NATIONAL TECHNICAL UNIVERSITY OF ATHENS

SCHOOL OF CIVIL ENGINEERING

DEPARTMENT OF WATER RESOURCES AND ENVIROMENTAL ENGINEERING

Diploma thesis:

Disentangling flow-energy transformations for small hydropower plants: from reverse engineering to uncertainty assessment and calibration

SAKKI GEORGIA KONSTANTINA

Supervisor: Andreas Efstratiadis, Assistant Professor, NTUA

TABLE of CONTENTS

Πρόλογος

Η εκπόνηση και παρουσίαση της παρούσας διπλωματικής εργασίας σηματοδοτούν το τέλος της φοίτησης μου στη σχολή Πολιτικών Μηχανικών στο Εθνικό Μετσόβιο Πολυτεχνείο καθώς και την απαρχή ενός νέου κεφαλαίου στη ζωή μου. Καθώς αυτή είναι η τελευταία σελίδα που γράφω για την εκπόνηση της εργασίας μου νιώθω την ανάγκη να ευχαριστήσω θερμά όλα τα πρόσωπα που συνέβαλλαν ουσιαστικά αλλά και ηθικά στην εκπόνησή της.

Αρχικά, θα ήθελα να ευχαριστήσω ιδιαίτερα τον κ. Α. Ευστρατιάδη, Επικ. Καθηγητή Ε.Μ.Π, που με την ιδιότητα του επιβλέποντος μου έδωσε την ευκαιρία να ασχοληθώ με ένα εξαιρετικά ενδιαφέρον και πρωτότυπο θέμα. Οι κρίσιμες επιστημονικά παρατηρήσεις και συμβουλές καθώς και το ειλικρινές ενδιαφέρον του για την εξέλιξη της διπλωματικής εργασίας βοήθησαν στην ολοκλήρωση της. Παρόλες τις δύσκολες καταστάσεις που αντιμετωπίζει η παγκόσμια κοινότητα λόγω της πανδημίας υπήρξε πάντα δίπλα μου με την ίδια αστείρευτη όρεξη. Οφείλω λοιπόν να τον ευχαριστήσω για τον χρόνο που διέθεσε σε συνεχείς τηλεδιασκέψεις καθώς και για την διαρκή πίστη του στις ικανότητες μου ακόμα και στις αστοχίες μου. Τέλος, είναι αναγκαίο να επισημάνω ότι το ήθος του και η αδιάλειπτη καθοδήγησή του τον κατέστησαν στα μάτια μου ως έναν αληθινό δάσκαλο.

Επίσης, οφείλω να ευχαριστήσω τον Δρ. Ιωάννη Τσουκαλά για την συνεισφορά του στην εκπόνηση της παρούσας εργασίας καθώς και για τον χρόνο που διέθεσε σε αυτήν. Η ενασχόληση του και μετά από την υπολογιστική διαδικασία συνέβαλε ουσιαστικά στην βελτίωση της συγκεκριμένης διπλωματικής εργασίας. Συγκεκριμένα χωρίς τη συμβολή του η παρούσα εργασία δε θα ήταν η ίδια. Ακόμη θα ήθελα να τον ευχαριστήσω για την ηθική του συνεισφορά στα μελλοντικά βήματα της επαγγελματικής μου σταδιοδρομίας.

Επίσης, θα ήθελα να ευχαριστήσω τους κ. Μακρόπουλο και Μαμάση για το ειλικρινές ενδιαφέρον τους σχετικά με την διπλωματική μου εργασία και τις συμβουλές του.

Ακολούθως, οφείλω να ευχαριστήσω τον Υποψήφιο Διδάκτωρ Διονύση Νικολόπουλο για την βοήθεια του σε ένα σημαντικό σημείο της παρούσας εργασίας. Ακόμη, θα ήθελα να ευχαριστήσω τον Δρ. Παναγιώτη Κοσσιέρη για την ηθική στήριξη και το ενδιαφέρον που έδειξε για την πρόοδο της εργασίας μου.

Τέλος, θα ήθελα να ευχαριστήσω τους φίλους και την οικογένεια μου για την πνευματική στήριξη τους κατά τη διάρκεια των σπουδών μου και για την πίστη στις δυνατότητες μου.

Σακκή Γεωργία – Κωνσταντίνα
Αθήνα, Ιούλιος 2020

Abstract

Due to their negligible storage capacity, small hydroelectric plants cannot offer regulation of flows, thus making the control of energy production a very difficult task, even for small time horizons. Further uncertainties arise due to limited information, both in terms of upstream inflow data and technical characteristics. Usually, the sole available measurements refer to power production, which is a nonlinear transformation of the river discharge. In this thesis we investigate the three configurations of this transformation, named the forward, the inverse and the calibration problem. The major outcome is a generic stochastic framework for the so-called *inverse problem of hydroelectricity*, i.e. the extraction of streamflow from observed energy data, focusing on two key potential sources of uncertainty, i.e. in energy production (observational error) and the efficiency curve of turbines (parameter error). Key issue of this *reverse engineering* approach is that the model error is expressed in stochastic terms, which allows for embedding uncertainties within calculations. Another interesting issue is the extrapolation of high and low flows outside of the range of operation of SHPs, which is employed by combining empirical hydrological rules for representing the rising and falling limbs. The methodology is tested in hypothetical problems as well as in a real-world case, i.e. the oldest (est. 1926) small hydroelectric plant of Greece, located at Glafkos river, in Northern Peloponnese. Among other complexities, this comprises a mixing of Pelton and Francis turbines, which makes the overall modelling procedure even more challenging and also requires to extract the efficiency curves of the two turbines through calibration. Our analyses indicate that the proposed framework may be the basis for handling several practical problems and open research questions in the broader area of simulation and optimization of small hydroelectric works.

Ελληνική περίληψη

Λόγω της αμελητέας ικανότητας αποθήκευσης, τα μικρά υδροηλεκτρικά έργα (ΜΥΗΕ) δεν μπορούν να προσφέρουν ρύθμιση των ροών, καθιστώντας έτσι τον έλεγχο της παραγωγής ενέργειας πολύ δύσκολο έργο, ακόμη και για μικρούς χρονικούς ορίζοντες. Περαιτέρω αβεβαιότητες προκύπτουν λόγω περιορισμένης πληροφόρησης, που αφορά είτε σε δεδομένα εισροών είτε σε τεχνικά χαρακτηριστικά του έργου. Συνήθως, οι μοναδικές διαθέσιμες μετρήσεις αναφέρονται στην παραγωγή ενέργειας, η οποία είναι ένας μη γραμμικός μετασχηματισμός της απορροής του ποταμού. Σε αυτήν τη διπλωματική εργασία διερευνώνται τρεις εκδοχές του μετασχηματισμού αυτού, που διαμορφώνουν αντίστοιχα το ευθύ και το αντίστροφο πρόβλημα καθώς και το πρόβλημα της βαθμονόμησης. Το κύριο αποτέλεσμα είναι ένα γενικό στοχαστικό πλαίσιο για το λεγόμενο αντίστροφο πρόβλημα της υδροηλεκτρικής ενέργειας, δηλαδή η εξαγωγή χρονοσειρών εισροής από δεδομένα παρατηρημένης ενέργειας, εστιάζοντας σε δύο βασικές πιθανές πηγές αβεβαιότητας, συγκεκριμένα στην παραγωγή ενέργειας (σφάλματα παρατηρήσεων) και στην καμπύλη απόδοσης των στροβίλων (σφάλματα παραμέτρων). Βασικό ζήτημα αυτής της αντίστροφης προσέγγισης είναι ότι το μοντέλο σφάλματος επιτρέπει την ενσωμάτωση της αβεβαιότητας στους υπολογισμούς, δεδομένου ότι εκφράζεται με στοχαστικούς όρους. Ένα άλλο ενδιαφέρον ζήτημα είναι η συμπλήρωση του υδρογραφήματος, δηλαδή ο υπολογισμός των υψηλών και χαμηλών ροών, εκτός του εύρους λειτουργίας των ΜΥΕ, κάτι που επιτυγχάνεται με τη χρήση εμπειρικών κανόνων για την αναπαράσταση των ανοδικών και καθοδικών κλάδων ροής. Η μεθοδολογία δοκιμάζεται σε πληθώρα υποθετικών προβλημάτων, καθώς επίσης και σε μια πραγματική περίπτωση, αυτή του παλαιότερου (περίπου το 1926) μικρού υδροηλεκτρικού έργου της Ελλάδας, που βρίσκεται στον ποταμό Γλαύκο, στη Βόρεια Πελοπόννησο. Μεταξύ άλλων περιπλοκοτήτων, το έργο αυτό περιλαμβάνει δύο στροβίλους, έναν τύπου Pelton και έναν Francis, γεγονός που καθιστά τη συνολική διαδικασία μοντελοποίησης ακόμη πιο δύσκολη μιας και απαιτεί την εξαγωγή των καμπυλών απόδοσης των δύο στροβίλων μέσω βαθμονόμησης. Οι αναλύσεις μας υποδεικνύουν ότι το προτεινόμενο πλαίσιο μπορεί να αποτελέσει τη βάση για τον χειρισμό πολλών πρακτικών προβλημάτων και ανοιχτών ερευνητικών ερωτημάτων στον ευρύτερο τομέα της προσομοίωσης και βελτιστοποίησης μικρών υδροηλεκτρικών έργων.

Εκτενής περίληψη

Αντικείμενο της παρούσας εργασίας αποτελεί η μοντελοποίηση της λειτουργίας μικρών υδροηλεκτρικών έργων υπό καθεστώς αβεβαιότητας. Συγκεκριμένα, αναπτύσσουμε ένα μοντέλο σε προγραμματιστικό περιβάλλον MATLAB το οποίο δέχεται δεδομένα παραγωγής ενέργειας και εξάγει την παροχή του υδατορεύματος, ποσοτικοποιώντας την αβεβαιότητα που προέρχεται τόσο από τα δεδομέαν εισόδου (παρατηρημενη ενέργεια) όσο και από τις εσωτερικές διεργασίες του συστήματος (π.χ. καμπύλες απόδοσης στροβίλων). Η παραπάνω προσέγγιση καλείται ως το «αντίστροφο ενεργειακό πρόβλημα», που στην πεούσα εργασία αντιμετωπίζεται ως πρόβλημα στοχαστικής προσομοίωσης.

Είναι γνωστό ότι το Ευρωπαϊκό Συμβούλιο προωθεί μια ολοκληρωμένη προσέγγιση για την κλιματική και ενεργειακή πολιτική, με στόχο την αποτροπή της αλλαγής του κλίματος καθώς και την αύξηση της ενεργειακή ασφάλειας της Ε.Ε. Ενδεικτικά, με βάση την γνωστή συμφωνία «20-20-20», μια σειρά μέτρων υιοθετήθηκαν από τα κράτη-μέλη με στόχο:

- Μείωση των εκπομπών αερίων θερμοκηπίου·
- Αύξηση της κατανάλωσης ενέργειας που προέρχεται από ανανεώσιμες πηγές ενέργειας (ΑΠΕ)·
- Μείωση στη χρήση πρωτογενούς ενέργειας.

Ακολούθως, η κυβερνητική πολιτική της Ελλάδας αποσύρει την εξάρτηση από τον λιγνίτη, προωθώντας επενδύσεις σε ΑΠΕ. Οι σχετικές επενδύσεις υπολογίζεται να φτάσουν 10 δισεκατομμύρια ευρώ έως το 2030. Πληθώρα ιδιωτικών εταιρειών σπεύδουν να βελτιστοποιήσουν την τεχνογνωσία και να καταρτίσουν εξειδικευμένο προσωπικό για να ανταποκριθούν στο νέο πλαίσιο της ενέργειας. Γίνεται κατανοητό ότι μεταβολή των μέσων παραγωγής ενέργειας σηματοδοτεί την βελτιστοποίηση των υφιστάμενων αιολικών πάρκων, υδροηλεκτρικών έργων κ.ά., καθώς επίσης και τη δημιουργία νέων. Η απεξάρτηση από τον λιγνίτη και η στροφή στις ΑΠΕ καθιστούν αναγκαία την μεγιστοποίηση της απόδοσης και διαχείρισης των υφιστάμενων υδροηλεκτρικών έργων και τον σχεδιασμό βελτιστοποιημένων υδροενεργειακών συστημάτων κάθε τύπου και κλίμακας (μεγάλα/μικρά υδροηλεκτρικά έργα, έργα αντλησιοταμίευσης).

Τα υδροηλεκτρικά έργα με εγκατεστημένη συνολική ισχύ κάτω των 15 MW νοούνται ως μικρά υδροηλεκτρικά εργοστάσια και η λειτουργία τους διαφέρει σε σημαντικό βαθμό από τα μεγάλα. Συγκεκριμένα, τα μικρά υδροηλεκτρικά έργα (ΜΥΗΕ) εκμεταλλεύονται μόνο τη ροή του ποταμού και τη διαφορά υψομέτρου που δημιουργεί το φυσικό ανάγλυφο για να παράγουν ενέργεια, απαιτώντας μικρής μόνο κλίμακας έργα. Εξαιτίας της μηδαμινής αποθήκευσης νερού λόγω της έλλειψης φράγματος, η παρακολούθηση της λειτουργίας των ΜΥΗΕ είναι εξαιρετικής σημασίας και καθοριστικός παράγοντας στην περίπτωση που μελετάται η αναβάθμισή τους. Ωστόσο, η σωστή και συστηματική παρακολούθηση της παραγωγής ενέργειας και απόδοσης των στροβίλων δεν είναι μία εύκολη και τυποποιημένη διαδικασία. Οι αβεβαιότητες στα τεχνικά μεγέθη (κυρίως στις καμπύλες απόδοσης των στροβίλων και στις υδραυλικές απώλειες στον αγωγό πτώσης) καθώς και τα λάθη στις

παρατηρήσεις ροής ή/ και ενέργειας, καθίστανται καθοριστικές για την λειτουργία ενός τέτοιου έργου.

Η ανάπτυξη ενός πλαισίου ποσοτικοποίησης των παραπάνω αβεβαιοτήτων κρίνεται εξαιρετικά χρήσιμη για τον σχεδιασμό και διαχείριση των ΜΥΗΕ, που σε κάθε περίπτωση προϋποθέτει τη μοντελοποίηση του μετασχηματισμού της παροχής του υδατορεύματος στη θέση της υδροληψίας (είσοδος συστήματος) σε ηλεκτρική ενέργεια που παράγεται από τον σταθμό παραγωγής (έξοδος συστήματος). Προκύπτουν τρεις διατυπώσεις του προβλήματος:

- *Ευθεία διατύπωση*, ήτοι εκτίμηση της παραγόμενης ενέργειας για δεδομένη παροχή και γνωστά τεχνικά χαρακτηριστικά του ΜΥΗΕ·
- *Αντίστροφη διατύπωση*, ήτοι εκτίμηση της παροχής από δεδομένα ενέργειας, και για γνωστά τεχνικά χαρακτηριστικά του ΜΥΗΕ·
- Εκτίμηση τεχνικών μεγεθών (παράμετροι) του ΜΥΗΕ μέσω *βαθμονόμησης*, με βάση γνωστά δεδομένα ενέργειας και παροχής.

Στην παρούσα διπλωματική εργασία δίνεται έμφαση στο αντίστροφο πρόβλημα, για το οποίο αναπτύσσεται ένα γενικό μεθοδολογικό πλαίσιο στοχαστικής προσομοίωσης, που περιγράφεται στο διάγραμμα της **Εικόνας 1**. Ειδικότερα, το μοντέλο που προτείνεται εξάγει καταρχήν ντετερμινιστικά, μέσω μιας επαναληπτικής διαδικασίας, τις παροχές για δεδομένη χρονοσειρά παραγωγής ενέργειας, με την προϋπόθεση ότι είναι στην εμβέλεια λειτουργίας των στροβίλων. Επίσης, για την ακριβή ποσοτικοποίηση των αβεβαιοτήτων που προκύπτουν ως αποκλίσεις από τις πραγματικές παροχές, κρίνεται απαραίτητη η στοχαστική περιγραφή των ανακτημένων παροχών του μοντέλου, μέσω διαστημάτων εμπιστοσύνης, όπως φαίνεται στο παράδειγμα της **Εικόνας 2**. Η στοχαστική προσέγγιση υλοποιείται με τη γένεση τυχαίων πραγματοποιήσεων για κάθε χρονικό βήμα, σύμφωνα με τα στατιστικά χαρακτηριστικά των σφαλμάτων του μοντέλου (περιθώρια κατανομή και δομή αυτοσυσχέτισης).

Όπως γίνεται σαφές το μοντέλο για το αντίστροφο πρόβλημα δύναται να εξάγει παροχές μόνο για το εύρος λειτουργίας των στροβίλων. Κάτω από το ελάχιστο και πάνω από το μέγιστο όριο παροχής η παραγόμενη ενέργεια είναι μηδέν ή είναι η μέγιστη (με βάση την ονομαστική ισχύ των στροβίλων), αντιστοίχως. Αυτός ο περιορισμός οδήγησε την έρευνα σε μια μεθοδολογία συμπλήρωσης για συμβάντα συνεχόμενων ελάχιστων ή μέγιστων παροχών, στην οποία επιδιώκεται η συμπλήρωση του υδρογραφήματος χρησιμοποιώντας εμπειρικούς κανόνες. Το υδρογράφημα διαχωρίζεται σε δύο κλάδους, ανοδικό και καθοδικό, και η συμπλήρωση γίνεται για κάθε κλάδο γνωρίζοντας τις δύο τελευταίες τιμές για τις οποίες έχουμε γνωστά δεδομένα ενέργειας. Στο υδρογράφημα υποθέτουμε ότι ο καθοδικός κλάδος ακολουθεί εκθετική στείρεση (μοντέλο γραμμικού ταμιευτήρα) ενώ ο ανοδικός μεταβάλλεται γραμμικά. Η συμπλήρωση του υδρογραφήματος σκοπεύει στην ολοκληρωμένη διατύπωση του μοντέλου, προκεμένου να εξάγεται η πλήρης χρονοσειρά παροχής. Είναι ενδιαφέρον να επισημάνουμε ότι για τις υψηλές παροχές η διαδικασία συμπλήρωσης μας επιτρέπει την πρόβλεψη της παροχής αιχμής καθώς και την ημέρα που συμβαίνει. Αντίστοιχη γνώση εξασφαλίζουμε και για την χαμηλές παροχές. Όπως και στην μεθοδολογία του αντίστροφου προβλήματος, εκφράζουμε στοχαστικά την συμπλήρωση του υδρογραφήματος.

$$if\ P_{obs} > P_{min}$$

NO **YES**

$$Q_{model} = "low"$$

Energy production data (**P**) $n(Q_t)$ H(Q_t)   Iterative numerical scheme

$$Q(t) = \frac{P(t)}{n(Q)H(Q)\gamma}$$

$$\left| Q^{[s-1]} - Q^{[s]} \right| > \Delta Q$$

NO   **YES**

$$Q_{model} = Q(t)$$

Comparison
$$Q_{model} \sim Q_{observed}$$

Generation of m synthetic error realizations

Creation of confidence interval for retrieved streamflow
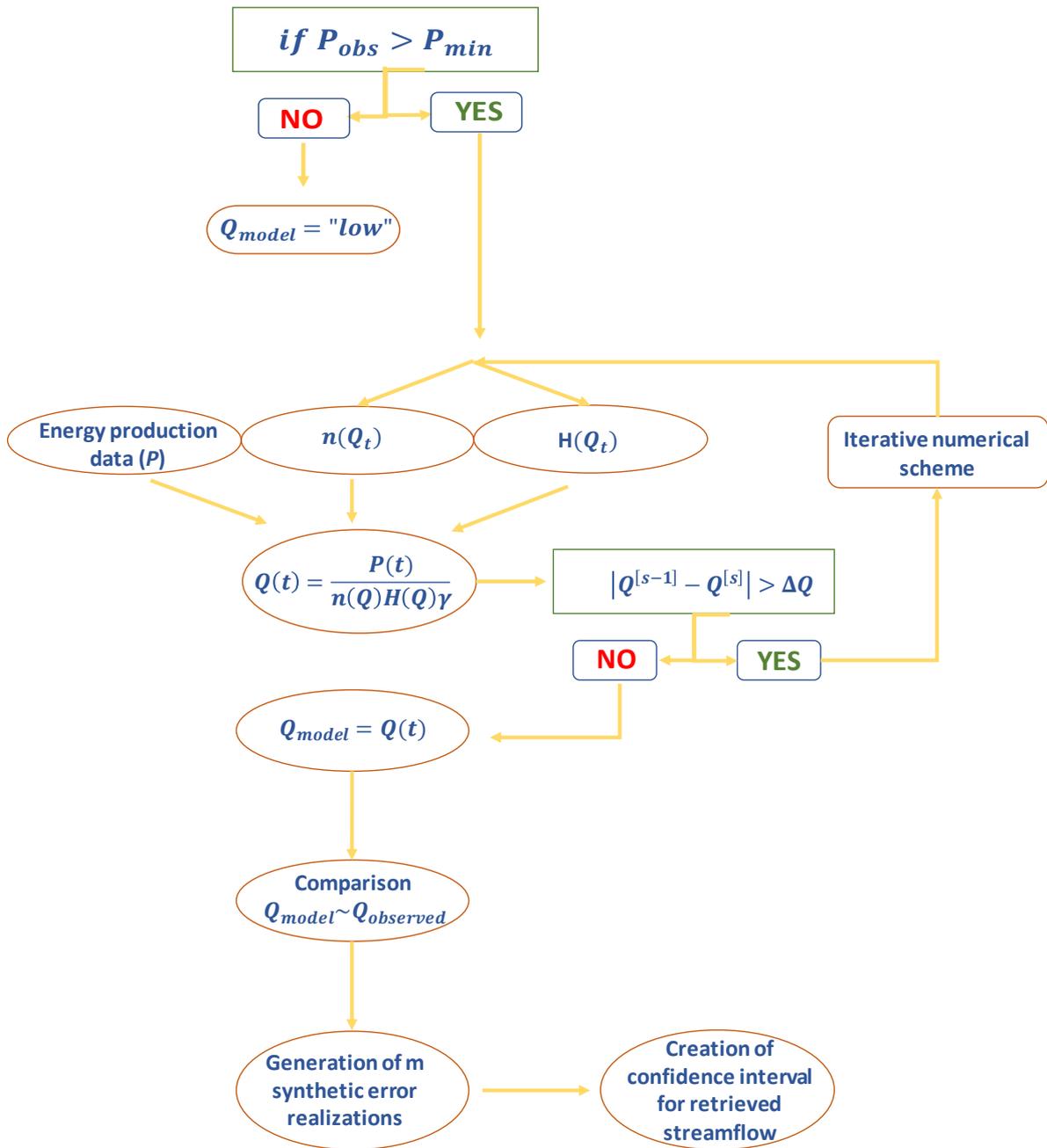
Εικόνα 1: Διάγραμμα ροής του προτεινόμενου μοντέλου ανάκτησης χρονοσειρών παροχής και του εύρους αβεβαιότητάς τους από δεδομένα παραγωγής ενέργειας.
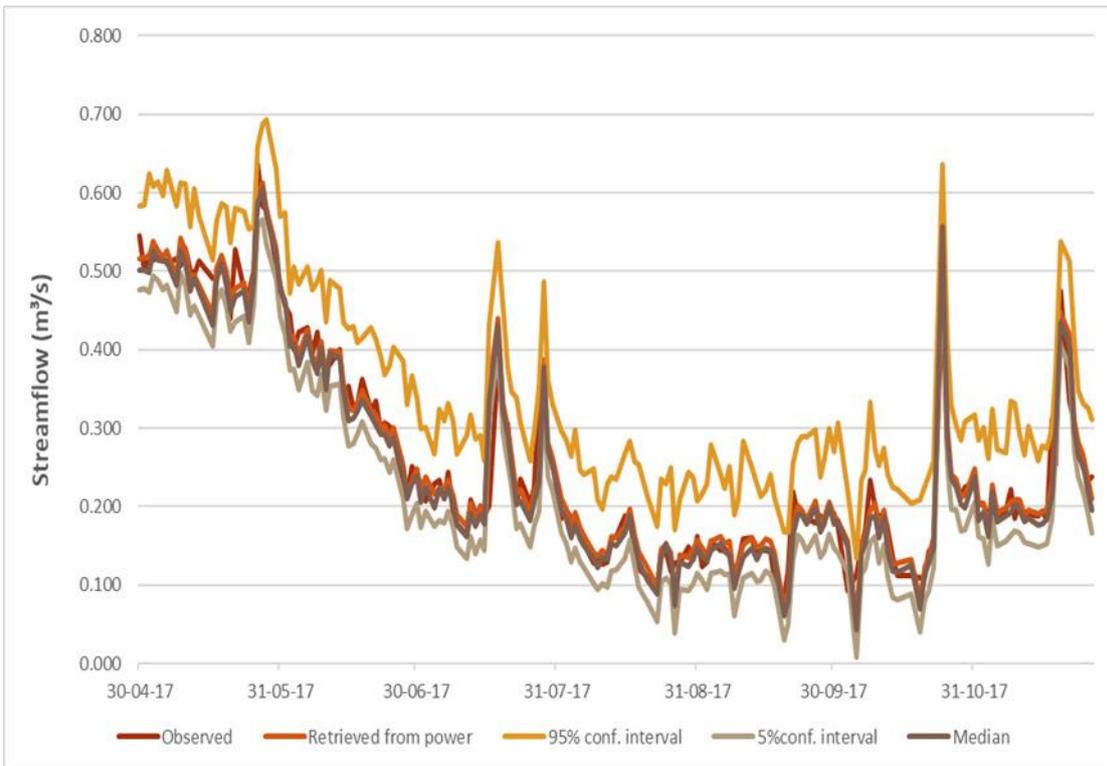
Εικόνα 2: Προσομοιωμένη παροχή με στοχαστική προσέγγιση για συνεχή λειτουργία του στροβίλου Pelton στο υδροηλεκτρικό «Γλαύκος». Απεικονίζονται η μετρημένη παροχή, η παροχή που προκύπτει από το ντετερμινιστικό μοντέλο, και τρεις χαρακτηριστικές τιμές παροχής από τη στοχαστική προσέγγιση (διάμεσος και όρια εμπιστοσύνης 90%).
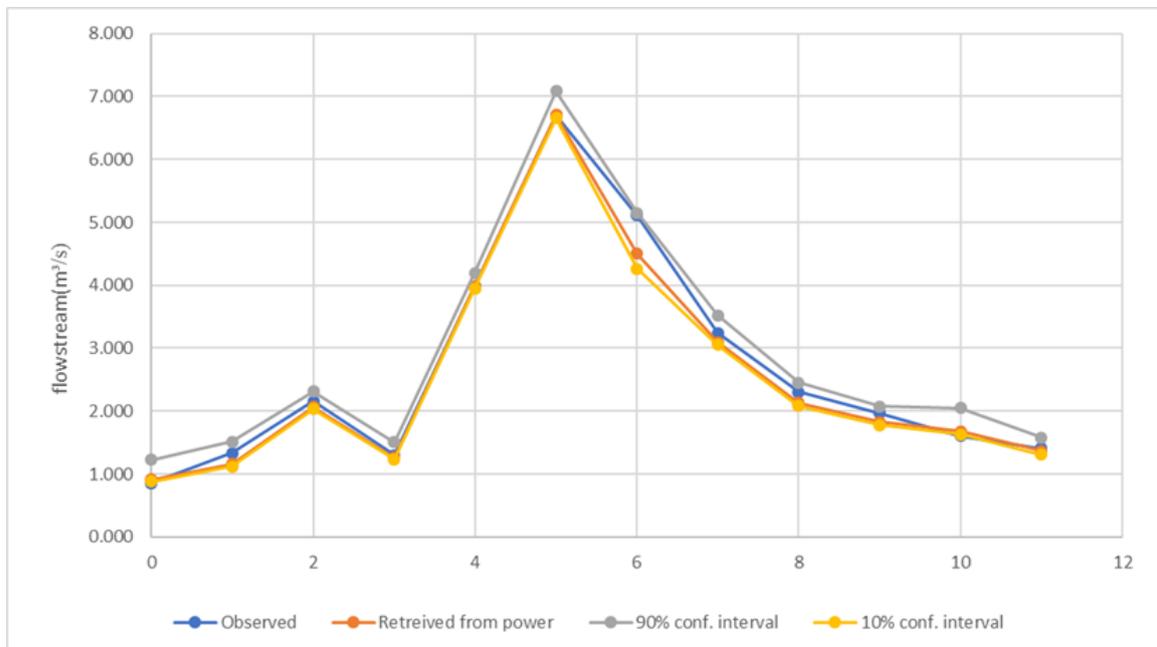
Εικόνα 3: Παράδειγμα συμπλήρωσης υδρογραφήματος για παροχές που υπερβαίνουν την ονομαστική παροχή των στροβίλων (στην προκειμένη περίπτωση 5.0 m^3/s) και αντίστοιχα όρια εμπιστοσύνης.
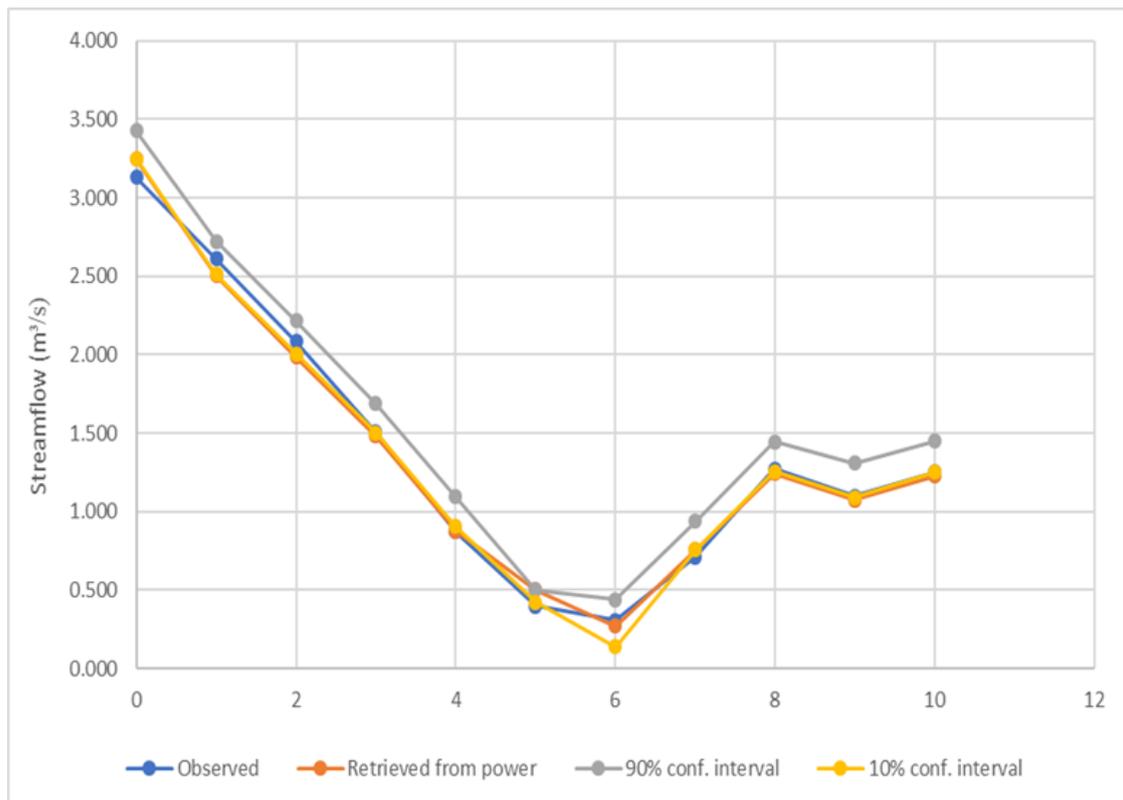
Εικόνα 4: Παράδειγμα συμπλήρωσης υδρογραφήματος για παροχές κάτω από το όριο λειτουργίας των στροβίλων (στην προκειμένη περίπτωση 0.5 m³/s) και αντίστοιχα όρια εμπιστοσύνης.

Το μοντέλο που προτείνεται εφαρμόστηκε σε ένα εικονικό και σε ένα υφιστάμενο έργο (ΜΥΗΕ Γλαύκου). Συγκεκριμένα, στο εικονικό έργο χρησιμοποιήθηκαν δύο διαφορετικοί τύποι στροβίλων, ενώ στο έργο του Γλαύκου μελετήθηκε η μίξη των στροβίλων καθώς και η λειτουργία κάθε στροβίλου ξεχωριστά. Ως πρωτογενή δεδομένα εισόδου ελήφθησαν ωριαία δεδομένα παραγωγής ενέργειας, ημερήσιες παροχές, η ισχύς του συστήματος, το ύψος πτώσης, η διάμετρος του αγωγού πτώσης καθώς και οι καμπύλες απόδοσης των στροβίλων.

Όσον αφορά στο εικονικό έργο, μελετήθηκαν δύο παράγοντες αβεβαιότητας:

- Αβεβαιότητα στα δεδομένα παραγωγής ενέργειας (σφάλματα εισόδου)
- Αβεβαιότητα στην καμπύλη απόδοσης των στροβίλων (σφάλματα παραμέτρων)

Σημειώνεται ότι ο βαθμός απόδοσης των υδροστροβίλων είναι συνάρτηση του λόγου της τρέχουσας προς την ονομαστική παροχή τους, και δίνεται σε εμπειρικά νομογραφήματα. Στην μελέτη ενός υδροηλεκτρικού έργου, ο βαθμός απόδοσης θεωρείται συχνά σταθερός. Αντιθέτως, κατά τη λειτουργία του ο βαθμός απόδοσης έχει διακυμάνσεις και εξαρτάται από την εισερχόμενη ροή στον στρόβιλο. Οι αναλύσεις μας έδειξαν ότι η διαφορά στη θεώρηση λειτουργίας-σχεδιασμού φάνηκε ότι είναι καθοριστική στα μικρά υδροηλεκτρικά έργα. Στην παρούσα εργασία μελετήθηκαν αρκετές καμπύλες στροβίλων, οι οποίες ακολουθούν μια παραμετρική αναλυτική φόρμουλα που μας επιτρέπει να προσαρμόζουμε οποιαδήποτε σχέση και να παράγουμε οικογένειες ισοπίθανων καμπυλών, θεωρώντας τις παραμέτρους της σχέσης ως τυχαίες μεταβλητές, όπως στο παράδειγμα της **Εικόνας 5**.
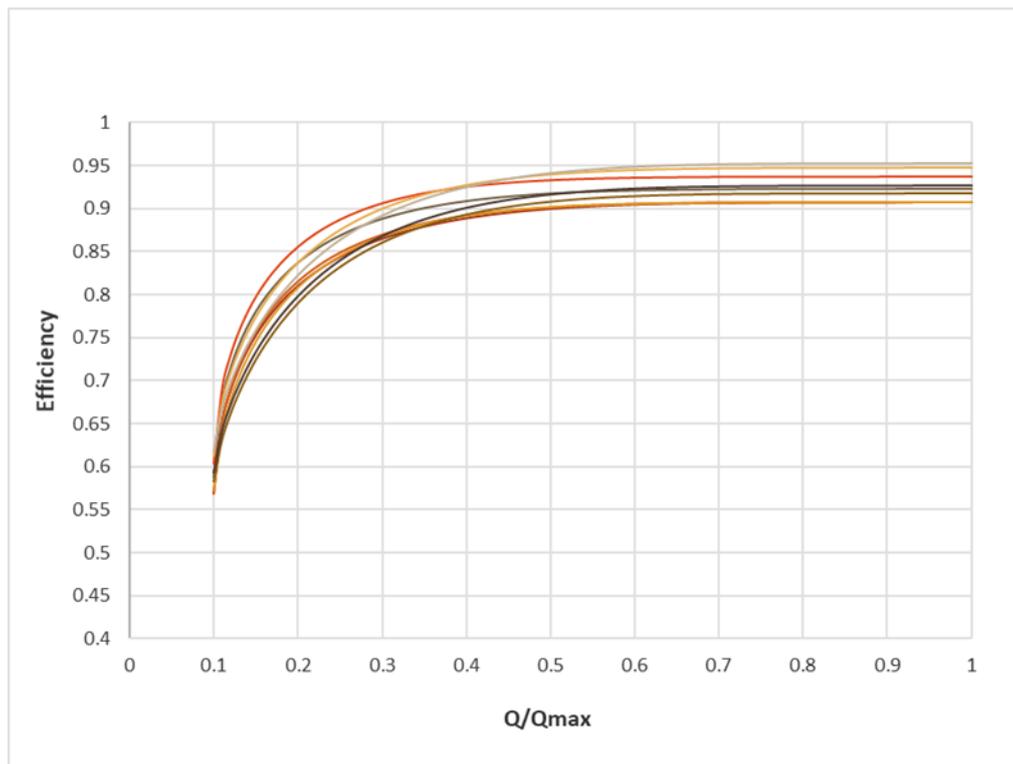
Εικόνα 5: Παράδειγμα παραγωγής τυχαίων καμπυλών απόδοσης για στρόβιλο τύπου Pelton.

Στο εικονικό έργο, τα σφάλματα στα «παρατηρημένα» δεδομένα παραγωγής ενέργειας. εισήχθησαν συνθετικά, με σκοπό να μελετηθεί η επιρροή τους στην αντίστροφη σχέση ενέργειας–παροχής. Εξετάστηκαν διάφοροι προσθετικοί τύποι σφαλμάτων που ακολουθούν κανονική ή Γάμμα κατανομή (με ασυμμετρία), καθώς και πολλαπλασιαστικά σφάλματα, και έγινε αντιπαραβολή τους με τα σφάλματα της εξαγόμενης παροχής (αποκλίσεις από την μετρημένη). Είναι ενδιαφέρον ότι το προσθετικό σφάλμα στην ενέργεια οδηγεί σε έντονα συσχετισμένα σφάλματα της προσομοιωμένης παροχής, αντίθετα το πολλαπλασιαστικό σφάλμα δημιουργεί σφάλματα μορφής λευκού θορύβου (με αμελητέα αυτοσυσχέτιση και ετεροσυσχέτιση με την παροχή).

Όσον αφορά το έργο του Γλαύκου προέκυψαν αρκετές δυσκολίες κυρίως λόγω έλλειψης δεδομένων. Ιδιαίτερα οι καμπύλες απόδοσης των στροβίλων ήταν άγνωστες και η προσέγγιση τους έγινε με βελτιστοποίηση μέσω γενετικών αλγορίθμων από τα δεδομένα ενέργειας και παροχής. Επίσης το δείγμα των δεδομένων παραγωγής ενέργειας για συνεχή και ταυτόχρονη λειτουργία των υδροστροβίλων ήταν αρκετά μικρό.

Καθίσταται σαφές ότι το προτεινόμενο στοχαστικό πλαίσιο αναλύει μια μη γραμμική σχέση, ποσοτικοποιώντας την υπαρκτή αβεβαιότητα σε όλες τις πτυχές της (απόδοση στροβίλων, καθαρό ύψος πτώσης, σφάλματα στα δεδομένα ενέργειας). Η ανάγκη ύπαρξης ενός τέτοιου μοντέλου διαφαίνεται κυρίως από τα αποτελέσματα στη μελέτη του υδροηλεκτρικού έργου στον Γλαύκο. Πιο συγκεκριμένα, εικάζουμε ότι οι αβεβαιότητες στην καμπύλη των στροβίλων καθώς και τα λάθη στην παρατήρηση της ενέργειας και της ροής έχουν ως αποτέλεσμα τη μη αποδοτική λειτουργία του συστήματος.

Το μοντέλο που προτείνουμε δύναται να εφαρμοστεί σε όλα τα μικρά υδροηλεκτρικά έργα, αφενός για τον έλεγχο της λειτουργίας τους και αφετέρου για την βελτιστοποίηση του σχεδιασμού τους αλλά και την επιχειρησιακή τους διαχείριση (πρόγνωση ενεργειακής παραγωγής). Συγκεκριμένα, είναι δυνατό να επιτυγχάνεται ο προγραμματισμός της παραγωγής ενέργειας μέσω του συνδυασμού ευθύ και αντίστροφου προβλήματος. Μέσω της αντίστροφης σχέσης εξάγονται οι πρόσφατες παροχές, δημιουργείται ένα σχήμα πρόβλεψης της παροχής και τέλος γίνεται η πρόβλεψη της ενέργειας στο επόμενο χρονικό βήμα μέσω της κλασσικής σχέσης. Επιπρόσθετα, η παρούσα έρευνα ανέδειξε την ανάγκη για διερεύνηση της βελτιστοποίησης της διαχειριστικής πολιτικής των στροβίλων στην ταυτόχρονη λειτουργία, προκειμένου να μεγιστοποιηθεί ο βαθμός απόδοσης του συστήματος.

1 Introduction

1.1 Motivation

In 2007, the European Council set a package of three key targets for year 2020, in an effort of making renewables the key player in energy production in the long term. These so-called "20-20-20" targets are:

- 20% cut in greenhouse gas emissions (from 1990 levels);
- 20% of EU energy production from renewables;
- 20% improvement in energy efficiency.

At this time, Greece's government policy withdraws its dependence on lignite, thus strongly promoting investments in RES. Relevant investments are expected to reach 10 billion euros by 2030. Numerous private companies are rushing to optimize know-how and train qualified personnel to meet the new energy framework. In is scene, it is necessary both to maximize the efficiency and optimize the management on the existing hydroelectric plants and to develop new hydropower plants of all types and scales, i.e. large, small, and particularly pumped-storage projects (Koutsoyiannis *et al.*, 2009).

Hydropower plants, which have a total installed capacity less than 15 MW are considered as "small" and their operation differs significantly from the large ones. In particular, SHPPs use the river's flow to produce energy directly. Due to their negligible storage capacity, small hydroelectric plants (SHPPs) cannot offer regulation of flows, thus making the scheduling of energy production a quite difficult task, even for small time horizons. Uncertainties in the technical characteristics (mainly in the performance curves of the turbines and the hydraulic losses in the pipe stock) as well as the observational errors in the flow and / or energy, become crucial for the operation of such projects. The creation of a quantitative framework for the above uncertainties is considered very useful for the design and the management of a SHPP. Subsequently, there are three formulations of the problem:

- Forward configuration, i.e. assessment of the energy produced for given inflow data and known technical characteristics;
- Inverse configuration by means of *reverse engineering*, i.e. estimation of the discharge by using energy production data, and known technical characteristics;
- Estimation of unknown or uncertain technical characteristics (handled as *parameters*) through calibration, based on known energy and flow data.

In this diploma thesis, we emphasize on the inverse problem of hydroelectricity, for which we develop a generic stochastic/probabilistic framework, and we also discuss and test the calibration problem. Preliminary results of the present study were presented at the General Assembly of the European Geosciences Union (Sakki *et al.*, 2020).

1.2   Research objectives

Considering the three possible expressions of the flow-energy transformation problem, in our research we set the following objectives:

- Formulation and computational implementation of each problem type;
- Recognition of uncertainties on technical characteristics;
- Quantification of uncertainties on observational errors;
- Configuration of efficiency curve by using analytical formula;
- Calibration of efficiency of each type, using the inflow and energy data;
- Stochastic approach of errors for the inverse engineering problem type.

The main focus of this research is the retrieval of flows from energy data, so-called the inverse problem of hydropower. The inverse engineering problem type involves the three flow ranges:

- Low flows, below the minimum operational discharge of turbines;

- High flows, exceeding the nominal discharge of turbines;

- Intermediate flows, which are directly estimated based on observed hydropower data.

The usefulness of such a model becomes apparent if we consider the huge uncertainties on river flow and finally on energy production and its cost.

1.3   Thesis outline

This thesis is divided into nine chapters and an appendix.

This **first chapter** introduces a preamble to the subject, the research objectives and the motivation of our work.

The **second chapter** provides a brief bibliographic overview on the meaning and usefulness of the hydroelectric plants, and especially of the small hydropower plants (SHPPs). Also this chapter presents the layout and the characteristics of a SHP.

Chapter three includes the literature review for the design, operation and maintenance of hydropower systems. In addition, this chapter discusses the issue of uncertainty on literature basis.

The **fourth chapter** discusses the three typical flow-energy transformation problems, i.e., the forward and inverse engineering approach, as well as the issue of calibration. After introducing the typical input data of SHPPs and their processing, it presents the formalization of the three problems and their challenges. Moreover, we explain in detail the hydraulic calculations and the estimation of efficiency.

The **fifth chapter** explains the core of our research, which is the stochastic modelling framework for the inverse problem of hydroelectricity. In particular, it presents the proposed numerical procedure for extracting the streamflow data under uncertainty, during the

operation of turbines within their flow limits. In the proposed framework, uncertainty is expressed by means of observational errors in energy data, as well as internal modelling errors with respect to the efficiency curves of turbines. For the latter, we develop an approximative parametric formula, which is also used in the context of calibration. Moreover, we provide a semi-empirical approach for the extrapolation of the hydrograph when the flow is outside of the range of the turbines.

The **sixth chapter** illustrates the model implementation in MATLAB environment. Specifically, we provide the code snippet for the whole numerical procedure.

In the **seventh chapter** we test our methodology in a hypothetical SHPP with two alternative turbines. In this example, we calibrate the efficiency curve, implement the reverse engineering procedure to reconstruct the streamflow and quantify the derived uncertainties for several error expressions and associated scenarios (e.g. normal, gamma-distributed). We also implement the extrapolation approach for the high and low flows, while the detailed results are given in the **Appendix**.

In the **eighth chapter** we implement our research in a real-world case, i.e. the Glafkos power plant, comprising a Pelton and a Francis turbine. Initially, we provide an overview of the study area, the system characteristics and its operation since its establishment (1926). In this study we extract the inflows for three time periods, i.e. the individual operation of the two turbines as well as their mixing. The issue of uncertainty, particularly regarding the efficiency curve of Francis turbine, as well as the observational errors in energy production data, are thoroughly discussed.

The **ninth chapter** summarizes the conclusions and the future perspective of our research.

2   Overview of small hydropower plants

2.1   About hydropower

Throughout history, human population growth has been supported by a steadily increasing production and consumption of energy. In the most recent five decades, the world energy consumption increased substantially. For instance, the electric power consumption per capita in 1971 was 1200 KWh, whereas in 2014 it has increased up to 3133 KWh (The World Bank, 2017). Specifically, the per capita energy consumption has risen from a global average of 1.56 tones of oil equivalent (toe) per person in 1973, to 1.66 toe per person in 2000 and to 1.92 toe per person in 2014 (The World Bank, 2017). This rapidly increasing energy demand raised the need for shifting to renewable energy sources, such as wind, solar, biomass, geothermal and hydropower. According to summary statistics for years 2017 and 2018, renewables contributed 18.1% to the world's energy consumption and 26% to its electricity generation, respectively (REN21's 2019 report).

Of these so-called green energy sources, hydropower is the most efficient, in both technical and economic terms, with a price competitive to fossil fuels. The idea of hydropower is simple. Stored water in a high elevation has a dynamic energy that turns into hydraulic energy, as water flows to lower areas. Next, the hydraulic energy is converted to mechanical, by using hydrodynamic machines (turbines). In particular, a hydro turbine converts the energy of water through continuous flow of fluid and constant rotary motion. Transforming the energy of the passing fluid under a constant supply to mechanical energy is done in the rotating part of the machine, which is called a rotor, by means of thrust. The drive torque is transferred to the rotor shaft, which is coupled to the electric generator shaft, which converts the mechanical power to electricity. A final conversion is employed through the transformer, in order to supply the high-voltage electricity grid.

The small hydropower plants are based on the exploitation of dynamics surface water energy, by converting it initially to kinetic and then to electricity, according to the laws of electromagnetic fields. Initially, running water is confined or water is stored in natural or artificial lakes. The kinetic energy of water is converted into mechanical energy by the rotation of the axle of a turbine impeller. Then, the turbine operates a generator, which converts mechanical energy into electricity.
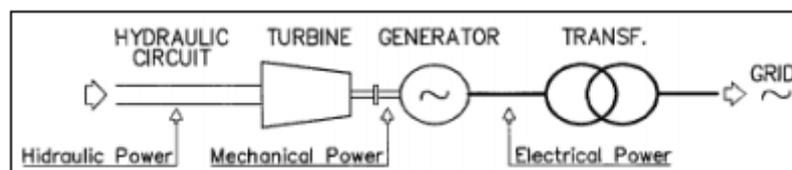

Figure 2.1: Serial conversion of hydrodynamic energy to electric energy at the grid through a hydropower system (Ramos & Betamio, 1999).
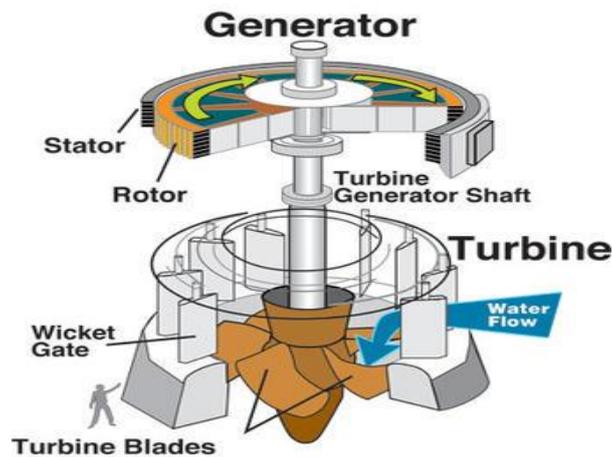
Figure 2.2: USGS

It is worth mentioning that the earliest evidence of taking advantage of hydraulic energy through water wheels and watermills goes back to the ancient Near East in the 4th century BC (Wikipedia,2020). It is also known that much earlier, namely in ancient Egyptian times, people have used energy in running water to operate machinery, grind grain and corn (Wikipedia, 2020). Nowadays, modern hydro plants produce electricity using turbines and generators. The first hydroelectric station was built in 1882 in Appleton, Wisconsin, and produced 12.5 kW, thus providing light to two papermakers and a house. Nowadays, the largest hydroelectric station, called the Three Gorges Dam, built in 2012 in China, has a capacity of 22 500 MW.

In general, the hydropower works are either dam-based or run-of-the-river; the latter belong to a broader category of the so-called Small HydroPower Plants (SHPPs), which is the focus of this research. Dam-based hydropower plants typically require the construction of large-scale infrastructures, in order to offer long-term regulation of flows through the reservoir storage. However, they also have significant impacts on the riverine ecosystem and the surrounding environment. On the contrary, RoR plants are quite simple structures, since they produce hydroelectric energy without requiring large-scale interventions in the river for employing water storage (reservoir). With respect to large reservoirs, they have limited socioeconomic and environmental impacts, thus making them more attractive.

Hydroelectric power has played an important role in worldwide spread of electricity and has helped to boost industrial development. Hydroelectric works continue to produce 16.6% of global electricity. Further growth of this mature technology is possible, though many countries have already developed cost-effective sites. The total installed capacity for hydroelectricity has now surpassed 1290 GW, and there remains vast untapped potentials around the world, especially in developing countries. There was more hydro commissioned than solar and wind energy and experts predict that hydropower capacity could double by 2050 (IHA, 2014). In Greece, the installed capacity is just under 3500 MW, while hydropower covers about 10% of our electric energy needs.

HYDROPOWER INSTALLED CAPACITY WORLDWIDE

REST OF THE WORLD **269**
COLOMBIA **12**
IRAN **12**
MEXICO **12**
AUSTRIA **15**
VENEZUELA **15**
SWEDEN **16**
VIETNAM **17**
SWITZERLAND **17**
SPAIN **20**
ITALY **23**
FRANCE **26**
TURKEY **28**
NORWAY **32**
RUSSIA **49**
INDIA **50**
JAPAN **50**

CHINA **352**

BRAZIL **104**
UNITED STATES **103**
CANADA **81**

4,200 TWh 2018

1,292 GW — Total hydropower installed capacity in 2018

Hydropower installed capacity (GW) of top 20 countries and rest of the world including pumped storage in 2018. Source: IHA 2018

iha International hydropower association

Figure 2.3: The total hydropower installed capacity IHA (2019)

2.2   Small hydropower plants

In order to define a Hydroelectric power plant as "small", the installed power must be under a certain limit, that is defined in the corresponding national legislation. This limit varies considerably among different countries, but the most common values are between 10 and 30 MW. For example, in California, hydroelectric generating stations with a maximum capacity of less than 30 MW are classified as small. The "small hydro" description may be stretched up to 50 MW in the United States, Canada and China (WIKIPEDIA). For the distinction between Small HydroPower Plants (SHPPs) and large ones, the Greek state has adopted a capacity limit of 15 MW. Most of SHPPs in Greece have a capacity from 0.5 to 3.0 MW. Such projects do not cause significant visual impacts and public opposition, because they involve neither large-scale water collection and storage works nor the construction of large dams, thus being quite compatible with the environment.

There are four different types of SHPPs, based on their storage capacity (Mamassis *et al.*, 2020). The first one is put at the outlet of a large dam, e.g. to exploit the environmental flow. In this case, the outflow target through the turbines is well-ensured, since there is a satisfactory storage of water (this target is small, if compared with other water uses, and is also put in priority). The second one is so-called run-of-river (RoR), which utilizes the streamflow as it comes, without the ability to store the water (water is captured and diverted to a forebay tank). This is the most common SHPP type. Another type involves the construction of a low-head dam across a large river or channel, which creates a small reservoir upstream of negligible regulation capacity. The last one is so-called in-stream, which utilizes the streamflow velocity to produce electric energy. Because of the fluctuations of river's streamflow very few projects of this type exist.

20
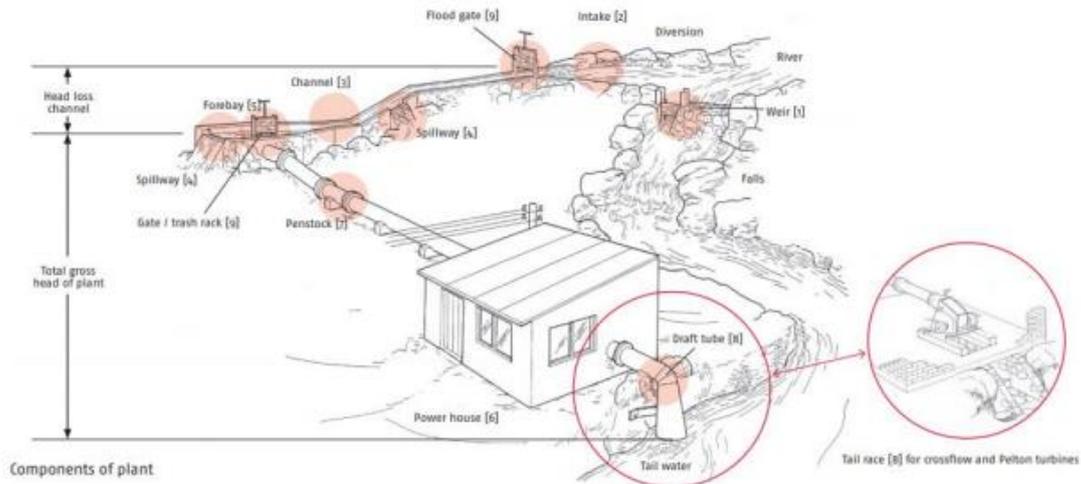
Figure 2.4: Components of a small hydropower plant (Source: www.energypedia.info).

2.3   Run-of-river plants: layout and operation

As mentioned before, the small hydroelectric plant utilizes the natural fall of the surface water, through a pressurized hydraulic system that sends water to a turbine. A general layout of a small hydroelectric station is demonstrated below.

Figure 2.4 illustrates a sketch of the most characteristic type of a small hydroelectric work, referred to as run-of-river plant (RoR). In this layout, the power station is located far away from the intake, to ensure an economically effective elevation difference between the forebay tank and the power station, but the case that it is embodied in the intake is also common. The main elements of this configuration, as moving from upstream to downstream, are:

(a)   A weir, comprising a water intake that controls the amount of river flow to be used for hydroelectricity, from which the exploitable water is abstracted from the stream or, more generally, from the water source. The water abstraction system is designed so that part of the flow (ecological supply) will be by priority conveyed to the downstream natural system, while surplus water is also spilling through the weir.

(b)   A channel, which is referred to as headrace, that conveys the water to a forebay tank. At the entrance of the channel there is sand trap and a desilter, which allows for managing sediment transport (a detailed layout is shown in **Figure 2.5**).

(c)   The forebay, which is designed to ensure the appropriate hydraulic conditions of the input into the penstock. The basic criterion for designing the forebay is the prevention of air into the supply pipeline, which can cause cavitation problems. Due to its small storage capacity, the forebay offers very limited regulation (e.g. for few hours) and also ensures a practically constant head.

(d)   The penstock system, basic component of which is the pipeline, through which the flow is conveyed to the turbine under pressure. The installation of the pipeline may be either underground or superficial. The pipeline is usually placed in a pit and then is buried, for environmental reasons as well as for the protection of the pipe from wear.

(e)   The power house, hosting the turbines and the generator. The power house is the place where the penstock ends and the electromechanical equipment (turbines), the transformers, the generator and the monitoring and control equipment are installed. The type and number of turbines is selected according to the flow rate and head of plant and the best-case scenario for the operation of the plant. The layout of the power house depends on the existing topography, the flow conditions of the natural water stream and the type of electromechanical equipment.

(f)   A tailrace that conveys the water back to the river, after exiting the turbine.
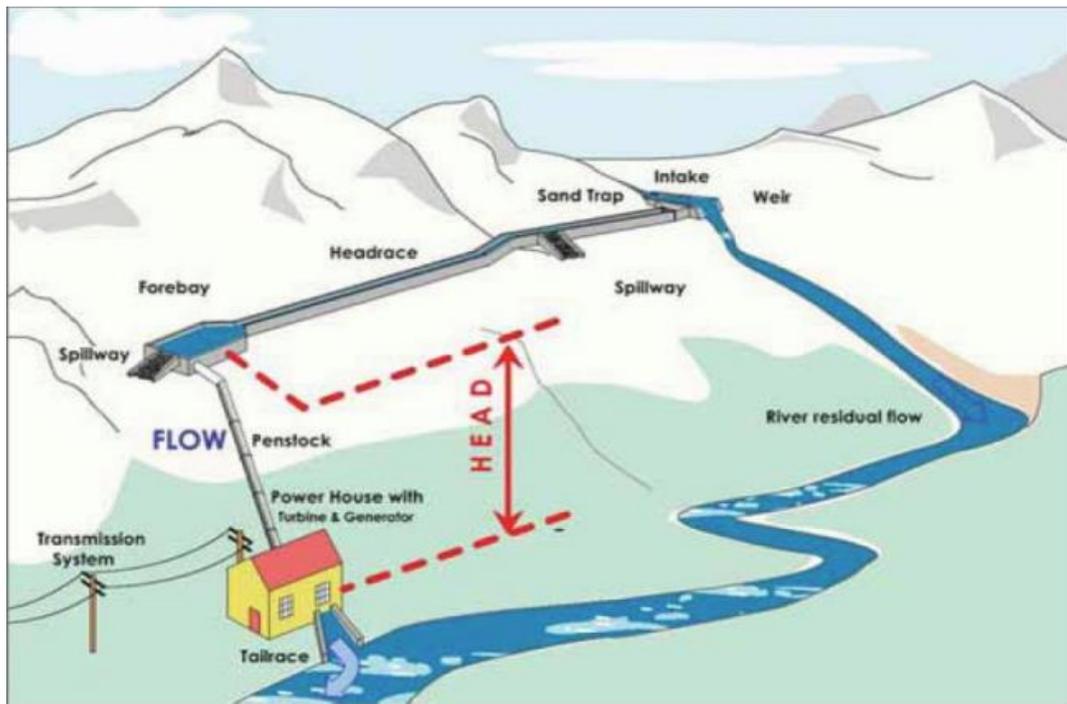
Figure 2.5: Overview of concept and main components of a RoR plant (GGF, 2012).

In order to define the exact design of a small hydropower plant it is essential to define of project layout and formulation and finally the layout optimization. Specifically, the following studies and optimization procedures are critical:

o   Hydrological study (streamflow data, preferably at daily basis or finer, flow-duration curve, environmental flows, flood regime, dry/wet year conditions);
o   Basic topographical overview (available head, siting of main system components, access conditions, existing roads);
o   Pre-design of hydraulic structures with cost estimations;
o   Optimisation of sizing;
o   Detailed field investigations;
o   Detailed engineering design and bill of quantities;
o   Choice of suitable equipment (turbines, penstock diameter etc.);
o   Budgetary quotations for equipment.
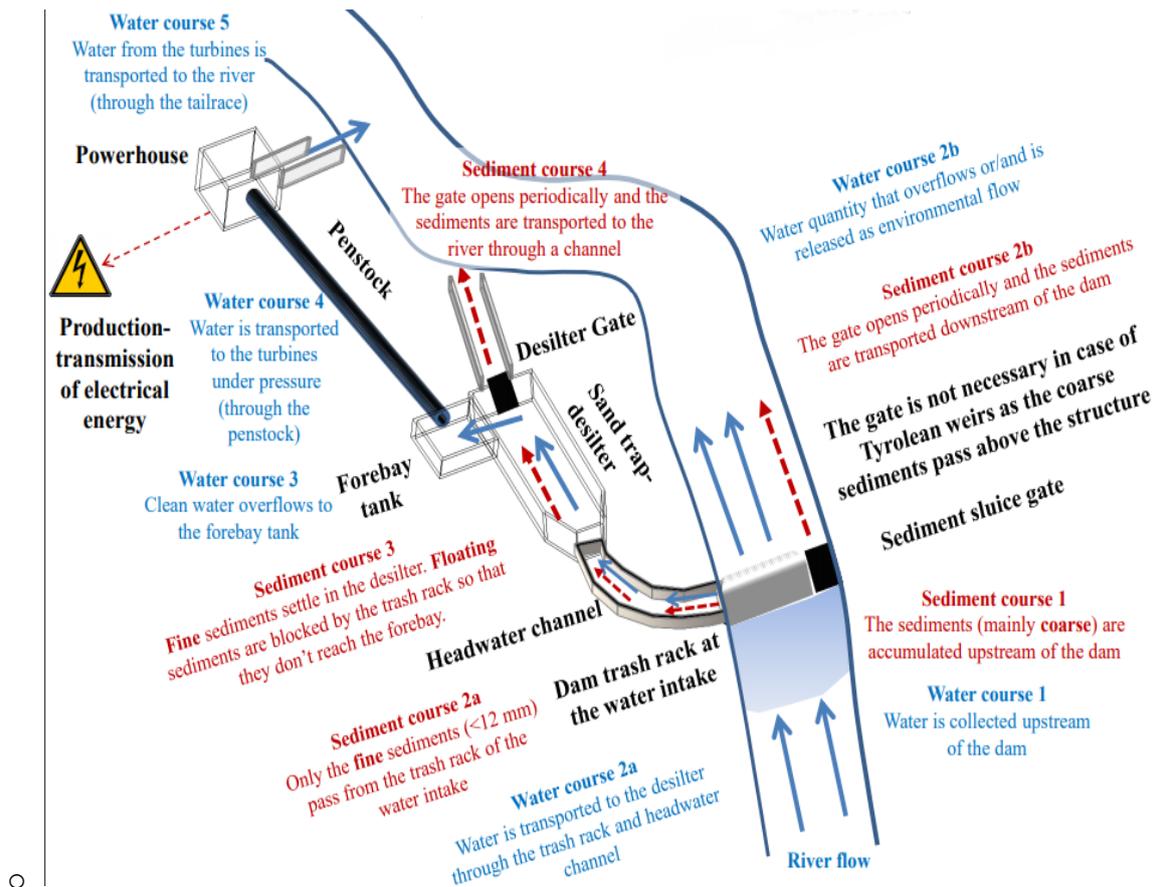
o **Figure 2.6**: Typical layout of intake works in a RoR plant (Mamassis *et al.*, 2019).

The above steps are necessary to design a small hydropower plant that uses with the most effective way the inflows of a river. If planned properly, hydropower offers the lowest generation cost at a very low risk and over a quite long life time. The hydrological study determines how much water will be available for electricity generation over the year, hence it provides the basis for the optimal siting and sizing of the system, in technical and economic terms.

2.4 Turbines

2.4.1 Classification and operation

The turbine system converts the hydraulic energy of the diverted river water, expressed in terms of net head, into electricity. Which turbine(s) to select depends in large part on site characteristics (e.g. available net head), and the river's discharge regime. In hydroelectric systems, turbines are generally classified into two categories:

i. impulse turbines (e.g. Pelton), taking advantage of the kinetic energy of water falling from a large elevation (outflow to the atmosphere); the flow velocity is substantially amplified by passing water through a nozzle;

ii. reaction turbines (e.g. Francis), operating under pressure, as the chamber of the runner remains completely filled by water.

Each turbine operates in a specific range of flows. The maximum flow, also referred to as nominal, is determined by power capacity of the turbine, while the minimum one ranges from 10-30% of maximum. Below this value the ability of the turbine to generate electrical power is negligible.

Next we will briefly mention the two major turbine types that are used in hydroelectricity, and particularly in run-of-river plants, i.e. Pelton and Francis.
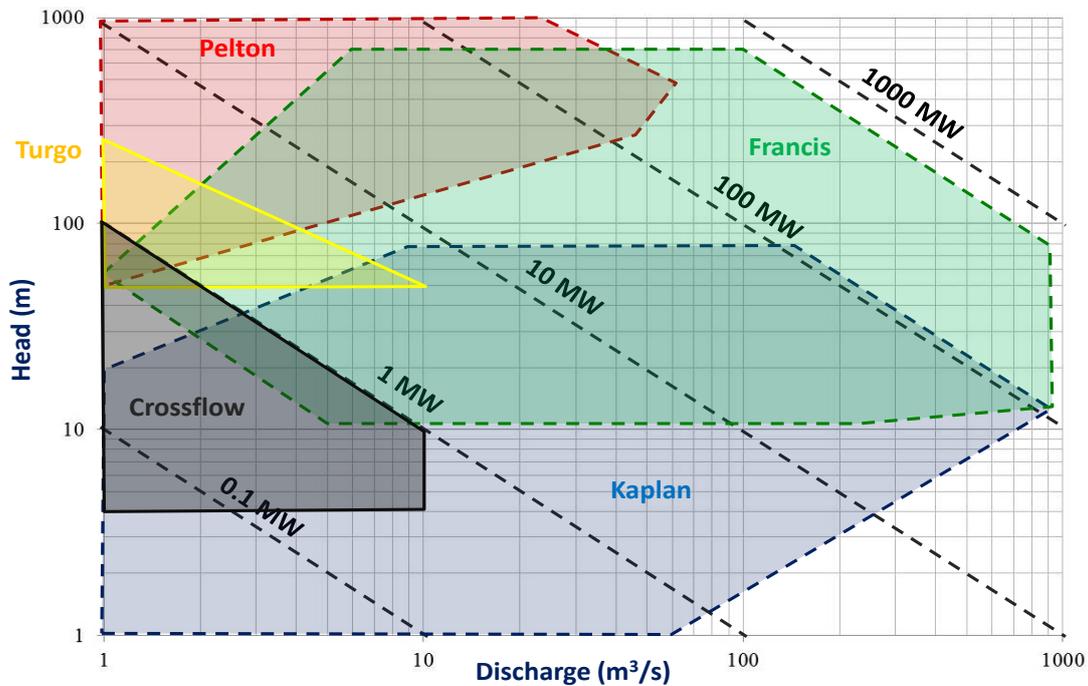

Figure 2.6: Typical recommendation ranges for turbine selection.

2.4.2   Pelton turbines

Pelton is one of the most effective hydro-turbine. Pelton is an impulse turbine. In 1889, the American engineer, Lester Allan Pelton, patented this machine by streamlining the traditional windmill technology. A jet of water passing from a contracting nozzle enters the double buckets of the turbine wheel, to produce energy as the runner rotates. After it is impinging the buckets, the water outflows freely (i.e., under atmospheric pressure). Since the jet flow is not axisymmetric, thus only part of the runner is activated (typically only two or three out of about 20 buckets), they are also referred to as partial admission. The idea of energy production the substantial increase of the flow velocity from V_1 to V_2 where V_1 is the velocity through the penstock, with diameter D_1, and V_2 is the velocity through the nozzle, with diameter $D_2 \ll D_1$. Generally, V_1 ranges from 4 to 6 m/s, while V_2 may exceed 100 m/s. Impulse turbines are applicable for large heads (H > 250 m) and relatively small Q.
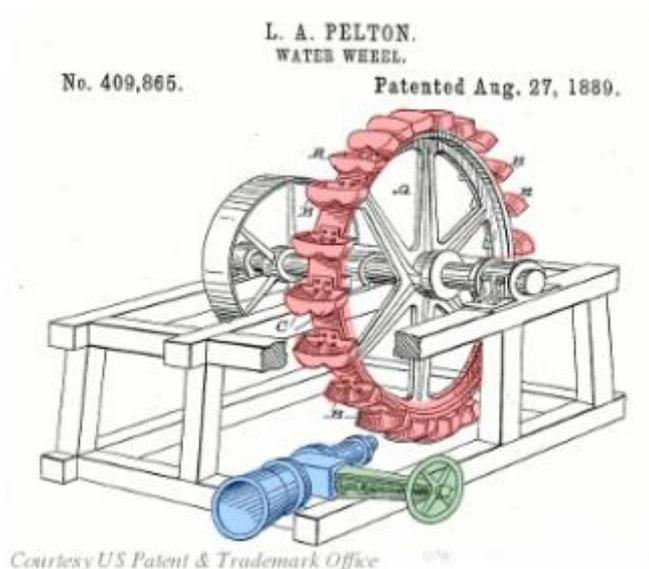
Figure 2.4: Sketch of the Pelton wheel (source: Wikipedia).

2.4.3   Francis turbines

In 1849, the American engineer, James B. Francis, built a new turbine, which has since bore this name and is the most common type of turbine in medium-sized hydroelectric projects. Francis The Francis turbine is a type of reaction turbine a category of turbine in which the working fluid comes to the turbine under immense pressure and the energy is extracted by the turbine blades from the working fluid. Part of the energy is given up by the fluid because of pressure changes occurring in the blades of the turbine, quantified by the expression of degree of reaction, while the remaining part of the energy is extracted by the volute casing of the turbine. At the exit, water acts on the spinning cup-shaped runner features, leaving at low velocity and low swirl with very little kinetic or potential energy left. The turbine's exit tube (also known as draft tube) is shaped to help decelerate the water flow and recover the pressure.

Francis turbines are suitable for a wide range of discharge and head conditions, thus they are applied most of hydroelectric works worldwide (all but two large hydropower systems in Greece employ Francis turbines). The Francis turbine is commonly used for heads from 40 to 600 m and for discharge values from 0.2 to 20 m³/s, thus resulting to power capacity values from 10 kW to 770 MW. The speed range of the turbine is from 75 to 1000 rpm. In contrast to the Pelton turbine, the Francis turbine operates at its best completely filled with water at all times. However, its efficiency ranges from very low to very high values, thus making it very difficult as for the optimal operation.
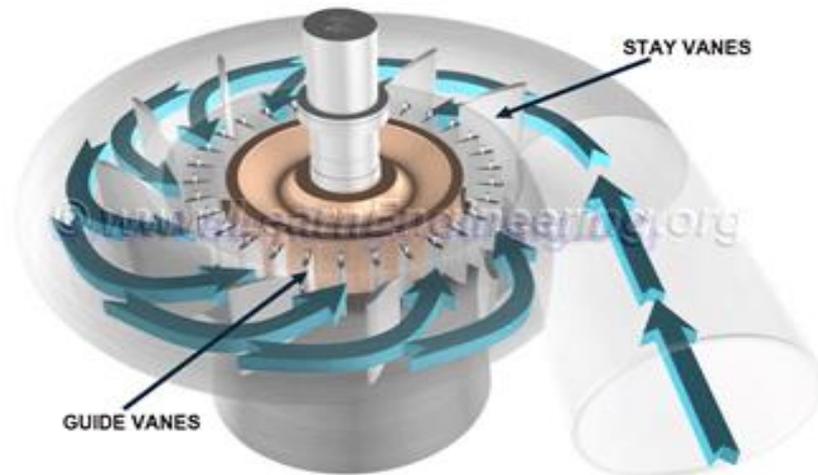
Figure 8.5: Stay vanes and guide vanes of a typical Francis turbine (www.theconstructor.org).

2.5   Advantages and disadvantages

Small hydroelectric power plants have a number of significant advantages, which establishes them as an effective source of energy. SHPPs are based on the idea to exploit the waterfalls, which are a renewable energy source and therefore do not face visible risk of depletion, as the contingency fuels. Contrary to what happens with fossil fuels, water is not disposed of in the production of electricity and can be used for other purposes. Specifically, small hydropower plants may be combined with parallel uses such as water supply and irrigation, helping to maximize the utilization of water resources. Furthermore, they have brief investment amortization time due to very low operational and maintenance costs and the cost of generating electricity has not huge fluctuations and essentially corresponds to the depreciation of the project. In environmental approach, the SHPPs do not have waste or residues, eventually do not pollute the environment. Due to the fact that small hydropower plants are constructed in isolated mountainous areas, the nuisance caused by them is minimal. The transport pipeline is usually underground, the building of the plant can be adapted to the local architecture, modern turbine technology ensures reduced sound nuisance and there is no need to store water. The result is not only not to be disturbed, but often for the visual environment area to be upgraded.

Despite their significant advantages, small hydropower plants present some disadvantages which they must be taken into account in order to maximize the benefits from the application of this technology. Besides the low operational cost, they have a high construction cost (of the order of 1000-2000 €/KW) and for this requires the allocation of relatively large funds. Although, the most crucial disadvantage of SHPPs is the uncertainty around energy production, due to lack of water storage. This feature, which is an advantage in terms of size of the environmental burden, implies zero flexibility in the management of energy in the Transmission System, since the energy produced should be consumed immediately.

Overall, small hydropower stations are a viable, clean and cost-effective alternative to dam-based plants, and provide the option of decentralized power production. The difficulties that occur by the small hydropower plants, should not, in any case, be considered as an inhibiting

factor in their promotion. The insurance of energy sustainability and the protection of the environment require the exploitation of every economically and environmentally sustainable energy source.

2.6   Development of small hydropower plants over Greece: current status and perspectives

An important qualitative feature in the field of small hydropower plants is their spatial distribution in Greek territory. The natural resource that they use for electricity production is water, i.e. rainfall or, in general precipitation and it is natural their development to be geared towards areas with rich water potential. In Greece the richest hydrological basins are concentrated mainly in the northern and western regions of the mainland, which are dominated by the mountain range of Pindos. The map below presents the distribution of small hydropower plants, depending on the stage of their implementation. The map also shows the spatial distribution of the mean annual rainfall over Greece.

As the investment interest in small hydropower plants has become particularly intense the last five years, the search for new sites has turned to the less developed areas. Generally, in Greece 107 small hydropower plants operate. Today, in Thessaly there are 28 projects under development, 29 in Western Macedonia and 9 in Peloponnese.
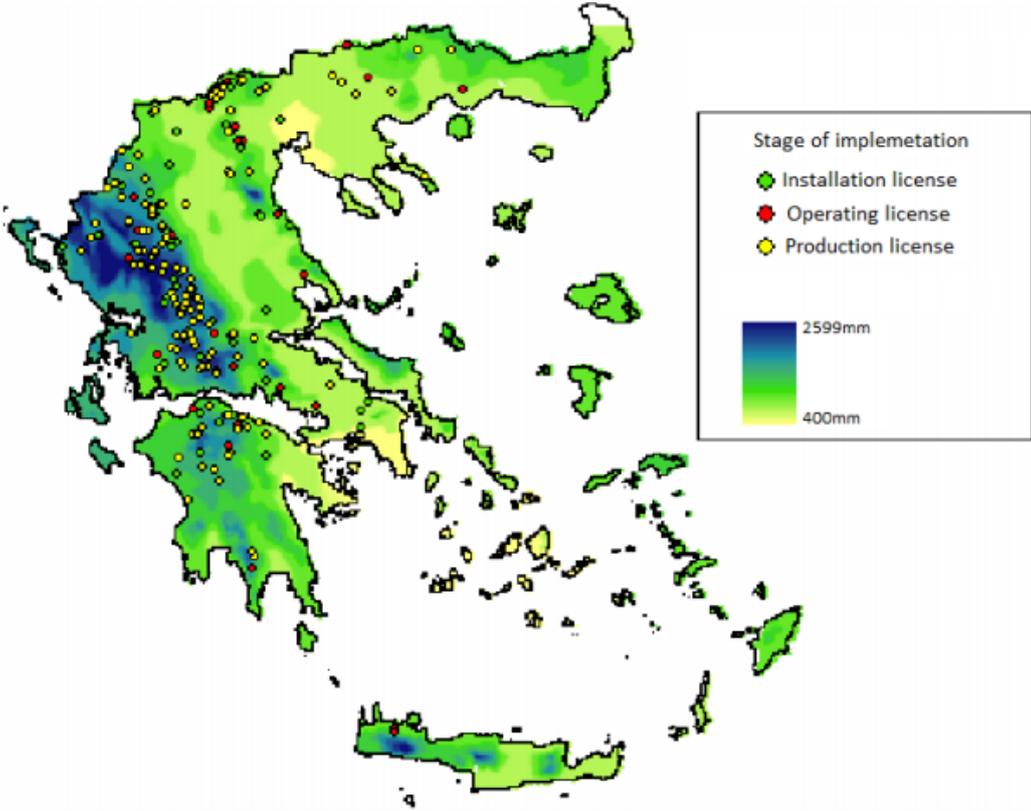

Figure 2.7: Elevation map of Greece, showing the locations of licensed small hydroelectric plants (Hellenic Ministry of Development).

3 Research advances in the design and operation of small hydropower plants

3.1 Literature review

During the past three decades many experts have employed comprehensive research on the optimal design, operation and performance of small hydropower plants. Yildiz and Vrugt (2019) mention that this research has primarily focused on five issues: (1) the determination of the optimal power capacity, (2) the development of specialized metrics (indices) that convey properly the economic performance (profitability) and energy production of power plants, (3) the development of fast and efficient optimization approaches for the design of the hydropower system, (4) the design, operation, analysis, and performance assessment of turbines, and (5) the importance of streamflow processes and surface hydrology on the overall performance of small plants.

Many researches focused on the optimum capacity of small hydroelectric plants as for their economic profitability. For instance, Santolin *et al.* (2011) proposed a model for the capacity sizing of a small hydropower plant on the basis of techno-economic analyses of the flow duration curve by using seven parameters. Montanari (2003) presented a method for finding the most economically advantageous choice for the installation of micro hydroelectric plants with small net head and modest flow rates. Anagnostopoulos and Papantonis (2007) found that the use of two turbines of different size can enhance sufficiently both the energy production of the plant, by optimizing the mix of turbines, and the economic results of the investment. In addition, they demonstrated that the optimum size of turbines depends strongly on the characteristics of the installation site and the actual turbines used. Mishra *et al.* (2011) concluded that the properties of the river discharge and number of poles of the generator determine the optimum size and investment costs of small hydropower plants, nevertheless, these variables are often ignored during design and optimization analyses.

The choice of one or more turbines in small hydropower plants is a multidimensional problem because their operation is based on many unknown characteristics. Research into turbine selection, design, analysis, operation and performance has led to approaches for direct measurement, monitoring, numerical simulation and optimization of the turbine efficiency. Cobb and Sharp (2013) studied a laboratory-scale test fixture in order to test the operating performance characteristics of impulse turbines (Pelton and Turgo). Elbatran *et al.* (2015) reviewed the selection of low head micro-hydropower turbines with emphasis to poorly developed areas, and looked forward to using simple turbines for achieving good performance with minimum initial and running cost. Finally, Skjelbred and Kong (2019) compared the performance of linear interpolation and spline interpolation for turbine efficiency curves, in the short-term hydropower scheduling (STHS) problem and the bidding strategy in intraday market.

3.2   Issues of uncertainty

Small hydropower plants have operational flexibility such as quick starting, stopping and load variations thus helping in improving the overall reliability of the power system. In this context, it is not surprising that this form of hydropower exhibited such an expansion during the past decades. On the other hand, these works are subject to multiple uncertainties that span over all aspects of flow-energy transformations, and affect many crucial tasks, including the optimization of turbines efficiency, the maximization of economic performance, the operational maintenance and the optimization of turbines mix.

The most apparent and well-studies issue of uncertainty involves the hydrological inputs. Evidently, due to their negligible storage capacity, small hydroelectric plants strongly depend on the sequence of hydrological periods, and particularly the low and medium flows. Casadei *et al.* (2014) proposed empirical methods to improve the performance of a SHPP according to the hydrological regime of the river, the frequency of dry and wet years, and the target energy production. Moreover, the fluctuations of demand and supply adjust more uncertainties in the operation and design of small hydropower plants. Bjerkholt and Olsen (1984) discuss the sizing and capacity utilization of a hydroelectric power system, when uncertainty in supply and demand are explicitly taken into consideration.

In a more general context, the quantification of hydrological uncertainty across water resource systems is a topic of extended research. This uncertainty either refers to the process of interest (in the particular case, streamflow) or the modelling procedure for extracting this process (e.g. through rainfall-runoff models). Regarding the first issue, hydrologists have long appreciated the usefulness of stochastic approaches and have applied them in a wide range of water resources applications, including the design and operation of hydropower systems (mainly large ones, comprising hydroelectric reservoirs). The most common use of stochastics is the generation of synthetic inflow data for the representation of all aspects of variability of streamflow and its statistical dependencies in space and time. The literature offers a plethora of models that reproduce the most important statistical characteristics of hydrological processes. Among many others, Koutsoyiannis (2000) proposed a framework for single- and multivariate simulation and forecasting problems in stochastic hydrology that allows for representing multiple persistence structures, while Tsoukalas *et al.* (2019) provided a flexible methodology for combining different stochastic models to represent any distribution and any dependence structure across any sequence of scales. The aforementioned methodologies have been implemented within time series generators, such as Castalia (Efstratiadis *et al.*, 2014) and the recently released AnySim package (Tsoukalas *et al.*, 2020).

Furthermore, the literature has also discussed the uncertainties induced by the use of hydrological models for representing the transformation of rainfall to runoff, when direct flow observations are limited or even missing. For instance, Vrugt *et al.* (2009) provided important advances in testing hydrologic theories, diagnosing structural errors in models, and appropriately benchmarking rainfall measurement devices by introducing a novel Markov Chain Monte Carlo (MCMC) sampler, entitled differential evolution adaptive Metropolis (DREAM). Sadegh *et al.* (2015) have used Bayesian inference with DREAM in the evaluation of

run-of-river hydroelectric plants, by proposing mathematical expressions of flow duration curves (FDC), coupled with uncertainty quantification.

A last issue of uncertainty involves the characteristics of hydraulic turbines, which are key component of hydropower systems. The experience so far reports many problems which degrade their condition and efficiency and require proper operation and maintenance. After only few years of operation, turbines can show significantly reduced performance due to various reasons such as cavitation, erosion, fatigue and material defects (cf. Kumar and Singal, 2015, also proposing methods for the effective maintenance of turbines). For this reason, the standard efficiency curves provided by the manufacturers may deviate significantly from the actual efficiency in the field, which is a major source of uncertainty affecting a wide range of applications, including performance assessment, real-time operation and power predictions. In this context, Abbas and Kumar (2019) mention that the total uncertainty in flow and efficiency measurements at the best efficiency point has been found to be the minimum one, when compared with other operating points.

4 Simulation problems in small hydropower plants: forward and inverse formulations

4.1 Input data and assumptions

The simulation problems in small hydropower plants are expressed either in forward or inverse mode. The forward simulation aims at estimating the energy produced by a system with given characteristics and given inflows. On the contrary, in the inverse simulation, the objective is to retrieve the overall input, i.e. the streamflow, for given system characteristics and given (observed) energy data.

Input data for the forward problem are:

- Streamflow upstream of the intake, Q;
- Gross head, H, expressed as the elevation difference between the forebay tank and the outlet level, which is practically constant;
- Geometrical and hydraulic characteristics of the penstock, which allow for estimating the hydraulic losses, h_L (section 4.3);
- Maximum discharge that can pass from the turbines, Q_{max}, which is also referred to as nominal flow;
- Minimum discharge for energy production, Q_{min}, which depends on the turbine type and is typically expressed as fraction of nominal flow, i.e. $Q_{min} = a \, Q_{max}$;
- Power plant efficiency, η, which is typically expressed as function of rated flow, Q/Q_{max} (section 4.4).

The nominal flow is associated with the power capacity of the plant, P_{max}, given that for $Q/Q_{max} = 1$ the efficiency is maximized. Under this premise we get:

$$Q_{max} = \frac{P_{max}}{\gamma \, \eta_{max} \, H_n} \tag{4.1}$$

We remark that the above relationship includes the net head term, H_n, which is function of Q_{max}. In this respect the formula cannot be solved explicitly, thus in the context of preliminary calculations, we can omit hydraulic losses and thus substitute H_n by the gross head, H. This approximation is valid only in case of large heads and penstocks with minimal losses. A more elegant approach, which is specific case of the inverse problem, is discussed in section 4.6.

It is important to remark that both problem configurations (forward, inverse) are subject to measurement errors and uncertainties that span over all elements of the governing formulas, and they are transferred to the simulated outputs. Herein we present the model formulation in deterministic terms, i.e. without accounting for uncertainties. In next chapter we will provide a more integrated approach, emphasized to the inverse problem, to allow embedding different sources of uncertainty within calculations.

4.2 The forward problem: converting discharge to hydroelectric energy

Let Q be the streamflow arriving at the intake of a RoR plant. The flow passing through the turbines is restricted by the discharge capacity Q_{max}, i.e.:

$$Q_T = \min(Q, Q_{max}) \tag{4.2}$$

If the flow is less than its minimum operational limit, the turbine efficiency is practically zero thus any anergy is produced. On the other hand, provided that $Q_T > Q_{min}$, the energy production rate, i.e. the power, is calculated by the relationship:

$$P = \eta(Q_T)\gamma\, Q_T\, H_n(Q_T) \tag{4.3}$$

where:

η is the power plant efficiency, expressed as function of discharge;

γ is the specific weight of water (9.81 KN/m^3);

Q_T is the flow passing through the turbines (m^3/s);

H_n is the net head, i.e. the constant gross head, H, after subtracting the flow-dependent hydraulic losses, h_L (m).

The estimated power production from the above relationship is approximative because of the input uncertainties (flow data) and the internal uncertainties of the system, i.e. in the power plant efficiency as well as in H_n. Hydraulic losses include friction and local ones, which are function of discharge and the penstock properties (roughness, length, diameter, geometrical transitions). Large hydroelectric reservoirs allow for controlling outflows; thus their turbines are normally working with the nominal flow, which maximizes efficiency. In contrast, SHPPs are operating with any flow conditions, where η is strongly varying across the feasible flow range (Q_{min}, Q_{max}).

The energy production during a time interval [t$_1$,t$_2$] is the integral of power, i.e.

$$E = \int_{t1}^{t2} P(t)dt \tag{4.4}$$

Also, assuming constant efficiency and net head, we get the following formula, expressing the energy produced over a specific time interval:

$$E = \eta\,\gamma\,V\,H_n \tag{4.5}$$

where V is the water volume passing the turbines during this time interval (m^3), and E is the energy, expressed in Joules.

4.3 Estimation of hydraulic losses

Gross head reduction is due to frictional losses across the penstock, as well as local energy losses that occur at all changes of the flow geometry. For given discharge, Q, and pipe diameter D, the flow velocity is given by:

$$V = \frac{4Q}{\pi D^2} \qquad (4.6)$$

For the above flow characteristics, the energy gradient J across the pipe is typically estimated by the so-called Darcy-Weisbach formula:

$$J = f \frac{1}{D} \frac{V^2}{2g} \qquad (4.7)$$

where f is a (dimensionless) friction factor. The latter is given by the Colebrook–White equation:

$$\frac{1}{\sqrt{f}} = -2 \log\left(\frac{\varepsilon}{3.7D} + \frac{2.51}{Re \sqrt{f}}\right) \qquad (4.8)$$

where $Re := V D/v$ is the *Reynolds number* and ε/D is the *relative roughness*, which are both dimensionless quantities, whereas ε is the absolute (surface) roughness of the specific pipe and v is the kinematic viscosity of water, which is function of temperature; e.g., for $T = 15$ °C, $v = 1.1 \times 10^{-6}$ m²/s.

For a pipe of length, L, and by considering steady uniform flow with discharge Q and diameter D, the *friction losses*, which are generally the main component of the total hydraulic losses, are given by:

$$h_f = fL \frac{8Q^2}{\pi g D^5} \qquad (4.9)$$

Due to the complexity of friction loss calculations through eq. (4.9), a number of simplified formulas have been developed in the literature (e.g., the Hazen-Williams expression), which are yet noticeably less accurate than the Darcy-Weisbach equation. A more consistent and accurate approximation is offered by the so-called *generalized Manning equation*, introduced by Koutsoyiannis (2008):

$$J = \left(\frac{4^{3+\beta} N^2 Q^2}{\pi^2 D^{5+\beta}}\right)^{1/(1+\gamma)} \qquad (4.10)$$

where β, γ and N are coefficients depending on roughness, for which Koutsoyiannis (2008) provides analytical expressions that are valid for specific velocity and diameter ranges. In particular, for large diameters (i.e., $D > 1$ m) and velocities (i.e., $V > 1$ m/s) that are typically applied in hydropower systems, we get:

33

$$\beta = 0.25 + 0.0006\varepsilon_* + \frac{0.024}{1 + 7.2\varepsilon_*}, \gamma = \frac{0.083}{1 + 0.42\varepsilon_*},$$

(4.11)

$$N = 0.00757(1 + 2.47\varepsilon_*)^{0.14}$$

where $\varepsilon_* := \varepsilon/\varepsilon_0$ is the so-called normalized roughness and $\varepsilon_0 := (v^2/g)^{1/3}$ = 0.05 mm, for temperature 15 °C.

The roughness coefficient, ε, is a characteristic hydraulic property of the pipe, mainly depending on the pipe material and age, where aging depends on the water quality. For design purposes, it is recommended to apply quite large roughness values, e.g. $\varepsilon = 1$ mm, in order to account for all above factors at the end of time life of the penstock. For the above value, we get ε_* = 1/0.05 = 20, and thus β = 0.262, γ = 0.009, and N = 0.0131.

On the other hand, local, also referred to as *minor hydraulic losses*, are occurring at every change of geometry (transition) and thus change of flow conditions (e.g. flow entrance through the intake, change of diameter, flow split, elbow, etc.). Each individual loss is generally estimated by:

$$h_{\text{L}} = k\frac{V^2}{2g}$$

(4.12)

where k is a dimensionless coefficient, depending on transition geometry. Classical hydraulic engineering handbooks (e.g., Roberson *et al.*, 1998) provide analytical relationships, empirical formulas and nomographs for estimating k as function of local geometrical characteristics, (e.g., ratio of upstream to downstream diameter).

Typical values that are applied in hydroelectric systems are:

- Intakes: k = 0.04
- Grids: k = 0.10-0.15
- Contractions: k = 0.08
- Elbows: k = 0.10
- Valves, fully open: k = 0.10-0.20
- Outflow to tailrace: k = 1

In preliminary design studies, local loss calculations can be generally omitted, since the geometrical details are not yet specified, or they are roughly estimated, by considering an aggregate value of k for all types of local losses. We remark that in case of reaction turbines (e.g. Francis, Kaplan), the outflow is by definition made under pressure through the draft tube to an open channel, thus the value k = 1 should always be applied. This case does not stand for Pelton turbines.

4.4 Estimation of efficiency

The total efficiency of a hydropower plant can be dissolved in four several factors as below:

$$\eta = \eta_T \, \eta_E \, \eta_{TR} \, \eta_G \qquad (4.13)$$

where:

η_T is the efficiency of the turbines;

η_G is the efficiency of the generator;

η_{TR} is the efficiency of the transformer;

η_E is the efficiency of the transmission lines;

Typical values for the three latter are 0.96, 0.98 and 0.98, respectively.

The power plant efficiency depends on the turbine types and the overall configuration of the hydroelectric power plant. This factor not only is crucial at the design stage but also in the operation of the power plant. Although in preliminary design and management studies efficiency is considered constant, it is actually function of head and flow. Both are varying, mainly due to fluctuations of the upstream level (case of hydroelectric reservoirs, where turbine flows are well-controllable) or due to the inherent variability of the flows captured by small hydropower plants.

The turbine efficiency, η_T, for specific dimensions (e.g., diameter runner) is usually expressed by means of nomographs as percentage of rated flow, Q_T/Q_{max} (Anagnostopoulos & Papantonis, 2003). **Figure 4.1** illustrates typical performance curves for turbines that are applied in small hydroelectric plants. We observe that the curves change significantly with turbine type and sizes. Other important issue is that there is a particular flow rate for which the turbine efficiency is maximized; this peak is practically achieved at the nominal discharge. It is worthy commendable that after years of operation the efficiency curves change.

We remark that the flow-efficiency nomographs are provided by the turbine manufacturer and they are obtained by data extrapolation from a reduced scale model. Since it is not possible to exactly preserve dynamical, geometrical, and kinematical similarity between the model and the prototype, it is also not possible to precisely estimate the efficiency. Although empirical corrections are employed to better reflect the prototype performance, actual efficiency is unknown, since it also depends on constructive and operational characteristics of the power plant, as well as changes due to deterioration, damage and aging of the equipment over time (Paish, 2002). In general, efficiency increases with scale, i.e. discharge and turbine Pelton, Crossflow and Kaplan machines retain high efficiency even when running below their design flow. In contrast, the efficiency of Francis turbines falls away sharply if run at below half its normal flow.
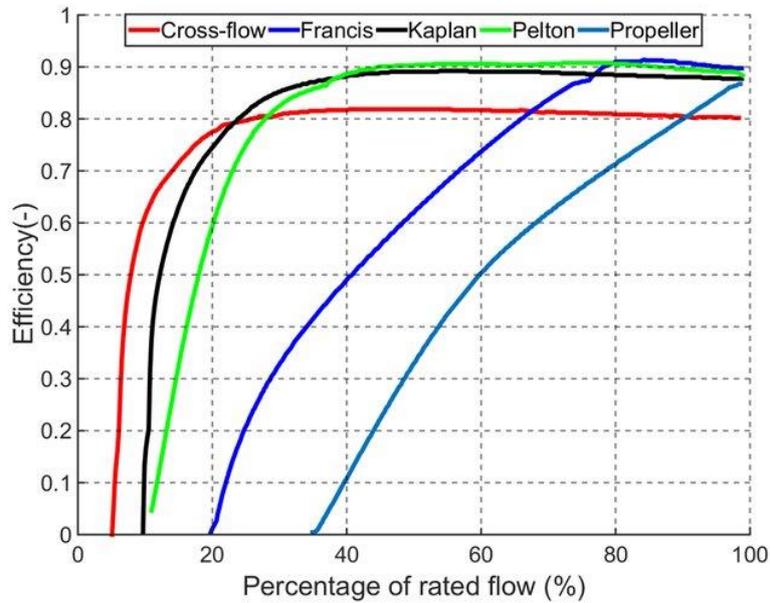
Figure 4.1: Typical efficiency curves for turbines applied in SHPPs.

In the present study, we investigate the performance of two commonly used turbines, namely Francis and Pelton. The Francis turbine belongs to the group of reaction turbines, and use the force exerted by the water to rotate the runner inside the turbine, in a way similar to how the engines of an airplane create trust. Reaction turbines exhibit a rather poor efficiency at low flows despite their relatively high specific speeds. As for the Pelton turbine, it is the typical case of impulse machines and its strong advantage over the Francis turbine is the approximately stable efficiency for quite a large range of flows.

As shown in the graph, between Pelton and Francis efficiency curves, the latter not only depends on the specific speed but also its efficiency varies from 0.08 to 0.96, thus making energy calculations very sensitive against errors induced by uncertain efficiency curves. Due to Francis efficiency variance, it is appropriate to approach the efficiency curve in stochastic terms. On the contrary, the Pelton's efficiency varies from 0.65 to 0.89.

4.5   The mixing of turbines

It is quite common that a small hydropower plant is equipped with more than one parallel turbines and the total flow is separated, as illustrated in the flowchart of **Figure 4.2**. Therefore, it is necessary to extend this procedure for the case of turbine mixing. The main difficulty in this problem is the consideration of the way these turbines operate. As mentioned in Chapter 3, many experts consider the problem of optimal mixing, generally involving the implementation of two turbines of the same or different type, which operate at different flow ranges in order to capture as much as more wide range of the flow variability. In general, there are two ways to define the operation of turbines:

- hierarchical operation, by assigning a master turbine and an auxiliary one, symbolized A and B, respectively;
- combined operation, where the sharing of flows is derived through optimization.

36

If the turbines are set in a specific priority order, the simulation problem is quite simple, because turbine A is systematically utilized up to its nominal discharge. The remaining flow passes through the turbine B, until reaching the nominal discharge of B, thus the surplus flow is spilling through the weir. The above policy is the simplest one, but not the overall optimal, because of the nonlinearities induced by the efficiency curves of turbines. In a more rigorous optimization context, the operation of two turbines accounts for the maximization of the combined efficiency of the system across all feasible flows, which ensures the maximum energy production. There are a lot of ways to separate the total inflow, on the basis of operation rules that account for different percentages for each turbine across different periods of operation.
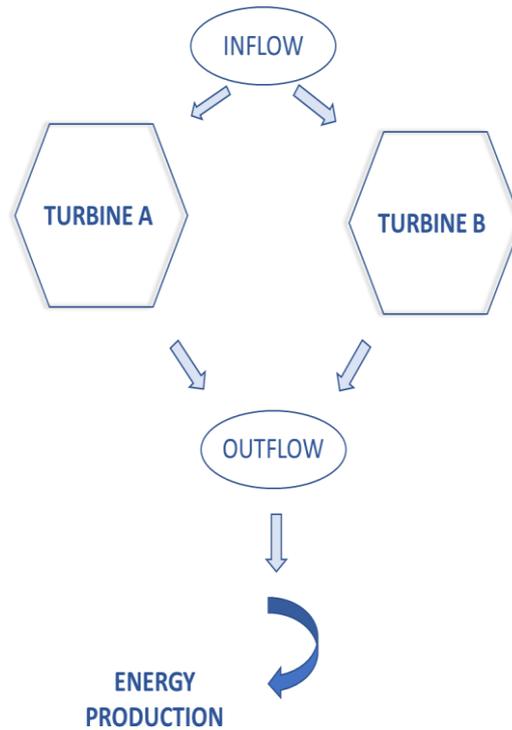

Figure 4.2: Operation of turbines in case of mixing.

4.6   The inverse problem: retrieving discharge from energy

In the inverse problem, we consider a given power production P, and solve for the flow that passes through the turbines, Q_T, which is calculated by:

$$Q_T = \frac{P}{\gamma \, \eta(Q_T) \, H_n(Q_T)}$$

(4.14)

The flow that passes through the turbines, inside of the range of operation of SHPPs, can be estimated through an iterative numerical scheme, accounting for nonlinearities induced by efficiency and net head formulas, $\eta(Q)$ and $H_n(Q)$. Details on the numerical procedure and its convergence properties are discussed in section 5.3.1.

Since, the turbines operate only in a certain range of flow, the power production fluctuates between zero and its maximum value, i.e. the installed power capacity, P_{max}. If the power production is zero, then we know that the streamflow is below the minimum discharge of turbines, Q_{min}, but we cannot retrieve its exact value. On the contrary, when the system produces its power capacity, we known that the streamflow certainly exceeds the nominal discharge, Q_{max}, yet its exact value is again unknown. Therefore, in contrast to the forward problem, for which we can extract the full time series of power production from a given streamflow sample, the inverse problem is not well-posed, since for a given power time series only part of the corresponding streamflow set can be retrieved.
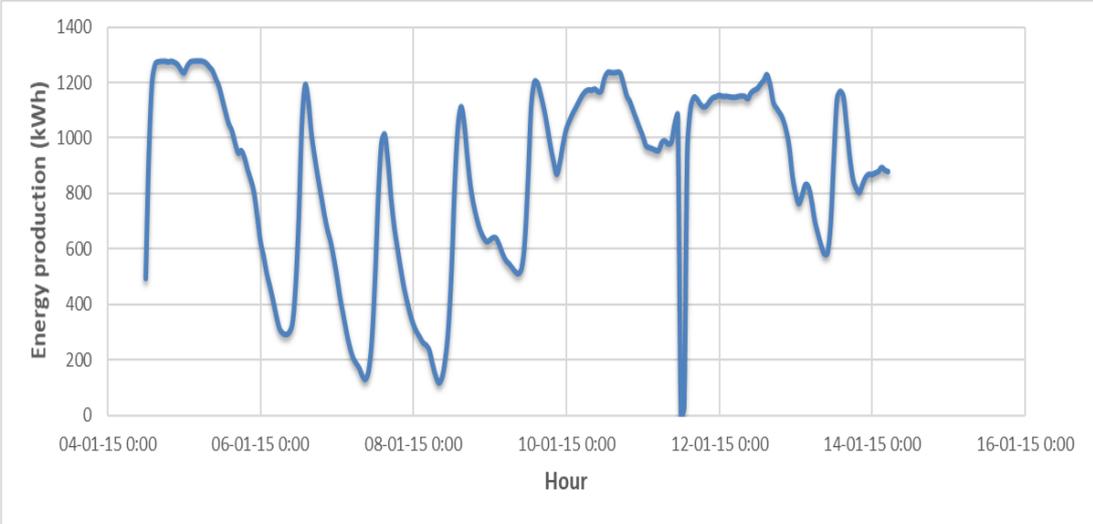

Figure 4.3: Example of hourly energy production time series (data derived from Glafkos plant, for a period of 10 days).
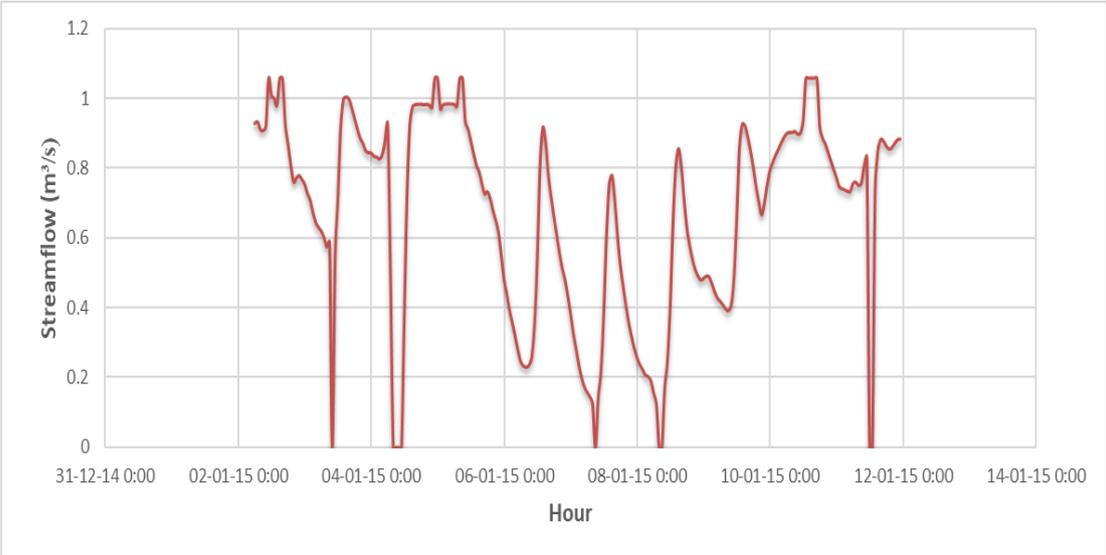

Figure 4.4: Example of extracting hourly streamflow time series from energy (data derived from Glafkos plant, for a period of 10 days).

4.7 The inverse problem in calibration setting: retrieving system properties from discharge and energy

Except from retrieving discharge from hydropower, another expression of the inverse problem involves the extraction of internal properties of the system through calibration, i.e. for given input (streamflow) and output (energy) data. This involves system components that are associated with energy conversions, both across the conveyance system (e.g., penstock roughness) as well as the mechanical equipment (efficiency of turbines and transformers). We remark that all these characteristics are not measured in the field, thus they are subject to uncertainties. The most crucial and at the same time interesting calibration problem is the extraction of efficiency curves. In Chapter 5 we also discuss a framework to optimize the efficiency curves by using an analytical parametric formula, which inspired by the Kumaraswamy distribution model.

5 Stochastic modelling framework for extracting streamflow time series from SHPP's energy data

5.1 Rationale and objectives

This chapter discusses the modeling framework that has been developed in this thesis. As mentioned before, the goal of our research is to extract the streamflow arriving at the inlet of a SHPP from energy production data, and evaluate its uncertainty. The data processing and the computational implementation of models, which will be described in this chapter, are done by using the MATLAB software. The code snippets as well as related comments are provided in Chapter 6.

Our rationale originates from the fact that in the case of small hydropower plant design and simulation, several components of water-energy transformations are handled as *constant* and *certain* quantities, while they are actually varying and uncertain. More precisely:

In the context of preliminary design of small hydropower plants, the main objective is the estimation of energy production from discharge. In this respect, crucial elements of the forward formula for the estimation of energy, such as net head and efficiency, are usually considered as constants. Similar approaches are also employed is common optimization studies (i.e. sizing of penstocks and turbines), where efficiency and net head are handled as constants. On the contrary, the formulas and procedures that are proposed in this study consider that efficiency and net head are not constant but they depend on the flow that passes through the turbines.

Furthermore, the usual practice to face both the forward and the inverse energy problems in a SHPP are handled as fully deterministic. Apparently, for a given discharge we can easily extract the power production, and vice versa, if the system properties are known. However, in real world studies the available data from a SHPP's operation may be quite limited or/and unreliable. It is a fact that the design of a hydroelectric power plant differs from its actual operation. This difference arises due to multiple uncertainties and errors both in design and operation. In the real-world there are several potential sources of uncertainty, such as the power data, hydraulic calculation, and flow-efficiency relationship.

In this research, we focus to two key uncertain issues, in particular the observed output (energy production), and the efficiency curve of turbines. As for the hydraulic calculations, uncertainties refer to parameters that are associated with friction and minor losses, e.g. the roughness coefficient, which also changes with time. Nevertheless, these errors affect the net head estimations, thus they become less important as the gross head increases, which is the typical case in run-of-river plants.

5.2 Model overview

As shown in **Figure 5.1**, the inverse problem in stochastic setting is posed as follows: First, we estimate the flow time series that passes from the turbines, through an iterative numerical scheme, using the energy production data. We highlight that this only involves part of the full hydrograph between the minimum and maximum (nominal) operational discharge of the system; the full streamflow data also comprises higher and lower values, which are estimated

in a different, semi-empirical manner (see sections 5.5.2 and 5.5.3, respectively). The next step is the comparison with the observed streamflow data. Following this, it is essential of express the model residuals through an error function, extract their statistical characteristics and fitting a suitable distribution, e.g. Gamma. After this, we generate *m* synthetic error realizations and the associated discharge ensembles. The latter are used to extract typical uncertainty metrics of the modelled flows, such as expected vales and confidence intervals.
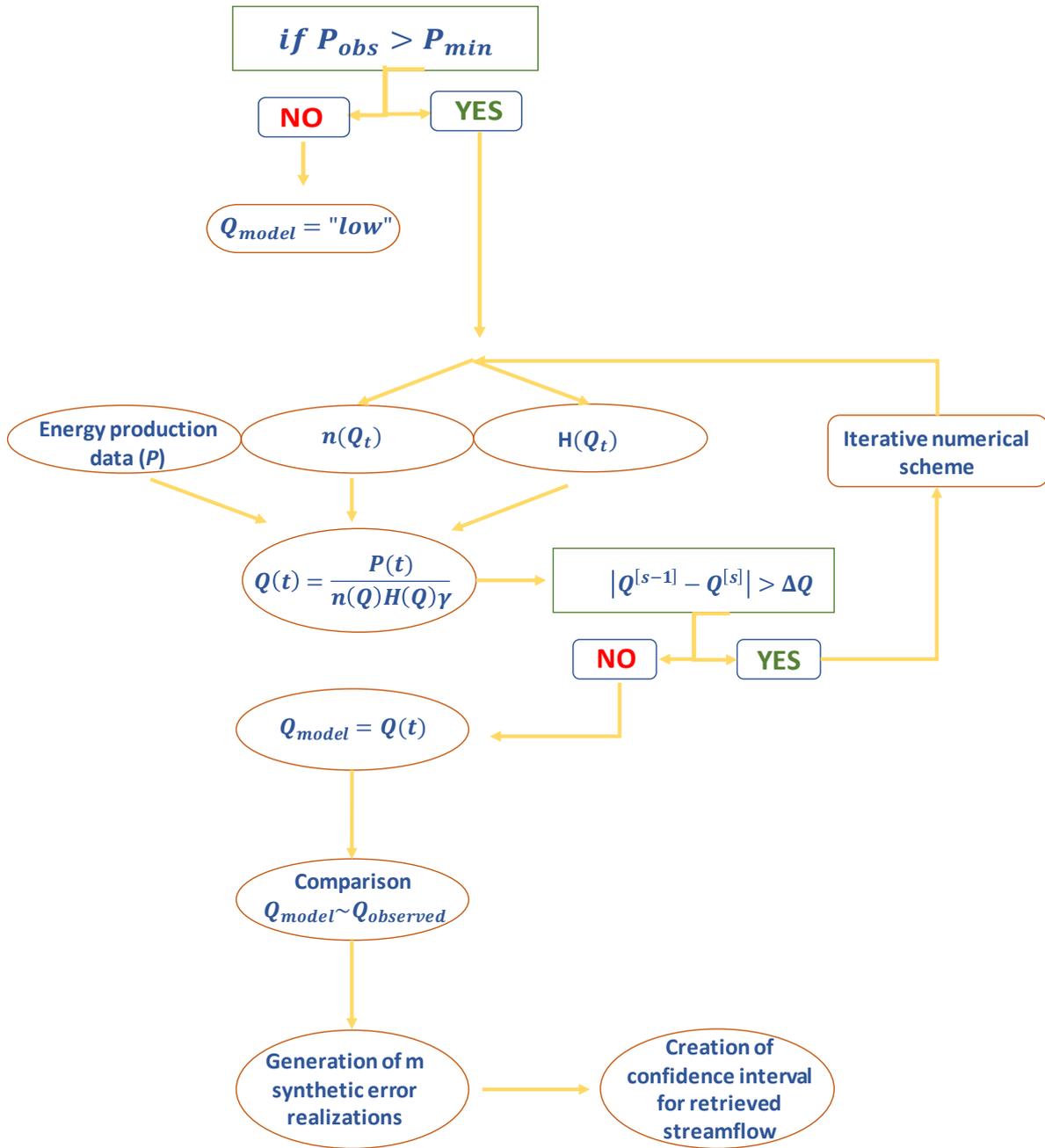
Figure 5.1: Flowchart of proposed model.

5.3   The inverse problem under uncertainty

The proposed model estimates the flow that passes through the turbines for a given value of energy production, while its deviation from the observed flow is handled as an error term that follows a specific distribution and has a specific autocorrelation structure. Herein we will use the Gamma distribution and express errors through a first-order autocorrelation model, but this can be generalized for any stochastic model. In this respect, the retrieved streamflow is expressed in stochastic terms, as the unique means for consistent quantification of uncertainty, thus allowing to express the overall uncertainties of the inverse transformation in typical statistical terms (e.g. marginal statistics and confidence intervals).

5.3.1   Numerical procedure

Firstly, it is necessary to check whether the flow passing through the turbines, Q_T, equals the input streamflow, Q, which is true only when the power production, P, is positive and less than P_{max}. The following cases arise:

- If $P = 0$ then $Q \leq Q_{min}$ (any energy is produced, since the streamflow arriving at the turbines is less than the minimum operational value);
- If $P = P_{max}$ then $Q \geq Q_{max}$ (the streamflow exceeds the nominal discharge of turbines, and the surplus quantity spills over the weir);
- If $0 < P < P_{max}$ then $Q = Q_T$

In the last case, we compute the turbine flow for time step t = 1, …, n by using the deterministic inverse formula $Q_T = f(P)$, which is expressed in the following recursive form:

$$Q_T^{[s+1]} = \frac{P}{\gamma \, \eta \left(Q_T^{[s]} \right) H_n \left(Q_T^{[s]} \right)}$$

(5.1)

where s is an iteration counter. For every time step, the above relationship is repeated until the flow converges. To run the formula, an initial flow value is assigned, typically the last known value of the simulated data. This iterative scheme usually converges after three repetitions. The upper limit in order to terminate this procedure is expressed in terms of absolute difference between subsequent flow values, ΔQ:

$$Q_T^{[s-1]} - Q_T^{[s]} > \Delta Q$$

(5.2)

If the above statement is true, then the relationship (5.1) is re-employed for $s + 1$, until (5.2) becomes false.

5.3.2   Stochastic modelling of errors

Apparently, in a real-world study, the flows extracted from energy data will deviate from actual ones, due to errors and uncertainties that appear in all components of the flow-energy transformation procedure. These involve energy data, internal properties and assumptions regarding the hydraulic and electromechanical equipment (penstock, turbines, generator, transformer), and even minor errors due to imperfect convergence of eq. (5.2). All these are

transferred as model errors i.e. deviations of simulated from actual flow data (also referred to as *residuals*).

Following this, it's crucial to investigate the way to express the model residuals, i.e. the discharge errors for each time step. In this research, three formulas are examined (Efstratiadis *et al.*, 2015):

$$w_t = Q_{T,t} - Q_{obs,t} \tag{5.3}$$

$$w_t = \frac{Q_{T,t} - Q_{obs,t}}{Q_{obs,t}} \tag{5.4}$$

$$w_t = \ln(Q_{T,t}) - \ln(Q_{obs,t}) \tag{5.5}$$

Although an ideal model error should follow the white noise properties, thus being homoscedastic and uncorrelated both in "space" (correlation with the parent process, e.g., flow) and time, in the real world we cannot avoid the existence of dependencies. In this respect, for the generic case we should represent the error through a *stochastic model*, not simply a statistical one.

The formulation of the stochastic model for residuals requires the computation of their marginal statistical characteristics and dependence properties, such as the mean, variance, skewness, autocorrelation, and the cross-correlation between the observed flows $Q_{obs,t}$ and the error data w_t. If the autocorrelations are large, it is suggested to use a stochastic model that allows to describe the dependence structure of the error process. In our analyses, the representation and synthesis of model residuals w_t is employed through a first order autoregressive (Markov) model, AR(1) as:

$$w_t = \varphi\, w_{t-1} + z_t \tag{5.6}$$

where w_t is the error process, with mean μ, standard deviation σ, skewness γ, and lag-1 autocorrelation coefficient ρ; $\varphi = \rho$ is the first order autoregression coefficient; and z_t is an i.i.d. process (white noise) with mean μ_z, standard deviation σ_z and skewness coefficient γ_z. The statistical characteristics of the white noise z_t are related with those of w_t by:

$$\mu_z = \mu_w (1 - \varphi) \tag{5.7}$$

$$\sigma_z = \sigma_w \sqrt{1 - \varphi^2} \tag{5.8}$$

$$\gamma_z = \gamma_w \frac{1 - \varphi^3}{(1 - \varphi^2)^{3/2}} \tag{5.9}$$

The next step is the generation of *m* synthetic error realizations ("ensembles"), by using the Gamma distribution. The Gamma distribution can be parameterized in terms of a shape parameter $a = k$ and an inverse scale parameter $b = 1/\theta$, called a rate parameter. A random variable X that is gamma-distributed with shape a and rate b is denoted. The corresponding probability density function (PDF) in the shape-rate parametrization is:

$$f(x) = \frac{\lambda^{\kappa}}{\Gamma(a)}(x-c)^{k-1}e^{-\lambda(x-c)}, x \geq 0 \; a > 0 \tag{5.10}$$

where $\Gamma(\alpha)$ is the gamma function

$$\Gamma(\alpha) = \int_0^{\infty} y^{a-1}\,e^{-iy}dy \tag{5.11}$$

The distribution's parameters are given by:

$$\kappa = \frac{4}{\xi_x^2} \tag{5.12}$$

$$\lambda = \frac{\sqrt{\kappa}}{s_x} \tag{5.13}$$

$$c = \mu_x - \frac{\kappa}{\lambda} \tag{5.14}$$

where μ_x is the mean, s_x is the standard deviation and ξ_x the skewness of the sample. In this case μ_x, s_x, ξ_x are the statistical characteristics of the residuals. The location parameter c allows for the better fitting of data, particularly when the latter is bounded (e.g., in the case of non-negative processes).

The Gamma distribution defined by the above relationships represents random processes that are always positively asymmetric. If the coefficient of asymmetry ξ_x is negative, the parameters are calculated as below:

$$\kappa = \frac{-4}{\xi_x^2} \tag{5.15}$$

$$\lambda = \frac{\sqrt{\kappa}}{s_x} \tag{5.16}$$

$$c = -\mu_x + \frac{\kappa}{\lambda} \tag{5.17}$$

For the generation of random numbers that follow a negatively-asymmetric gamma distribution, we can use the same generators as before, by setting $\kappa = |\kappa|$ and change the sign of the final result.

5.3.3 Generation of flow ensembles and uncertainty assessment

The stochastic model runs to generate m sets of synthetic error realizations $w_{j,t}$ (also referred to as *ensembles*) for the same time horizon n with the observed flow data. The number of ensembles should be large enough to allow for describing the model uncertainty as much as more accurately (in our analyses we generate 100 ensembles). These are next used to get the associated discharge scenarios (turbine flows) for each ensemble $j = 1, \dots, m$ by employing the appropriate inverse transformation for each error expression, i.e.

$$Q_{T,j,t} = f(P_t) + w_{j,t} \tag{5.18}$$

$$Q_{T,j,t} = \exp[f(P_t)] + w_{j,t} \tag{5.19}$$

$$Q_{T,j,t} = f(P_t)\, w_{j,t} \tag{5.20}$$

The quantification of uncertainty for each time step t is employed by estimating the statistical characteristics of the corresponding sample of synthetic flow values $Q_{T,j,t}$. The latter are empirically expressed in terms of quantiles, e.g. median. In this respect, we also provide confidence intervals based on empirical estimation of two characteristic quantiles (low, high) for each time step t, for a given confidence level (the latter describes the uncertainty of a sampling method). It is necessary to select a confidence level γ, such as 90, 95, or 99%; but any percentage can be used, depending on the size of sample, i.e. the number of ensembles, m. In this respect, for each time step we create the upper and lower limits of the confidence interval using the following functions:

$$Q_{upper} = Q_{(1+\gamma)/2} \tag{5.21}$$

$$Q_{lower} = Q_{(1-\gamma)/2} \tag{5.22}$$

where the subscript denotes the quantile of simulated flow values for each specific time step. For instance, for $m = 100$ and $\gamma = 90\%$, the confidence limits are captured by the 5th larger and 5th smaller flow value, and they are generally not symmetric with respect to the median.

5.4   Parametric model for deriving efficiency curves

The efficiency-discharge relationship can be well approximated by the following analytical formula, inspired by the generalized probability density function proposed by Kumaraswamy (1980). In probability theory and statistics, the Kumaraswamy's double bounded distribution is a family of continuous probability distribution functions defined in the interval (0, 1). The probability density function of the distribution, without considering any inflation, is:

$$f(x; a; b) = abx^{a-1}(1 - x^a)(1 - x^a)^{b-1} \tag{5.23}$$

Easily, we can extract the cumulative distribution function:

$$F(x; a; b) = 1 - (1 - x^a)^b \tag{5.24}$$

where a and b are non-negative shape parameters.

In its simplest form, the distribution takes values in the interval (0, 1). In a more general form, the normalized variable x is replaced by the unshifted and unscaled variable z, where:

$$x = \frac{z - z_{min}}{z_{max} - z_{min}}, \ z_{min} \leq z \leq z_{max} \tag{5.25}$$

For different values of a and b the Kumaraswamy distribution formula creates a wide range of curve shapes that may fit to multiple function types, such as power, exponential, logarithmic, sigmoid, logistic, etc. (**Figure 5.2**). In this respect, an analytical formula for turbine efficiency nomographs can also be well-approximated by the Kumaraswamy function. By turning its two shape parameters, we can fit the model to any empirically derived curve, thus significantly facilitating calculations.
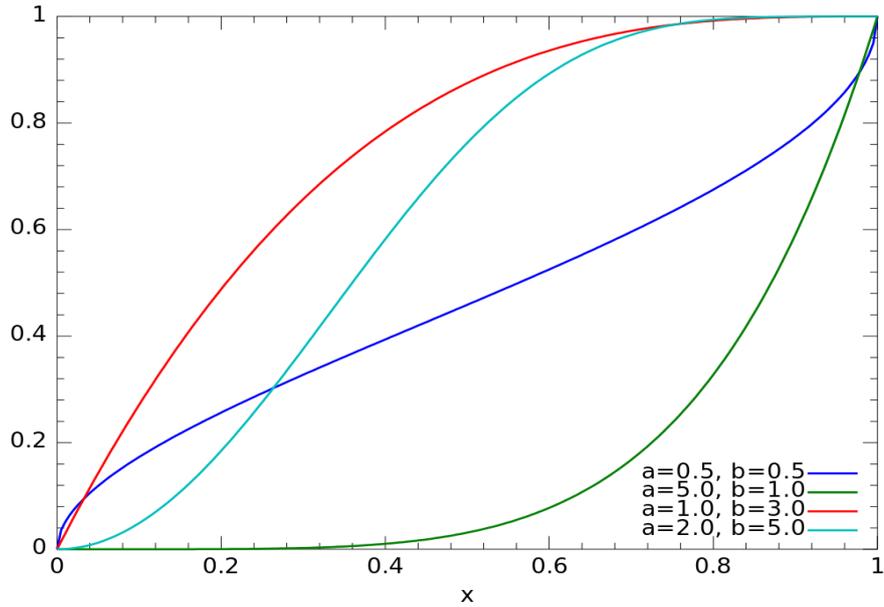
Figure 5.2: Plots of Kumaraswamy function for different values of shape parameters *a* and *b* (Wikipedia, 2020).

Under this premise, the generic efficiency-discharge relationship can be approximated by the following analytical formula:

$$n = n_{min} + \left(1 - \left(1 - \left(\frac{Q - Q_{min}}{Q_{max} - Q_{min}}\right)^{a}\right)^{b}\right)(n_{max} - n_{min}) \tag{5.26}$$

This formula uses a dimensionless expression of discharge, based on Q_{min} and Q_{max}, two efficiency limits, n_{min} and n_{max}, and the two shape parameters, *a* and *b.* We remark that the above formula has in fact four free parameters, since for a given power capacity P, and after empoying an iterative procedure as described in section 5.3.1, we get:

$$Q_{max} = \frac{P}{\gamma \, \eta_{max} \, H_n(Q_{max})} \tag{5.27}$$

$$Q_{min} = \frac{P}{\gamma \, \eta_{min} \, H_n(Q_{min})} \tag{5.28}$$

Figure 5.3 illustrates different efficiency curves which are extracted from the analytical formulas, as described before. This formula allows to shape the efficiency curve by changing the parameters *a, b,* n_{min}, n_{max}. This change is not just about the limits to which the curve fluctuates (n_{min}, n_{max}), but also is concerned about the camber and generally the way this curve reaches n_{max}. The procedure for efficiency curve construction presented here is rather simple and generic. Its main advantage is that it is transparent and allows for reaching almost perfect accuracy, depending on the data quality and knowledge about the turbine characteristics. It is essential to remark that since the nomographs typically refer to the turbine efficiency, for the extraction of total efficiency we should also account for additional energy losses in the generator and the transformer. Typically, an overall correction is employed, by multiplying the data by a constant value that may range from 0.88 to 0.97 (Anagnostopoulos, I., personal communication, 2020).

We should also highlight that using the empirical nomographs is a usual practice, and most of times effective, at least for preliminary design purposes. However, the uncertainties, which arise in the real-world operation of hydropower plants make these nomographs obsolete. In the case study of Chapter 8 (Glafkos power plant), this consideration will be verified. In this context, another major advantage of the proposed approach is the opportunity for expressing efficiency under uncertainty, by considering the four model parameters as random variables that follow a known distribution function. Furthermore, by considering these parameters as unknown, we can establish a calibration framework, to extract efficiency curves from given power and turbine flow data (cf. Hidalgo *et al.*).
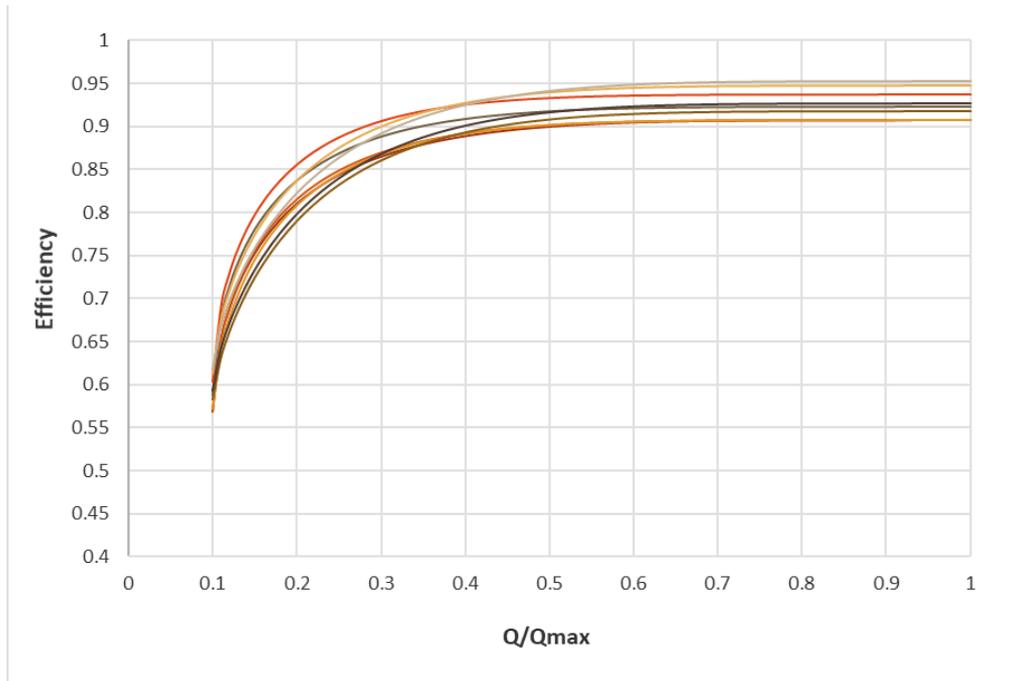
Figure 5.3: Example of randomly generated efficiency curves.

5.5   Extrapolation outside the operational flow limits

5.5.1   Problem setting

As mentioned in the Chapter 4, the proposed methodology for the inverse problem extracts only discharges, which range between Q_{min} and Q_{max}. Actually, the methodology, that will be described, completes the missing data by extrapolating the simulated turbine flows outside this range, thus obtaining the upper and lower part of the hydrograph that cannot be extracted from the inverse problem. We remind that the maximum discharge that can pass from the turbines, also named the nominal flow, is the upper limit that we can extract from the energy production data. Following this, the minimum discharge that can pass from the turbines, which is typically the 10-30% of the nominal flow (depends on turbine type), is the lower limit we can extract from energy. When the power production is zero, then the flow is under the lower limit, Q_{min}. On the contrary, when the system produces its power capacity, then the flow is over or equal with its nominal discharge, Q_{max}.

47

In order to determine the extrapolation procedure, it is necessary to mention our two basic principles:

- the rising limb follows a linearly increasing function;
- the falling limb follows a negative exponential recession function.

Moreover, the extrapolation is made by linking the two last known discharge values both for the rising and falling limbs. As before, the approach is not deterministic, since the extrapolation procedure is employed for all synthetically-generated flow ensembles, thus also obtaining ensembles of the full streamflow process. In this vein, confidence intervals are created for low and high periods, which are outside of the range of operation of a SHPP.

Subsequently, the extrapolation of the hydrograph for high and low flows is crucial for the real-time operation of a small hydropower plant. Particularly for high flows, this extrapolation allows not also the estimation of the peak flows, but also the recession rate that is representative of the flood propagation over the basin. Furthermore, the knowledge of last flow values is essential for short-term planning purposes, involving the prediction of expected energy on the basis of discharge forecasting scenarios. Preliminary ideas on this topic of major importance have been recently demonstrated in a research work presented in the General Assembly of the European Geosciences Union (Sakki *et al.*, 2020).

5.5.2   High flows

The flood flows upper the discharge capacity, Q_{max}, that arrive at the inlet of a small hydropower plant as well as the flood duration are essential elements of its operation, during which the surplus inflow spills over the weir. Their estimation is based on the extrapolation of the rising and falling limb of the flood hydrograph, for a given sequence of known turbine flow values little before and little after the operation of turbines in their maximum capacity, respectively. We remind that the computation of turbine flows is made by using the deterministic inverse formula, which allows us to extract the "intermediate" discharge values within the range (Q_{min}, Q_{max}).

For the rising limb we employ a linear extrapolation, while for the falling limb we consider an exponential extrapolation. Both are reasonable assumptions, justified by empirical evidence worldwide, and also validated by recent research aiming at the development of dynamic unit hydrographs (Michailidi, 2018).

Let Q_{t-2} and Q_{t-1} be the last known turbine flow values that are extracted from the inverse formula during the operation of the power station below its capacity, and Δt is a unit time interval (since t is a time index, not a time variable). In order to approximate and eventually extrapolate the hydrograph forward, it is required to compute the slope of the linear rising limb, which is:

$$\varphi = \frac{Q_{t-1} - Q_{t-2}}{\Delta t} \tag{5.29}$$

Any forward discharge value is calculated by using the relationship:

$$Q_t = max(Q_{max}, Q_{t-1} + \varphi \, t) \tag{5.30}$$

The above formula ensures that all estimated flow values in the rising limb will exceed the nominal flow, Q_{max}, otherwise they are manually set equal to Q_{max}.

As for the falling limb, the extrapolation is employed backwards, following a negative exponential law, based on the well-known linear reservoir approach, which is a simple yet effective model for describing recession phenomena, e.g. low flows through the groundwater zone (Risva *et al.*, 2018). Under this assumption, any discharge value after a given peak flow, Q_0, can be calculated by using the relationship below:

$$Q_t = Q_0 \exp(-kt) \tag{5.31}$$

where k is a recession parameter. For a known pair of subsequent turbine flow values t steps after the peak, i.e. Q_{t+1} and Q_{t+2}, the characteristic properties of the falling limb k and Q_0 are extracted by solving the system:

$$Q_{t+1} = Q_0 \exp(-k(t+1)) \tag{5.32}$$

$$Q_{t+2} = Q_0 \exp(-k(t+2)) \tag{5.33}$$

from which we get:

$$k = ln\left(\frac{Q_{t+1}}{Q_{t+2}}\right) \tag{5.34}$$

Apparently, the intercept point of the two extrapolations (forward linear and backward exponential) is the estimator of the peak discharge. In general, this occurs in an intermediate time between two subsequent time indices.
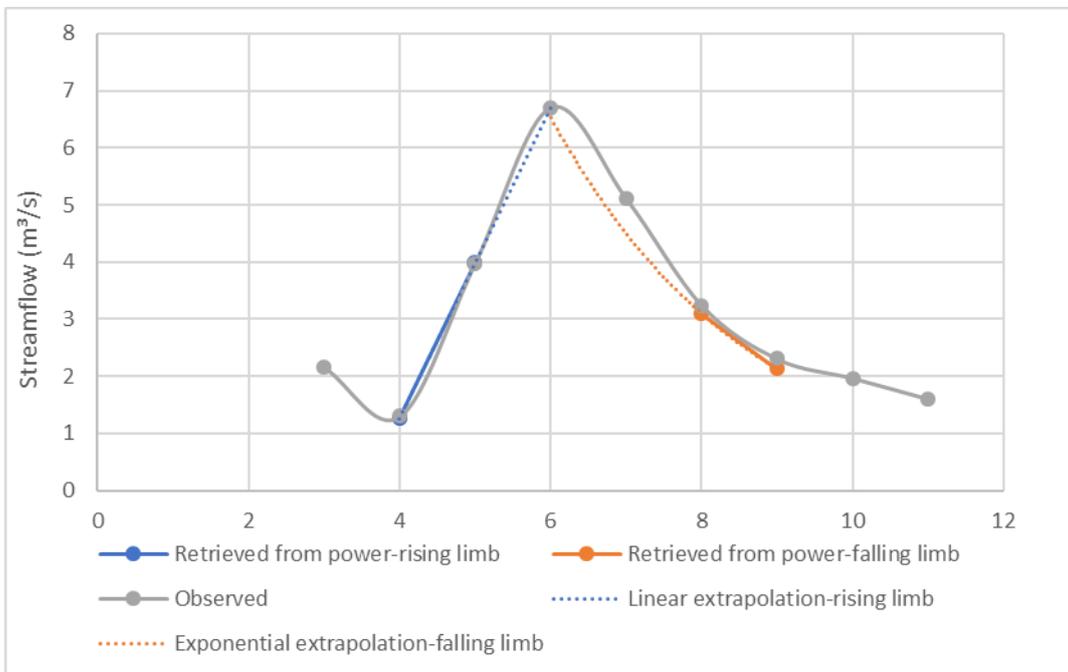
Figure 5.4: Example of extrapolating high flow values for missing days 6 and 7, when the streamflow exceeds the upper discharge limit (turbine capacity) of 5.0 m³/s.
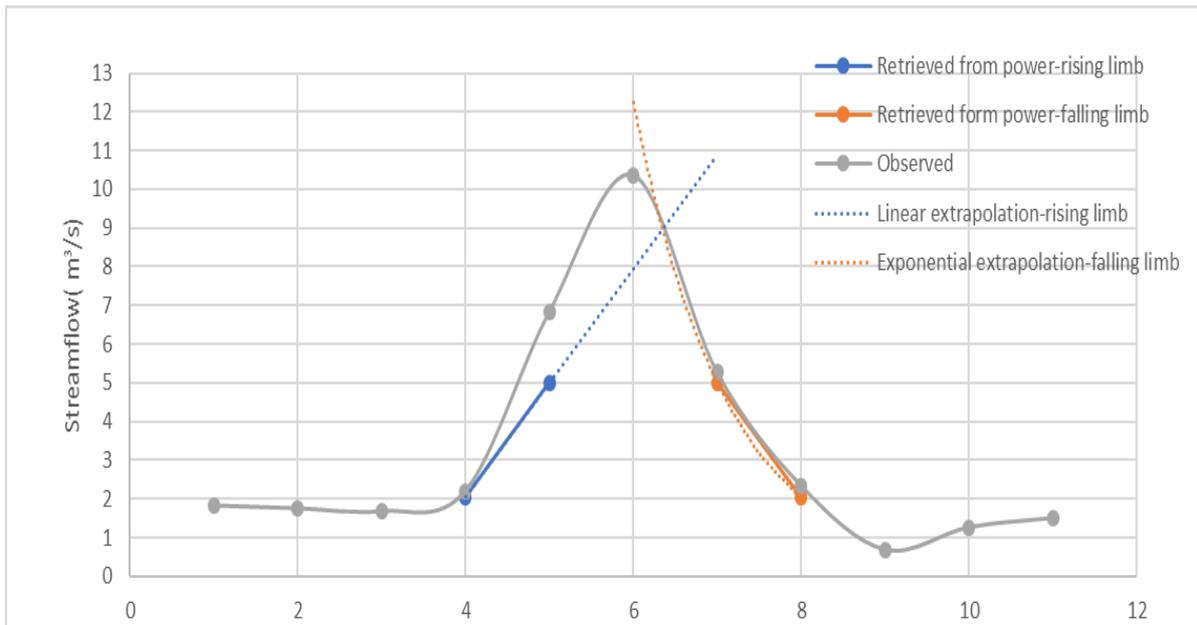
Figure 5.4: Example of extrapolating high flow values for missing days 5, 6 and 7, when the streamflow exceeds the upper discharge limit (turbine capacity) of 5.0 m³/s. The first value of the rising limb is manually set equal to the nominal discharge, since the last two known values do not allow for estimating the slope of the hydrograph.

Figures 5.4 and **5.5** demonstrate two examples of extrapolating high flows. In both cases the maximum discharge that can pass through the turbines is 5.0 m³/s. In the first example, the last known discharges in the rising and the falling limbs are 4.0 and 3.0 m³/s, respectively. The fitting to the known hydrograph and particularly the estimation of the peak value and time are almost perfect. On the other hand, in the second example the rising limb cannot be well-approximated, since the last two known values at days 3 and 4 do not capture the flood phenomenon, thus resulting to a very small slope. However, by manually setting the unknown flow value of day 5 equal to the nominal discharge, i.e. 5.9 m³/s, we obtain a peak flow up to 9.0 m³/s, which is quite close to the real value of 10.3 m³/s. Regarding the falling limb, in both cases the fitting is very satisfactory, since the recession parameter of both flood events is quite well approximated by the two first known discharge values after the nominal one.

As for the stochastic approach, we implement almost the same procedure with the inverse model for retrieving turbine flows. Firstly, it is necessary to estimate the model residuals, by comparing with real discharge data, next formulate an appropriate stochastic model for the residuals, accounting for their marginal and dependence properties, and eventually generate a number of synthetic error realizations ("ensembles") and associated discharge scenarios. For each scenario, we run the extrapolation method thus obtaining ensembles for the full hydrograph, i.e. low, intermediate and high flows, and also estimate their uncertainty bounds. **Figure 5.6** provides an example, which refers to the part of the flow time series that has been discussed before (**Figure 5.4**).
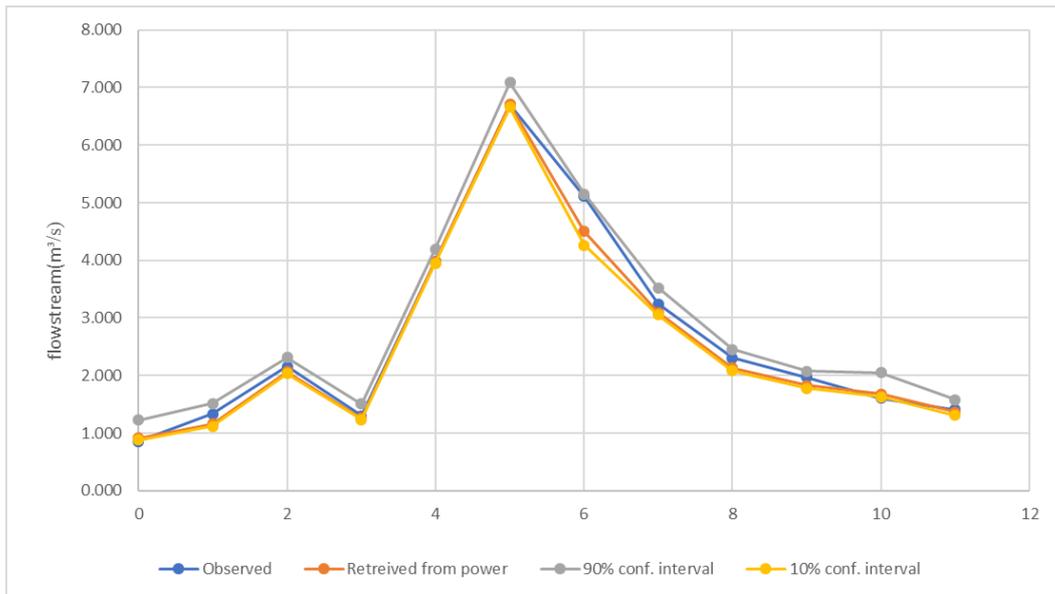
Figure 5.5: Example of extracting uncertainty bounds for extrapolated values.

5.5.3   Low flows

Similarly to the estimation of high flows, it is necessary to represent the period of low flows. As already mentioned, the turbines operate only for flows over Q_{min}, while for lower flows any energy is produced. This extrapolation is very important for a small hydropower plant, because the duration and the frequency of these periods may be crucial for the scheduling of the operation of power plant and the prediction of its performance. For instance, if these period are extended or they happen too often, then the plant is not efficient. Due to all uncertainties, which are also mentioned before, it is possible that a plant will not be as efficient as hypothesized in its design.

The hydrograph extrapolation for low flows follows the same idea with the extrapolation of high ones. The recognition of periods of low flows is straightforward, since during this period the power production is zero. The estimation is based on the forward extrapolation of the falling limb and the backward of the rising one, using the same assumptions with high flows, i.e. the rising limb is linear the falling exponential. It is worthy commendable that if the any estimated discharge value exceeds the minimum flow, it is manually set equal to Q_{min}.

Figures 5.7 and **5.8** illustrate the extrapolation of the hydrographs when the discharges are below Q_{min}. The difference between these figures is concerned about the last known discharge in falling limb. Specifically, in **Figure 5.8** the falling limb declines sharply and the last known discharge is under the minimum discharge. In order to extrapolate the falling limb, we manually set the last known streamflow to Q_{min}.

Again, the approach is stochastic with very interesting results. Due to the importance of this estimation, it is essential to provide confidence intervals for each examined period of low flows. As shown in the example of **Figure 5.9**, the most noticeable feature is that in day 6 the confidence interval cannot capture the observed flow. The lower limit is over the real flow in fifth day.
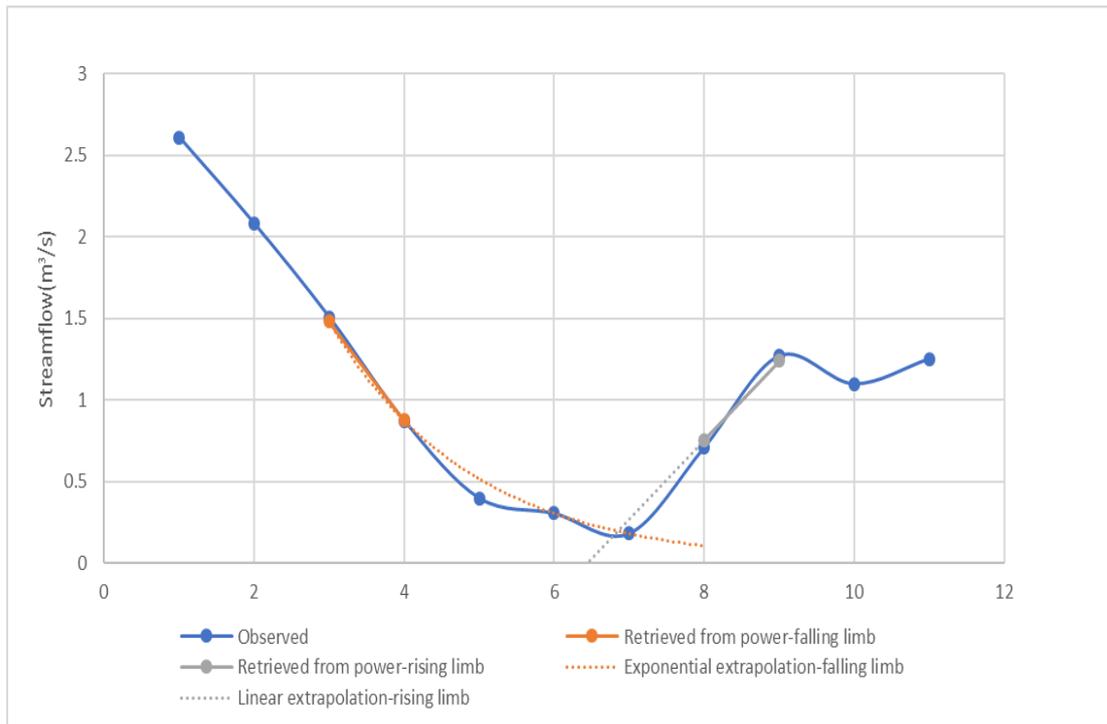
Figure 5.6: Example of extrapolating low flow values for missing days 5, 6 and 7, when the streamflow is below the lower operational discharge limit of 0.5 m³/s.
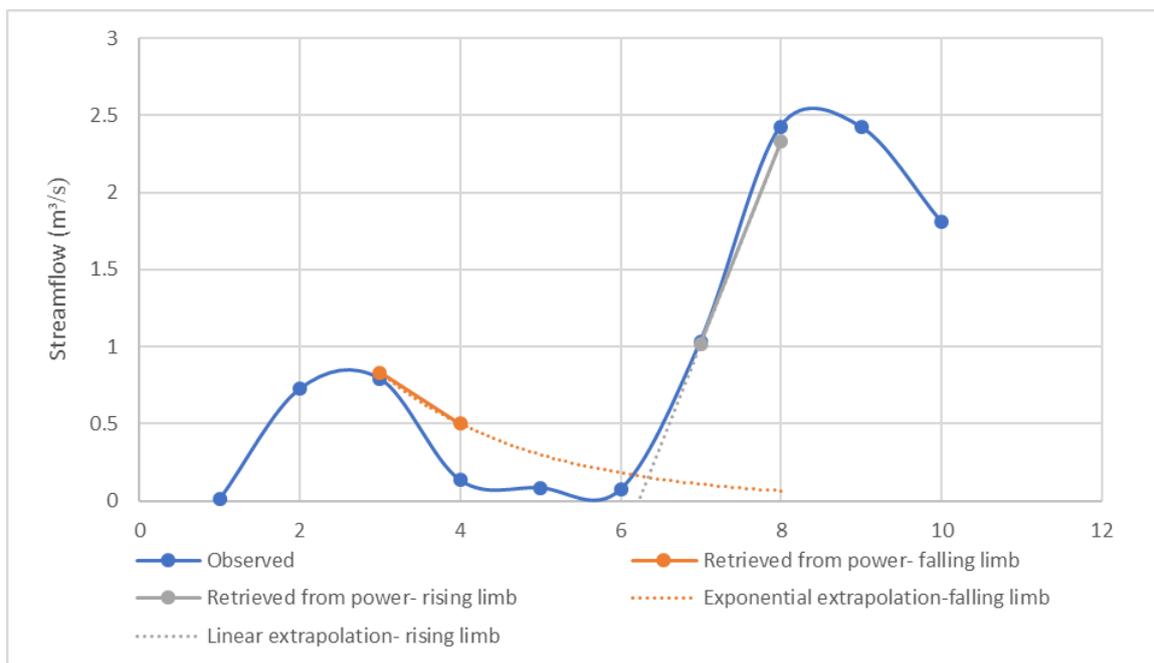

Figure 5.7: Example of extrapolating low flow values for missing days 4, 5 and 6, when the streamflow is below the lower operational discharge limit of 0.5 m³/s.
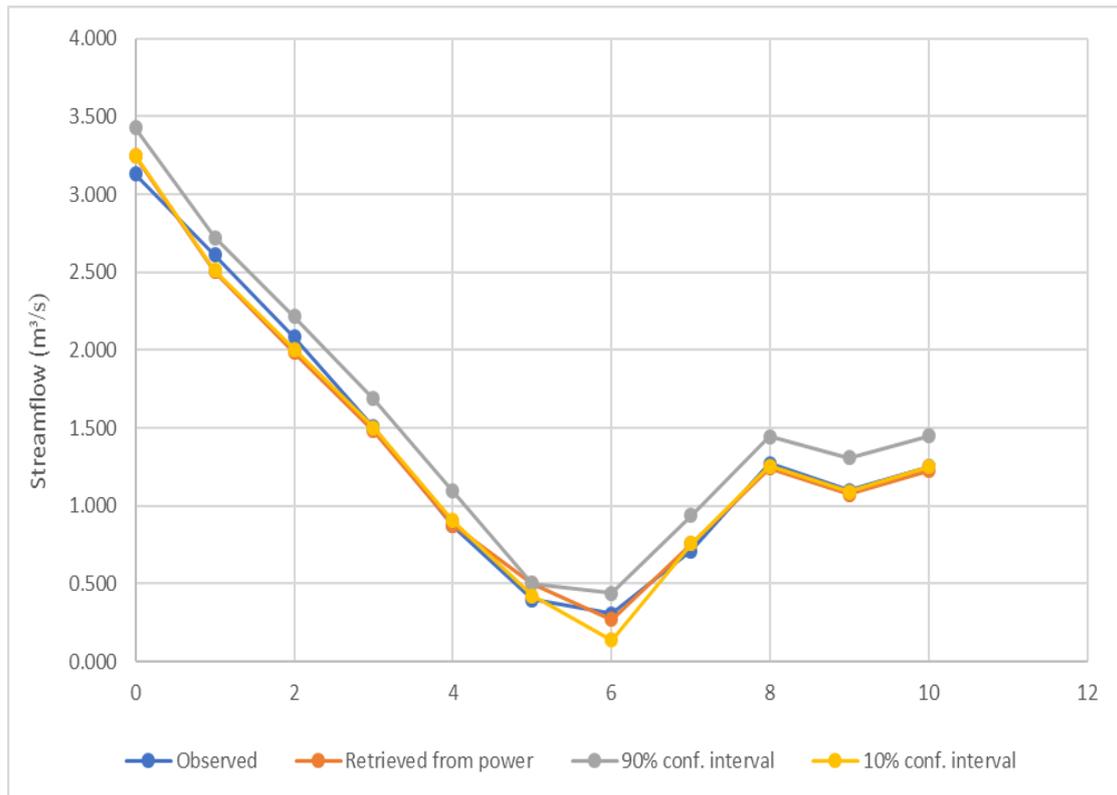
Figure 5.8: Example of extracting uncertainty bounds for extrapolated values.

6   Model implementation in MATLAB environment

6.1   Data insert-matrix pre-allocation

The code snippet below demonstrates the following actions:

o   Insert in the MATLAB workspace the data from a MS Excel spreadsheet in the form of one dimensional index;

- Edailydata1: the observed daily energy production

- Qobseved: the observed daily flow

o   Determining the size of the registers used below in order to increase computational speed. These registers are:

- D: the diameter of penstock

- A: the cross-section area of penstock

- Hol: the gross head

- n1: the starting efficiency

- L: the length of penstock

- e: the normalized roughness

- Qmodelhour: the extracted hourly streamflow

- Qmodeldaily: the extracted daily streamflow

- error1: $w_t = Q_{T,t} - Q_{obs,t}$

- error2: $w_t = \frac{Q_{T,t} - Q_{obs,t}}{Q_{obs,t}}$

- error3: $w_t = \ln(Q_{T,t}) - \ln(Q_{obs,t})$

- rndm: the random numbers in order to generate synthetic errors realizations

```
prompt='doste xronoseires dedomenon';
Edailydata1=xlsread('DATAEIK.xlsx','Sheet1','B3:B3653');
Ehourdata=Edailydata1/24
Qobserved=xlsread('DATAEIK.xlsx','Sheet1','C3:C3653');
hours=size(Ehourdata,1);
days=size(Edailydata1,1);
D=xlsread('DATAEIK.xlsx','Sheet1','D1');
A=(pi*D^2)/4;
Hol=xlsread('DATAEIK.xlsx','Sheet1','D2');
n1=xlsread('DATAEIK.xlsx','Sheet1','D3')
g=9.81;
L=xlsread('DATAEIK.xlsx','Sheet1','D4');
e=xlsread('DATAEIK.xlsx','Sheet1','D5');
error=I*0.01;
Qmodelhour=zeros(1,hours);
Qmodeldaily=zeros(1,days);
error1=zeros(1,days);
error2=zeros(1,days);
error3=zeros(1,days);
rndm=zeros(days,100);
```

6.2   Useful functions

6.2.1   Friction losses

The function above is called to calculate the energy losses for given flow, diameter, normalized roughness and length of penstock.

```
function [ Hf ] = energy_loss_eik( q,D,e,L )
b=0.25+0.0006*e+0.024/(1+7.2*e);
g=0.083/(1+0.42*e);
N=0.00757*((1+2.47*e)^0.14);
p=4^(3+b);
k=D^(5+b);
o=1/(1+g);
J=(p*(N^2)*(q^2)/(pi^2)/k)^o;
Hf=J*L;
end
```

6.2.2   Efficiency

These functions compute the efficiency for each time step. The first one calculates the efficiency for given changing the parameters a, b, n_{min}, n_{max} and the streamflow from turbine. The second one calculates the efficiency by using the empirical nomograph.

```
function [n]=coef_francis_eik_cal(a,b,nmin,nmax,q)
qmin=0.5;
qmax=5;
n=real(nmin+(1-(1-((q-qmin)/(qmax-qmin))^a)^b)*(nmax-nmin));
end
```

```
function [n]=coef_francis_eik(q)
if (0.49<=q)&&(q<=0.95)
    n=0.16*q+0.7
elseif (0.95<q)&&(q<=1.35)
        n=-6*10^(-14)*q^2+0.04*q+0.82
elseif (1.35<q)&&(q<=2)
        n=-0.0135*q^2+0.0673*q+0.8087
elseif (0<=q)&&(q<0.49)
    n=0
elseif q>2
            n=0.89
elseif q<=0
    n=0



end
end
```

6.3   Inverse problem

This code snippet calculates the deterministic formula for the so-called inverse energy problem. It is worth noting that, this code calculates only the streamflow, which extracted from the energy production. If the energy production is over the installed power the model ,for this time step, the extracted streamflow is the nominal discharge. On the contrary, if the power production is zero, then the flow is outside of the range of operation of SHPP's. In this case, the code characterize this flow as "low".

```
for k=1:hours                              elseif abs(dQ)<0.05
    Eep=Ehourdata(k);                          if s>2
    if Eep>I1                                  Q(t)=Qdok(s);
    de=E(1)-Ehourdata(k);                      H(t)=Hdok(s);
    t=2;                                       elseif s<=2
     while abs(de)>=error                          Q(t)=Qdok(1);
     Hf=energy_loss_eik(q,D,e,L);                  H(t)=Hdok(1);
     kt=2;                                     end
     V=q/A;                                 s=s+1;
     Ht=kt*(V^2)/2/g;                       end
     H(t)=Hol-Hf-Ht;                        E(t)=Q(t)*g*n*H(t);
     n=coef_francis_eik(q);                 de=E(t)-Ehourdata(k);
     Q(t)=Ehourdata(k)/(g*n*H(t));          E1=E(t);
     q=Q(t);                                q=Q(t);
     dQ=Q(t)-Q(t-1) ;                       H1=H(t);
     Qdok(1)=Q(t);                          t=t+1;
     Hdok(1)=H(t);                          end
     s=2;                                   Hmodel(k)=H1;
     if abs(dQ)>=0.05                       nmodel(k)=n;
      n=coef_francis_eik(q);                Emodel(k)=E1;
      Hf=energy_loss_eik(q,D,e,L);          Qmodelhour(k)=q;
      kt=2;                                 elseif Eep<=I1
      V=q/A;                                Hmodel(k)=Hol;
      Ht=kt*(V^2)/2/g;                      nmodel(k)=low;
      Hdok(s)=Hol-Hf-Ht;                    Emodel(k)=low;
      Qdok(s)=Eep/(g*n*Hdok(s));            Qmodelhour(k)=low;
      dQ=Qdok(s)-Qdok(s-1);                 end
      H(t)=Hdok(s);                      end
      Q(t)=Qdok(s)   ;
```

6.4   Model residuals (errors)

The following code snippet illustrates the calculations for the model residuals, as described at the previous chapter. The two first moments, mean and standard deviation, are calculated as well. These error index is essential to approach the flow stochastically.

```
for p=1:t-1
    if (Qdata(p)>qmin) && (Qdata(p)<qmax)
    error1(p)=Qobserved(p)-Qmodelhour(p)
    error2(p)=log(Qobserved(p))-log(Qmodelhour(p))
    error3(p)=(Qobserved(p)-Qmodelhour(p))./Qobserved(p)
    end
end
mean1=mean(error1)
mean2=mean(error2)
mean3=mean(error3)
stdev=std(error1)
stdev2=std(error2)
stdev3=std(error3)
```

6.5   Synthetic error realizations

As for the generation of m synthetic error realizations, it's essential to calculate the statistical characteristics of each error (mean, standard deviation, skewness, correlation, cross correlation). In this study, the correlation between error and retrieved discharge as well as the

correlation of error are too large As a result, the AR1 model is required. This extract demonstrates the calculation of the statistical characteristics of the white noise.

The code snippet below shows the generation of 100 synthetic error realizations and the association with the first kind of error. Moreover, as can be seen clearly the intervals at this example are slightly strict (90% confidence level).

Firstly, the script creates in the first row random numbers, which follow the Gamma distribution with the error's statistical characteristics. The rest of the synthetic errors for each time step and for every realization concern the correlation of error as well. Moreover, the synthetic errors are sorted, in order to extract the confidence intervals. Finally, the intervals are extracted from the association of the error and the simulated streamflow. In the provided example this error is simply added to the retrieved discharge.

```
error=xlsread('DATAEIK.xlsx','Sheet1','E2:1600');
merror=mean(error);
stdeverror=std(error);
skewerror=skewness(error);
correlerror=xlsread('DATAEIK.xlsx','Sheet1','D6');
mwn=merror*(1-correlerror);
stdwn=stdeverror*sqrt(1-correlerror^2);
cswn=skewerror*(1-correlerror^3)/((1-correlerror^2)^1.5);
a=4/(cswn^2);
b=sqrt(a)/stdwn;
c=mwn-a/b;
rndm=zeros(days,100)
```

```
for i=1:100
    rndm(1,i)=gaminv(rand,a,1/b)+c;
     for t=2:days
      rndm(t,i)=gaminv(rand,a,1/b)+c +correlerror.*rndm(t-1,i);

     end

end
medgam=median(rndm,2);
sorted=sort(rndm,2);
lowergam=zeros(1,days);
upergam=zeros(1,days);

for i=1:days
    lowergam(1,i)=sorted(i,10);
    upergam(1,i)=sorted(i,90);
end
lower=zeros(1,days);
uper=zeros(1,days);
med=zeros(1,days);
for i=1:days
    lower(1,i)=Qdailymodel(i,1)+lowergam(1,i);
    uper(1,i)=Qdailymodel(i,1)+upergam(1,i);
    med(1,i)=Qdailymodel(i,1)+medgam(i,1);
end
```

7   Theoretical investigations

7.1   Problem configuration and input data

In order to put in practice, the "inverse energy problem" and the extrapolation of high and low flows, we first formulate a theoretical example of a hypothetical small hydropower plant. The plant contains a single turbine of 10.8 MW power capacity and its operation is tested by using daily inflows over a ten-year period. In order to present a holistic study of this problem two alternative turbines are considered, i.e., Pelton or Francis, operating at low flow limits of 10 and 20%, respectively. This approach is ideal due to the differences of efficiency curves of these turbines. Specifically, the efficiency of Pelton's turbines do not exhibit significant fluctuations against discharge, and usually range between 0.65 and 0.89. On the contrary, the efficiency of Francis turbines range between 0.08 and 0.96, also depending on the specific speed of the turbine.

To evaluate the methodology, as described in previous chapters, it is required to extract the actual power production depending on inflows (initial data, obtained by solving the forward problem), the net head, the average efficiency and the installed power. The hypothetic plant has net head $H_n = 260\,m$, which is considered constant for the forward problem, and an average efficiency $\eta = 0.85$. Following this, the installed power is 10.8 MW and the maximum discharge of turbines is 5.0 m³/s. On the contrary, the minimum discharge is 0.5 m³/s and 1.0 m³/s for Pelton and Francis turbines, respectively. The **Table 7.1** demonstrates the characteristics statistical and not of the hypothetical SHPP, which is used for the test of our methodology. Furthermore, **Figure 7.1** illustrates the inflows at the entrance of the SHPP, whereas **Figure 7.2** and **Figure 7.3** represent the energy production the two alternatives turbines Francis and Pelton, respectively.

Table 7.1: Characteristics of the hypothetical SHPP.

|	Pelton	Francis
Minimum operational discharge Q_{min} (m³/s)	5.0	5.0
Maximum operational discharge Q_{max} (m³/s)	0.5	1.0
Power capacity I_{max} (MW)	10.8	10.8
Operating time ratio	0.30	0.30
Ratio of volume passed from turbines to total runoff	0.75	0.75
Mean annual production (GWh)	11.8	10.9
Average daily energy (MWh)	37.9	32.2
Standard deviation (MWh)	55.0	56.5
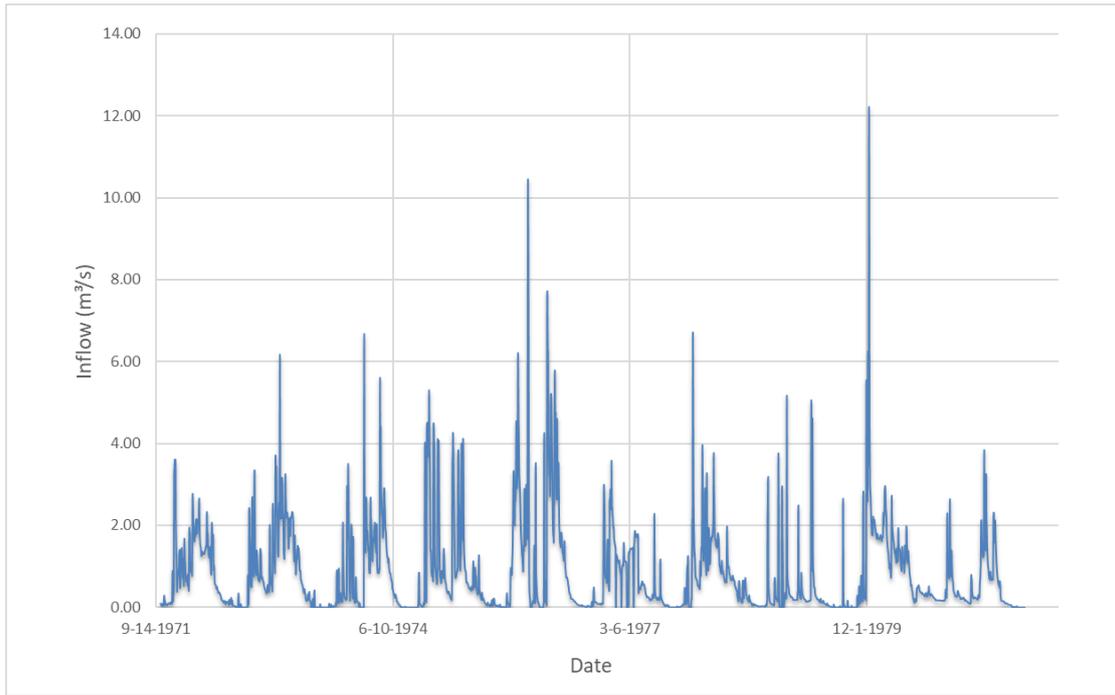
Figure 7.1: Inflow time series at the entrance of the hypothetical small hydropower plant.
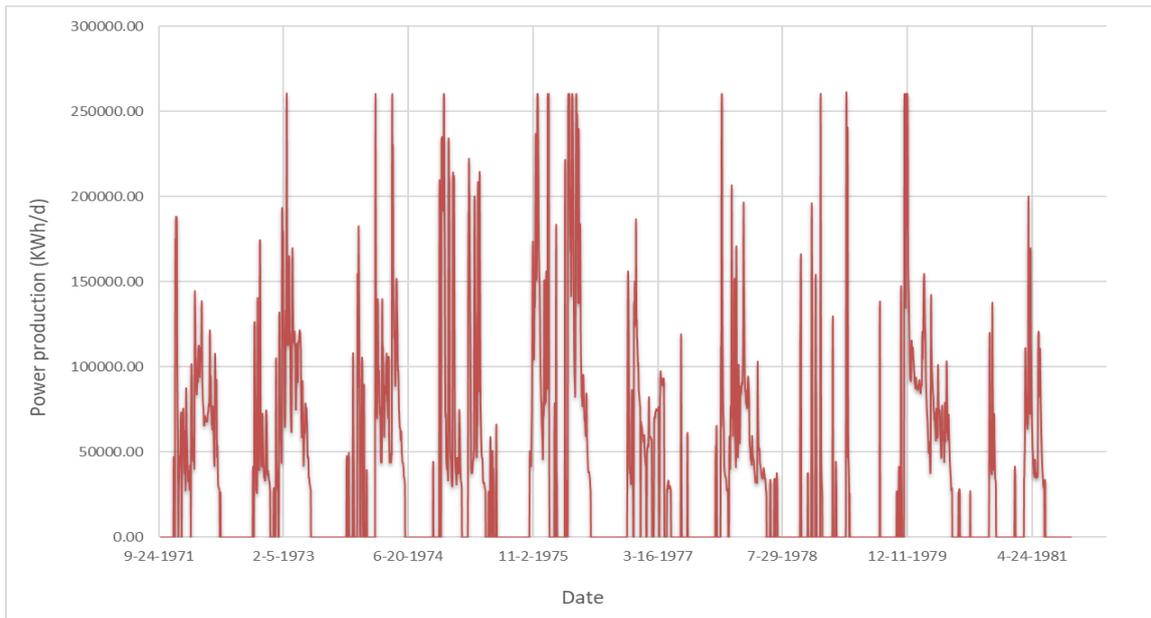

**Figure 7.2**: Simulated energy data through the Pelton turbine using actual inflows.
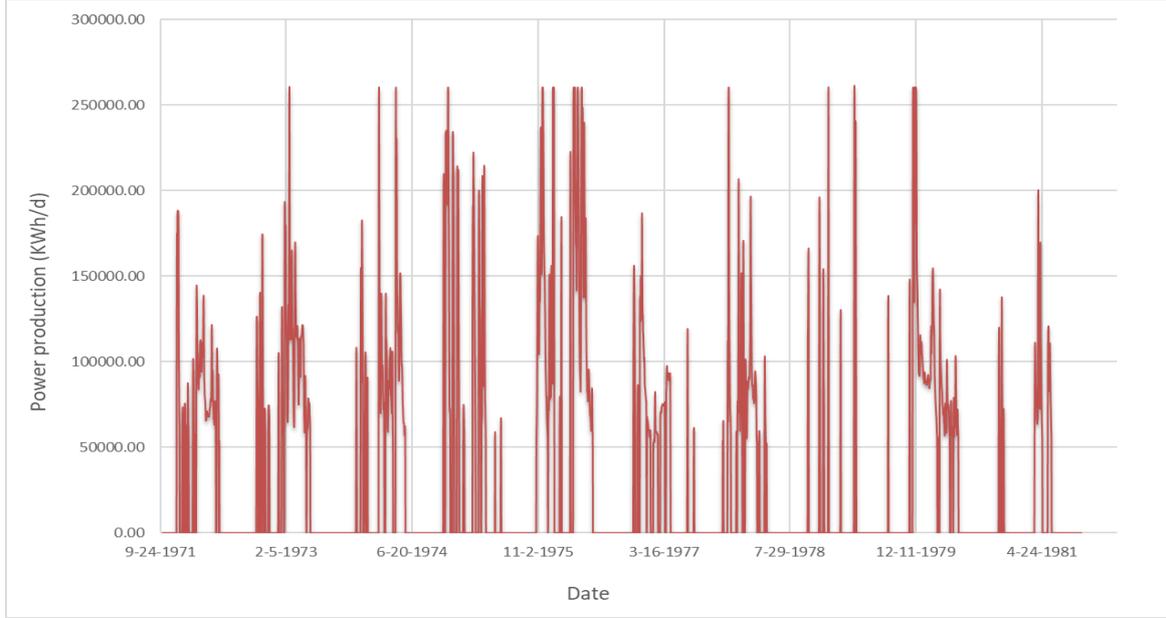
Figure 7.3: Simulated energy data through the Francis turbine using actual inflows.

7.2 Assignment of artificial uncertainties

7.2.1 Overview

The implementation of the inverse problem under uncertainty, and eventually the investigation of the arising uncertainties, requires the assignment of artificial errors to crucial factors of the hydroelectric plant. In this study, the error expressions are either observational or parametric. Observation errors are expressed as random perturbations of energy generation data, by assigning an additive or multiplicative error term to simulated energy that follows either a normal or a skewed (Gamma) distribution. On the other hand, the extraction of discharge data under parameter uncertainty is made by using a set of 100 randomly generated efficiency curves around the "actual" ones (Pelton or Francis), to represent the inherent uncertainties of the modelling procedure. In the first setting, the uncertain discharge data are represented in stochastic terms, i.e. by employing the AR(1) model to residuals, while in the second setting the ensembles are directly obtained by solving the inverse problem for each equifinal efficiency curve (term "equifinal" is applied to denote that all curves are equivalently possible to be the true ones).

7.2.2 Uncertain energy

The uncertain energy production is expressed in two ways. The first is by adding or multiply to the actual energy data $e_t(Q_t)$, which is obtained from the known inflows Q_t, an error term Δe_t, as follows:

$$e_t^* = e_t(Q_t) + \Delta e_t \tag{7.1}$$

$$e_t^* = e_t(Q_t)\, \Delta e_t \tag{7.2}$$

where Δe_t is expressed by means of unbiased noise. The distributions which describe the artificial error are the Normal $N(\mu, \sigma)$ and the three-parameter Gamma with skewness γ_ε. As

for the Normal distribution and **7.1**, the mean is zero and the standard deviation is expressed as percentage of the standard deviation of simulated energy production, i.e. 1%, 5% and 10% of σ_e. Also, as for the **7.2** and the Normal distribution the mean is 1 and the standard deviation is 0.1 and 0.2. This range of errors demonstrates how much is the uncertainty and how can the possible measurement errors in energy production affect the streamflow estimations. The uncertainty of inflows that are retrieved by the inverse procedure is quantified in terms of key statistical characteristics of residuals, namely:

- mean, variance, skewness
- lag-one autocorrelations
- cross-correlations with actual flow data

In this study the error is expressed as the difference:

$$w_t = Q_{t,T} - Q_{obs,t} \tag{7.3}$$

Table 7.2 demonstrates the statistical characteristics of the three types of errors for the two alternatives turbines, by assigning a small variance to energy data, i.e. 1%. A common conclusion for all error configurations is that there exist obvious differences between the two turbine types. In particular, the estimated flows for the Pelton case exhibit errors that are highly correlated, both in time and space (cross-correlation with discharge), while in the case of Francis the errors exhibit significantly smaller dependencies, yet they are highly skewed. Regarding the differences among the three error types per se, we remark that the formula (7.3) has "better" statistical behavior, due to the relatively smaller lag-one autocorrelations and cross-correlations. In this respect, this formula will be next generally used as the overall expression for error modelling.

Table 7.2: Statistical characteristics of different types of errors.

	PELTON			FRANCIS		
	Error 1	**Error 2**	**Error 3**	**Error 1**	**Error 2**	**Error 3**
Mean	0.04	0.01	0.01	-0.11	-0.08	-0.09
St. deviation	0.06	0.07	0.04	0.20	0.19	0.11
Skewness	1.41	0.88	-1.06	1.21	-2.50	-1.42
Autocorrelation	0.62	0.75	0.80	0.77	0.82	0.78
Cross-correl.	0.78	0.82	0.88	0.31	0.96	0.88

7.2.3 Uncertain efficiency curve

As it commonly known, the data sets of hydropower plants may be subject to measurement errors regarding energy production data as well as inflows. The examples above are the so-called observational errors and may due to imperfect measurement systems and human faults, as well. On the contrary, one of the most important factor, the efficiency of turbines, at hydropower plants many times seems to have errors. As mentioned in previous chapters, the efficiency is not constant and depend on the turbine type and the flow. In addition, the initial efficiency curve, which be used to primary study of plant is, at majority, empirical and

the actual efficiency is still indefinite. Also, this efficiency curve changes due to deterioration, damage and aging of the equipment over time. For instance, it is possible that not only the maximum efficiency will decrease with time but also the minimum operational flow will also increase, thus reducing the effective flow range of the turbine. As can be understood, the study of a hydropower plant may be totally different from its operation.

In order to focus on the impacts of efficiency on the relationship energy production and stream flow it is necessary to create different efficiency curves for one turbine. The calibrated initial efficiency curve is given in analytical form, which described before. Firstly, it is necessary to consider a turbine with known efficiency curve and known inflows and extract the energy production through the forward formula. This energy production is essential information to move on the inverse problem and the investigation of the efficiency's uncertainties. The generation of 100 synthetic efficiency curves around the known one allows to represent these uncertainties in stochastic terms. This generation is a result of changes in four parameters a, b, n_{min}, n_{max}. The changes in parameters a and b are around 10% of the known value. Also, a realistic change of n_{min} and n_{max} is considered 0.1 around the known value. The extraction of stochastic flow series in this case becomes directly for the inverse formula.

Table 7.3: Efficiency curve parameters for the two problem settings.

	a	b	n_{max}	n_{min}
PELTON	0.51	10.56	0.83	0.30
FRANCIS	0.59	3.95	0.91	0.70

7.3   Results of inverse problem under uncertainty

7.3.1   Observational uncertainties (errors in energy)

The statistical characteristics of simulated discharge errors provided below, after adding a normal error term to actual energy data (zero bias, standard deviation 1, 5 and 10% of energy standard deviation).

Following this, the statistical characteristics of simulated discharge errors, after adding a gamma-distributed error to actual energy data (zero bias, standard deviation 1% of energy, skewness coefficients 0.3, 1, 5).

Even if this formula seems to have better correlations than the others formula, it is necessary to use the AR(1) model to residuals because the autocorrelation is still big. The most important feature is that when the standard deviation is increasing the autocorrelation is decreasing. On the contrary, when the skewness is rising the autocorrelation fall.

The statistical characteristics above demonstrated at the timeseries of streamflow, which retrieved by the inverse problem. For instance, two line graphs are represented below and as can be seen the increase of standard deviation from 1% to 10% of observed energy standard deviation not only affect the retrieval discharge a lot, but also the confidence interval are

extended. Specifically, when the maximum gap between upper and lower limit in first scenario is 0.2 m³/s, in second scenario with one size class up this gap is 0.46 m³/s.

On the other hand, when skewness changes the flow from the inverse formula don't be affected dramatically. This feature can be released from the timeseries below.

Table 7.4: Statistical characteristics of error type 1 for alternative turbines by adding artificial error with standard deviation

	$\sigma = 1\%$		$\sigma = 5\%$		$\sigma = 10\%$	
	PELTON	FRANCIS	PELTON	FRANCIS	PELTON	FRANCIS
Mean	0.037	-0.109	0.044	-0.115	0.049	-0.109
St. deviation	0.065	0.201	0.100	0.196	0.139	0.205
Skewness	1.411	1.212	1.968	1.225	1.154	0.921
Autocorrelation	0.619	0.768	0.243	0.736	0.125	0.672
Cross-correl.	0.777	0.312	0.398	0.947	0.310	0.900

Table 7.5: Statistical characteristics of error type 1 for alternative turbines by adding artificial error with skewness

	$\gamma = 0.3$		$\gamma = 1.0$		$\gamma = 5.0$	
	PELTON	FRANCIS	PELTON	FRANCIS	PELTON	FRANCIS
Mean	0.037	-0.117	0.037	-0.116	0.036	-0.116
St. deviation	0.064	0.179	0.064	0.180	0.060	0.179
Skewness	1.442	0.674	1.174	0.683	0.573	0.680
Autocorrelation	0.600	0.794	0.633	0.795	0.723	0.796
Cross-correl.	0.773	0.968	0.780	0.968	0.862	0.968

Table 7.6: Statistical characteristics of error type 1 for alternative turbines by multiplying artificial error with standard deviation

	$\sigma = 0.1$		$\sigma = 0.2$	
	PELTON	FRANCIS	PELTON	FRANCIS
Mean	0.05	-0.06	0.06	-0.08
St. deviation	0.19	0.13	0.36	0.15
Skewness	0.84	0.93	0.21	0.75
Autocorrelation	0.03	0.07	0.06	0.08
Cross-correl.	0.23	0.51	0.11	0.22
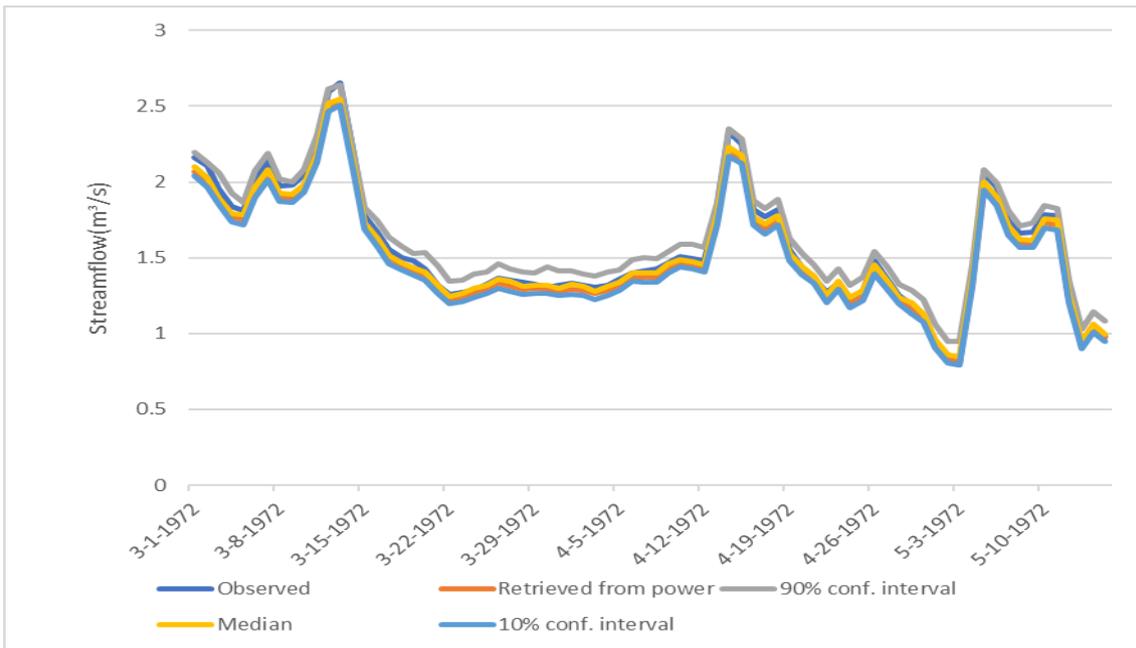
Figure 7.4: Simulated flows and its uncertainty for additive error following Normal distribution with $\sigma = 1\%\sigma_{observed}$.
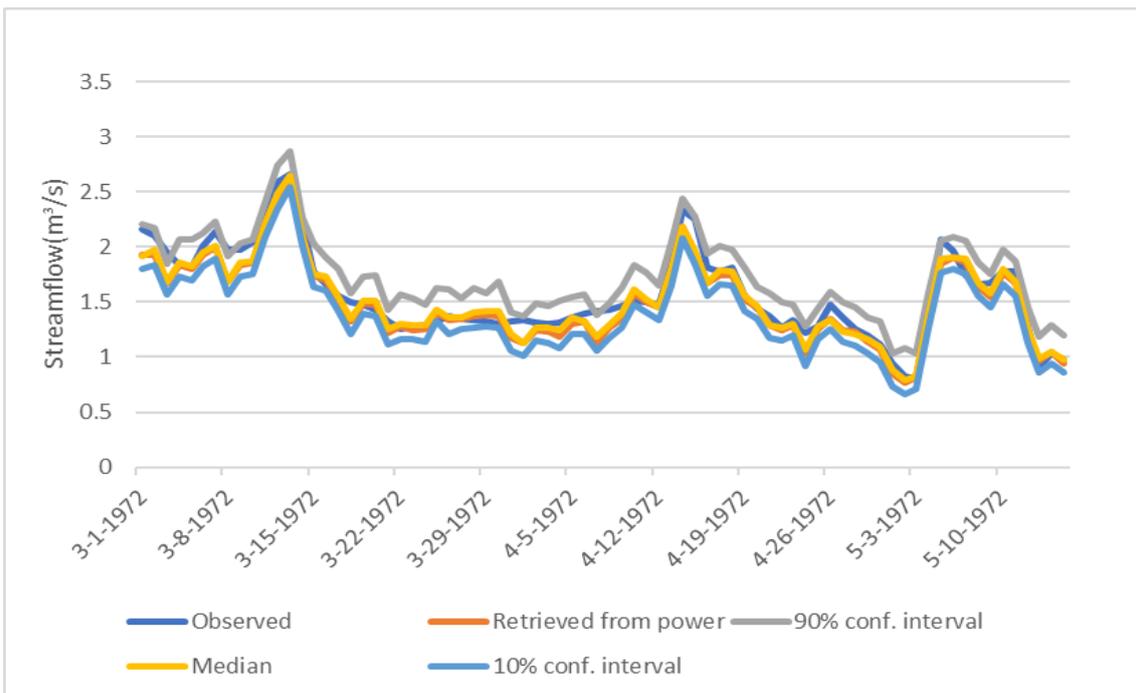
Figure 7.5: Simulated flows and its uncertainty for additive error following Normal distribution with $\sigma = 10\%\sigma_{observed}$.
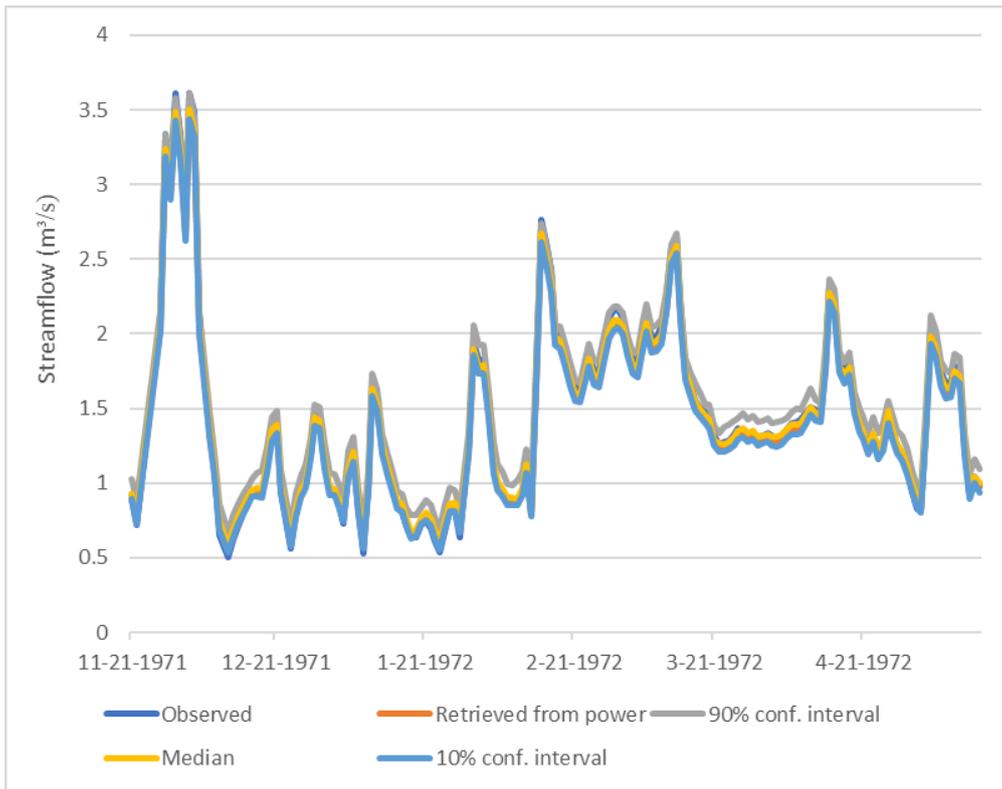
Figure 7.6: Simulated flows and its uncertainty for additive error following Gamma distribution with $\gamma = 0.30$.
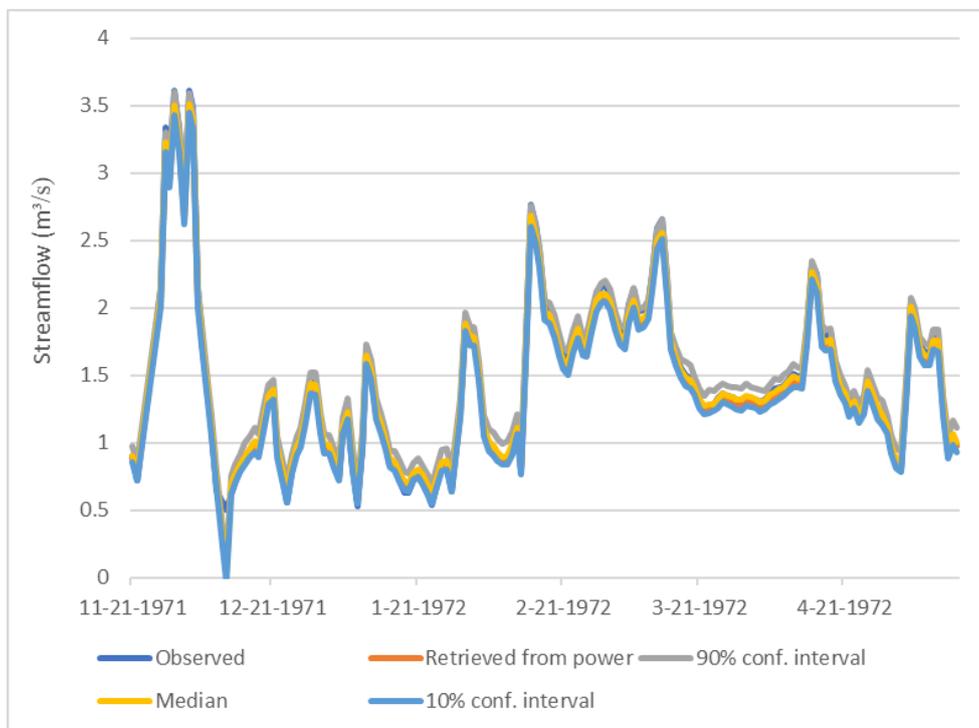
Figure 7.7: Simulated flows and its uncertainty for additive error following Gamma distribution with $\gamma = 5.0$.
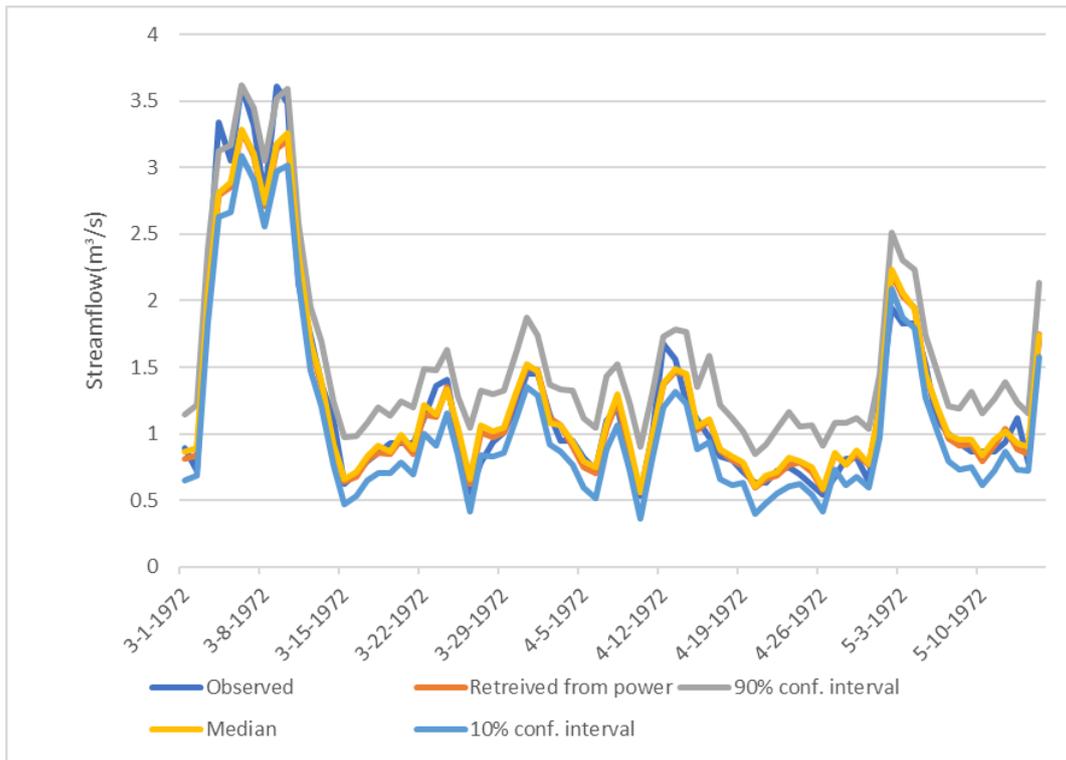
Figure 7.8: Simulated flows and its uncertainty for multiplicative error following Normal distribution with $\sigma = 0.1$ & $\mu = 1.0$.
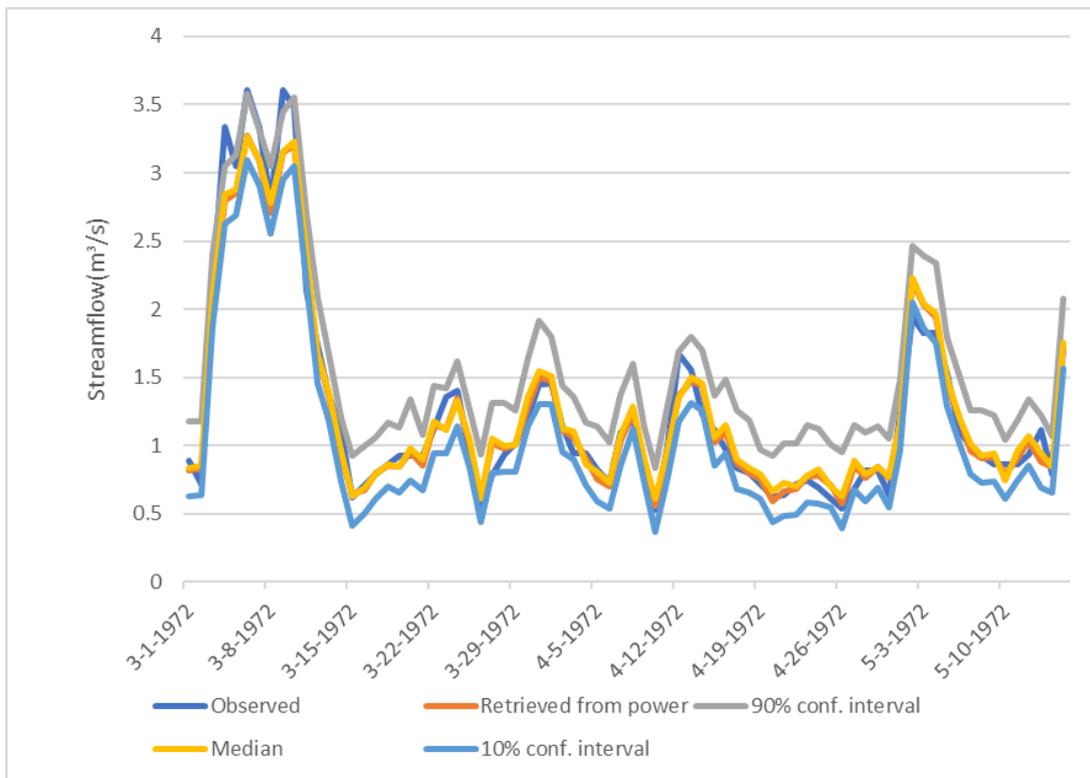
Figure 7.9: Simulated flows and its uncertainty for multiplicative error following Normal distribution with $\sigma = 0.2$ & $\mu = 1.0$.

7.3.2 Parameter uncertainties (errors in efficiency)

This subchapter discuss the impact of the possible changes in efficiency by using the analytical formula, which we proposed in Chapter 4. These changes are due to deterioration, damage and aging of the equipment over time. Furthermore the choice of a turbine in design maybe is not be the same in operation. Thus allows us to investigate not only the minimum and maximum efficiency n_{min}, n_{max} but also the whole efficiency curve by changing the shape parameters a and b. The synthetic curves are around the "true" one, which is extracted from the optimization of the Francis turbine. The optimization in turbine was a necessary step in order to pass from the empirical efficiency curve to analytical one.

Table 7.3 Parameters of synthetic curves and the optimal one

	Optimal efficiency curve	Synthetic efficiency curve 1	Synthetic efficiency curve 2	Synthetic efficiency curve 3	Synthetic efficiency curve 4	Synthetic efficiency curve 5	Synthetic efficiency curve 6
a	0.593	0.738	0.750	0.714	0.677	0.787	0.700
b	3.946	4.444	4.221	4.589	4.764	4.633	4.240
n_{max}	0.568	0.623	0.598	0.583	0.573	0.578	0.568
n_{min}	0.907	0.957	0.932	0.857	0.907	0.912	0.793
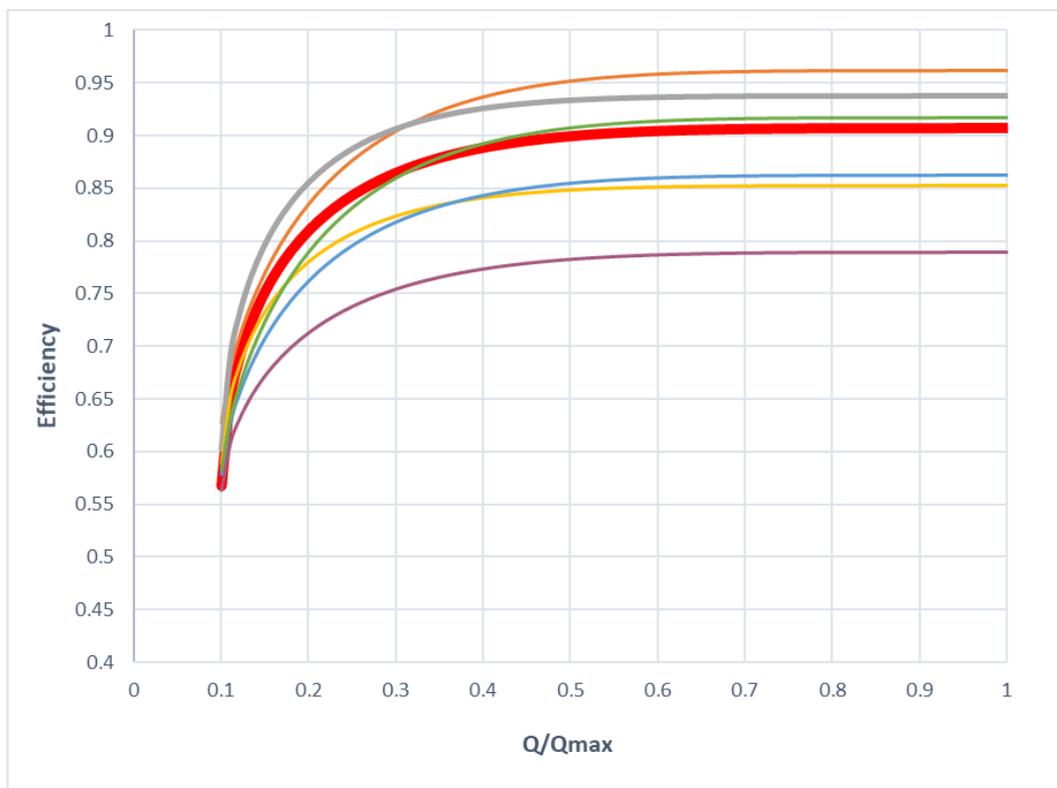
Figure 7.10: Synthetic efficiency curves (six out of 100) around the "true" one (red line).
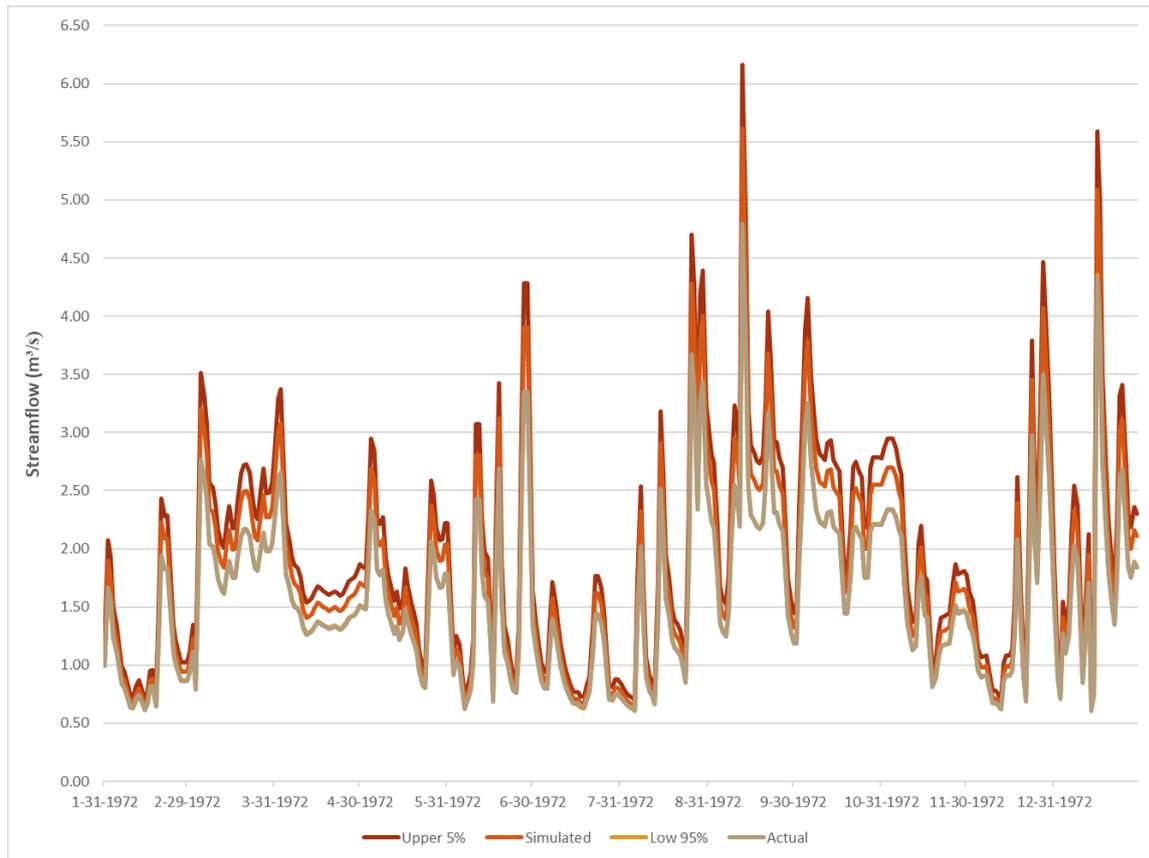
Figure 7.11: Simulated flows and its uncertainty for errors in efficiency curves.

From **Figure 7.11** (simulated flow data for one year period) we see that the uncertainties in efficiency have an important impact in the energy-flow transformation. The most noticeable feature is that the extraction of low flows (0.5-1.0 m³/s) is not affected importantly from the parameter changes. On the contrary, the uncertainties around the efficiency curve have a significant impact on the retrieved streamflow over the value of 1.0 m³/s.

7.3.3   Extrapolation of high and low flows

For one of the problem settings, namely the extraction of flows from the Pelton case, considering an additive error $N(0, 0.1\sigma_e)$, we detected all events for which the estimated flow should exceed the nominal one, i.e. 5.0 m³/s (11 events), or be less than the minimum one, i.e. 0.5 m³/s (8 events). Characteristic examples have been already discussed in section 5.5, while the full cases are given in the Appendix.

8 Real-world case study: Glafkos power plant

8.1 Study area and data

8.1.1 Glafkos river basin

In this case study we examine the real-world small hydropower plant of Glafkos, located in South-Western Greece. Glafkos is a small river in the city of Patras, flowing into the Gulf of Patras (Ionian Sea), south of the city centre. The study basin extends over the Northern Peloponnese Water Department (EL02), and drains an area of 7.4 km². Its relief is generally characterized as mountainous, in the upstream part, semi-mountainous in its outer perimeter and lowland in its coastal zone. Specifically, the catchment includes several tributaries, i.e.:

o   Malamamoutis
o   Romanos
o   Diakoniaris
o   Elexistra
o   Glafkos (main watercourse)
o   Filiouras and Xiropotamos
o   Neromanas
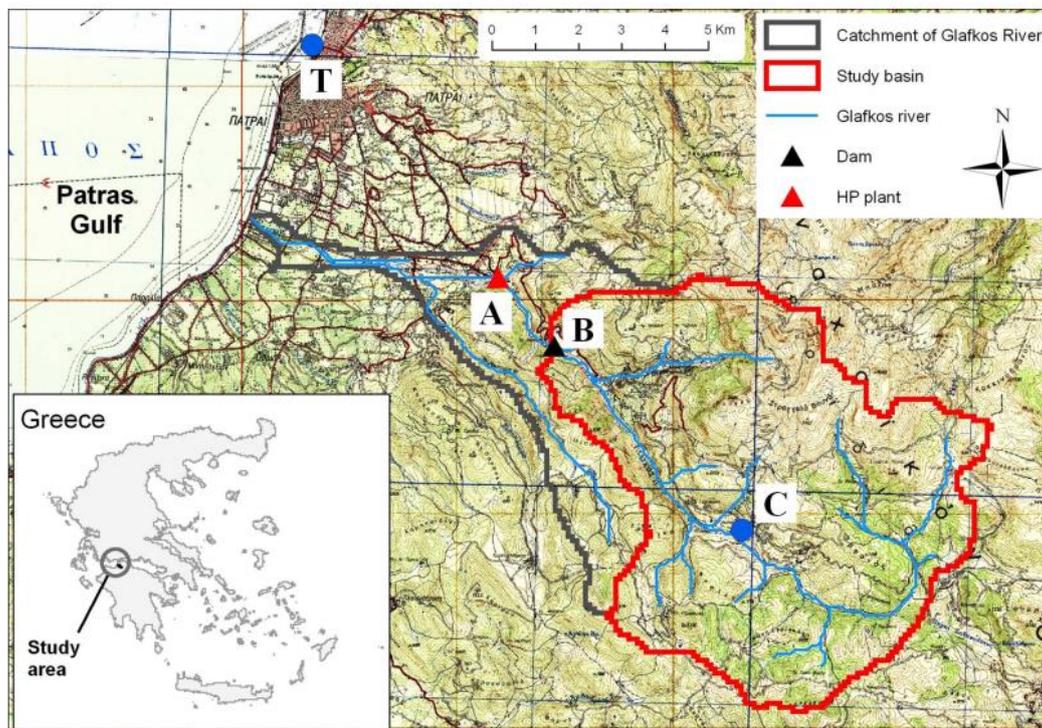
Figure 8.1: Glafkos basin upstream of the diversion dam (Langousis and Kaleris, 2013).

70

8.1.2   Project details

The hydroelectric plant of Glafkos was built in the period of 1922-1926 and it was the first project of this type in Greece. As shown in **Figure 8.2**, the system comprises a run-of-river plant, with a small diversion dam upstream (i.e., at the inlet). Initially, it was intended to fulfill both the water and power supply of the city of Patras, from the waters of the homonymous river. The first dam had a water gate and it was completely different than the current one. In 1968, PPC bought the plant from the municipality of Patras and included it in the network of its hydroelectric power plants under the administration of Ladonas HPP (Wikipedia). Although Glafkos now produces very little energy in relation to the needs of Patras, it covers almost the entire water supply needs of the city for a large portion of time within each hydrological year, i.e. from mid-November to the end of April. As made for all projects of this type, it mainly exploits the baseflow of the river. In case of flood events, if the inflows exceed the conveyance capacity of the system, the surplus water is drained downstream by opening of the water gates, since the flood control capacity of the project is negligible.
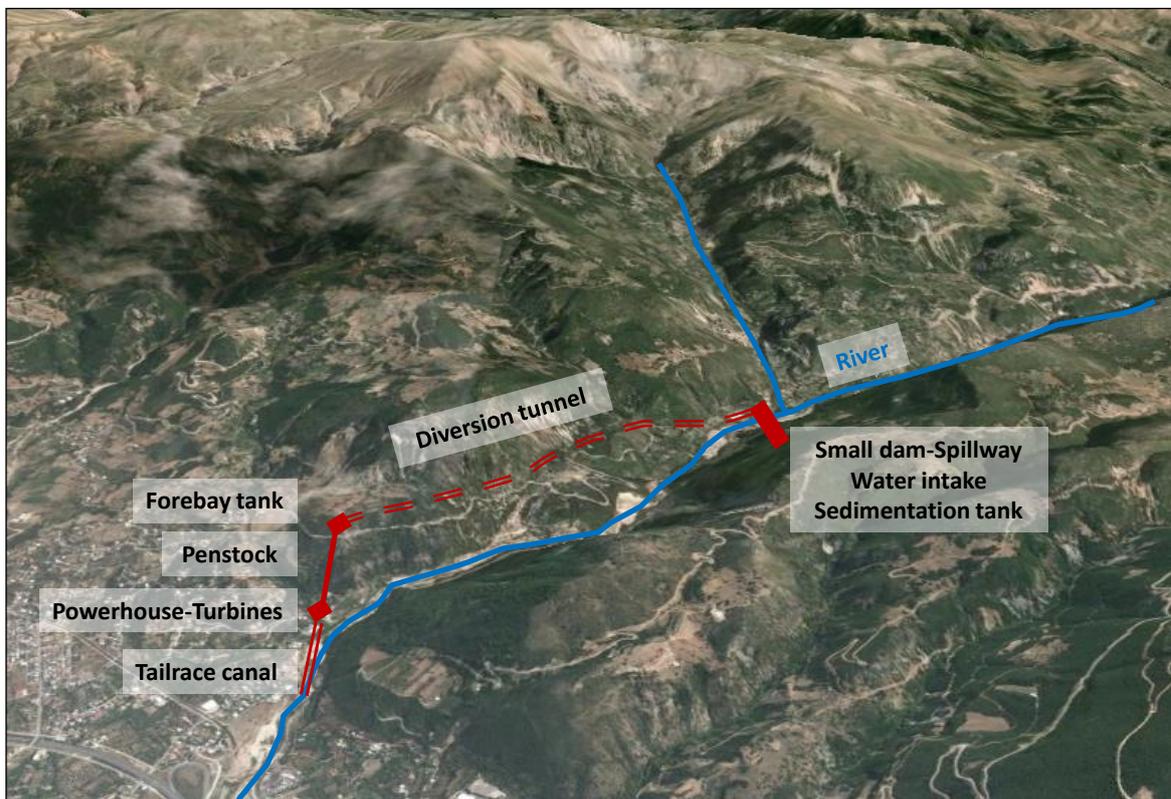
Figure 8.2: Layout of Glafkos hydropower system (Efstratiadis *et al.*, 2020).

Initially, the total installed power capacity was 2.25 MW (3 Francis turbines of 750 kW each). However, due to the small capacity of the Francis units, their old technology and the damages occurred so far, their performance gradually fell by 60% and they were eventually put out of operation. In 1997, two new turbines have been installed, i.e. a Francis-type (2.3 MW) and a Pelton-type (1.4 MW), thus the station's total power capacity rose to 3.7 MW. In mean annual basis, the hydropower plant produces 10.4 GWh, covering about 1/30 of the electricity needs of the city of Patras. In term of capacity, the installed power of Glafkos is 3.7

MW, while the city of Patras needs up to 80 MW. After passing the turbines, the flow is used for irrigation and water supply.

The hydropower system is a typical run-of-river scheme. The small diversion dam, shown in **Figure 8.3**, receives a mean annual inflow of 39 hm³. The water intake is located at an altitude of 339 m and serves to create a small tank to drive water to a diversion tunnel. Upstream of the entrance of the tunnel there are two sand collectors, equipped with valves at their bed to drain the solids. To protect this dam, a cofferdam has been laid at 400 meters. For the conveyance of flood flows, there are two gateways, one automatic (electric) and one manual.

The length of the diversion tunnel is 1 695 m and its cross section is not constant, but ranges from 1.64 m² up to 1.95 m². At the end of the tunnel there is a tank from reinforced concrete, with an inner diameter of 9 m and a height of 9 m, serving as surge chamber. At its bottom there is a conical opening with a diameter of 1.50 m towards the penstock. This is used to protect the penstock and the turbines from excess pressure in case of water hammers, as well as to provide the additional amount of water required when starting the units. At its bed there is also a small drain pipe which is used to clean the water tower from rubble.

As shown in **Figure 8.4**, the penstock is made of concrete and steel and it is placed in the surface, both for economic reasons and also for ensuring easy supervision and maintenance. The pipe conveys the water from the forebay to the power station and after passing it through the power generation units to the downstream river. Its length is 308 m, its diameter 0.90 m, the average slope is about 48% and its thickness ranges from 7 to 14 mm.
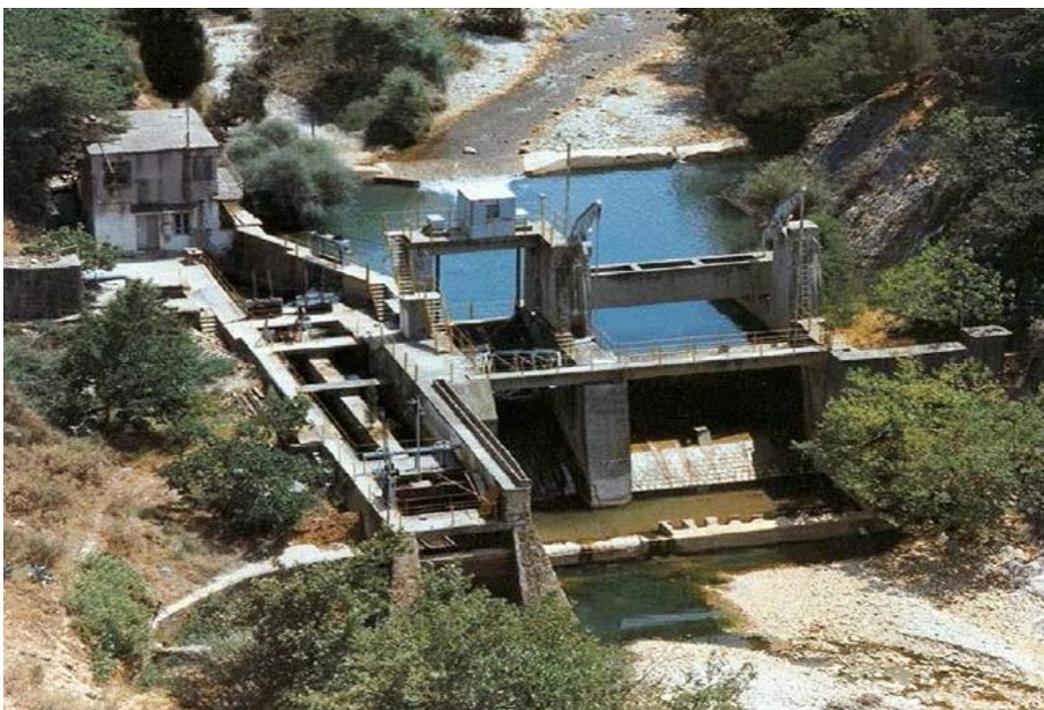
Figure 8.3: View of the diversion dam (Evaggelatos, 2016).

Figure 8.4: View of the penstock (Evaggelatos, 2016).

8.2   Problem setting

Apart from the aforementioned technical characteristics, in order to solve the inverse problem, the following data are also necessary:

- Observed energy production;
- Observed flows at the inlet of the diversion tunnel;
- Efficiency curves for each turbine.
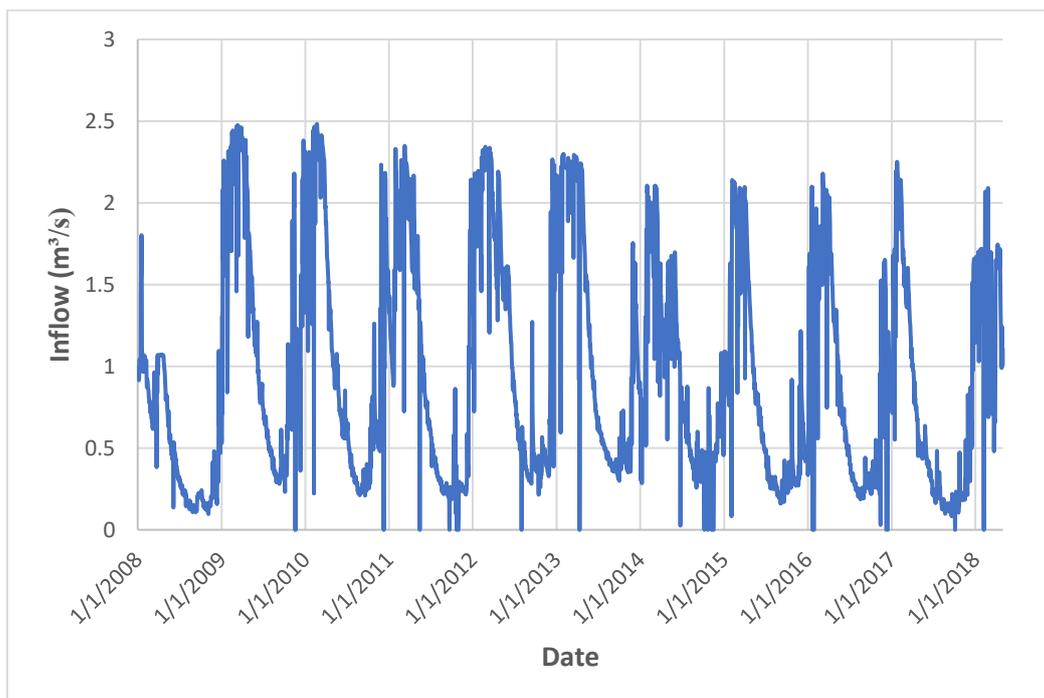
Figure 8.5: Inflow time series diverted to the turbines (full data).

73
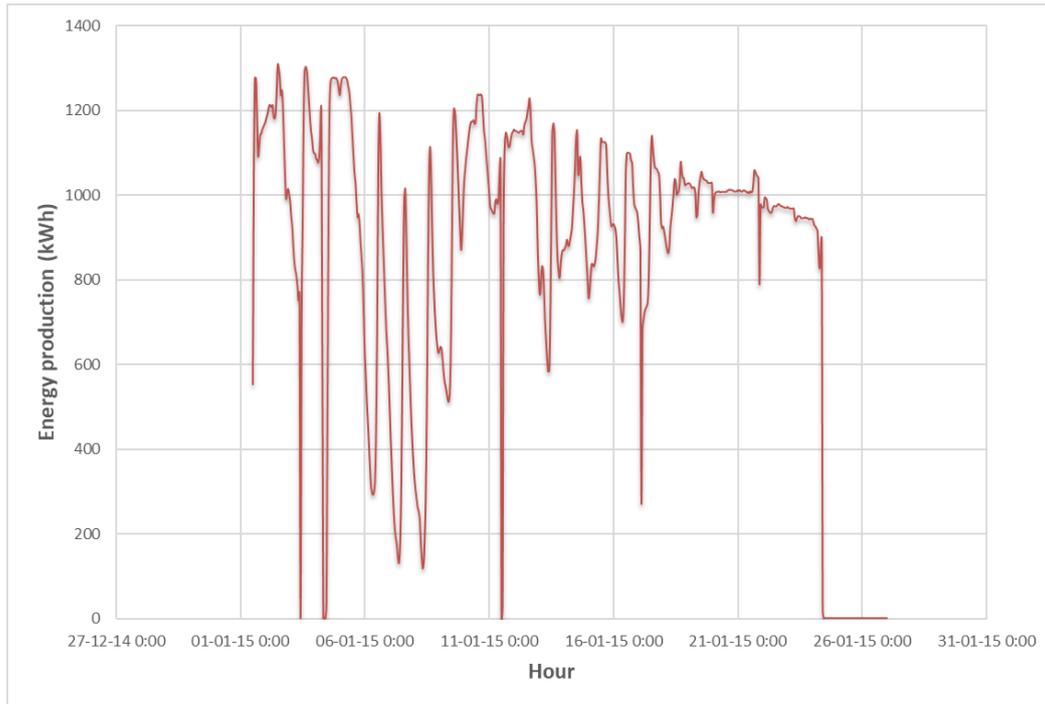
Figure 8.6: Hourly energy production through the individual operation of the Pelton turbine for one-month period.

In Glafkos we used inflow and energy production for a common period of three years, i.e. 2015-2018 (J. Stefanakos, 2019, personal communication). One of the key challenges of this problem was the different temporal resolution of the two data types. In particular, the energy production data from each turbine was provided in hourly resolution (**Figure 8.6**), while the inflow data in daily (**Figure 8.5**). The efficiency curves for both turbines, Pelton and Francis, were unknown, thus making this problem even more challenging. In the figures below are demonstrated the timeseries of Pelton's energy production for one-month period.

8.3   Turbine characteristics and efficiency curves

As mentioned before, the hydropower plant includes a Pelton turbine, with installed power capacity 1.4 MW, and a Francis-type, with installed power 2.3 MW. The efficiency curves of both turbines were unknown. Hence, we initially tested several empirical curves that are given in the literature (Papantonis, 2008), before selecting the ones illustrated in **Figure 8.7**. All values are multiplied by 0.95, since the original curves only refer to turbine efficiency.

In order to improve the model fitting, we next employed a calibration approach to determine the two curves in analytical terms, i.e. by means of the parameter efficiency formula. The results of this approach are presented in **section 8.5**.

Table 8.1: Efficiency curve parameters for Francis and Pelton turbines.

	a	b	n_{max}	n_{min}
PELTON	0.51	10.56	0.83	0.30
FRANCIS	0.59	3.95	0.91	0.70

74
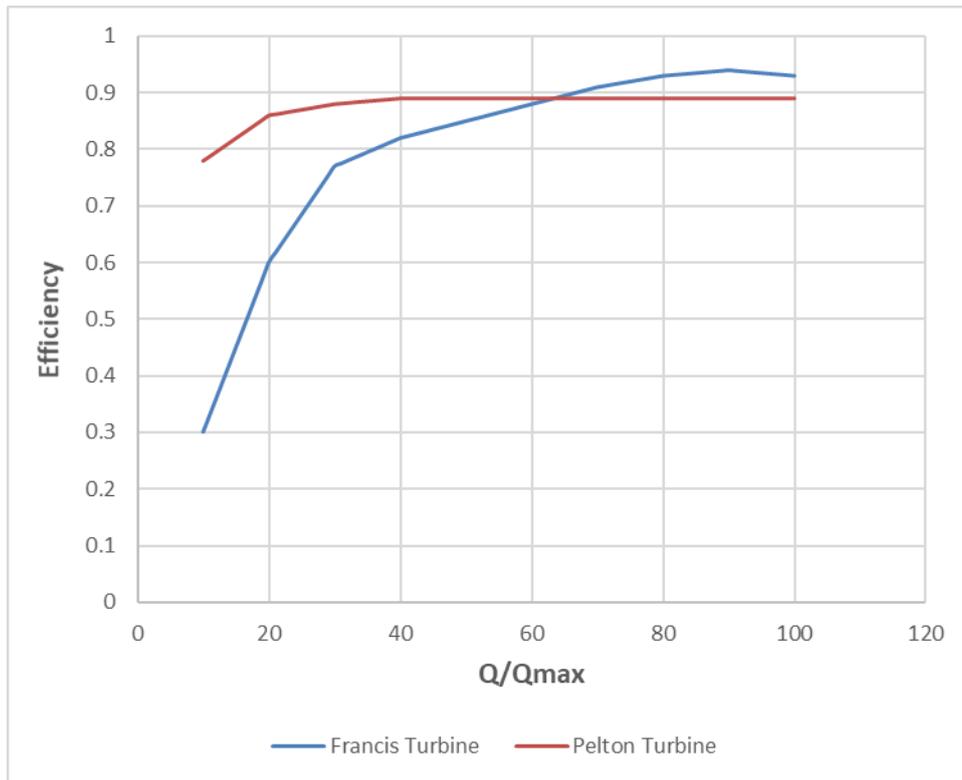
Figure 8.7: Empirical efficiency curves for the two turbines of the system, i.e. Pelton and Francis (for specific speed $n_s = 21$ and $n_s = 100$, respectively).

8.4 Computational procedure

Although the available inflow data are from 2008 to 2018, we only took advantage of specific sub-periods, in order to investigate the flow-energy transformations under different modes. In particular:

- A continuous period of 7 months, from April to November 2017, when only the Pelton turbine was in operation;
- Non-continuous periods of individual operation of the Francis turbine;
- 21 days of continuous operation of both turbines.

The computational procedure is as follows:

i. Retrieval of hourly flows from hourly energy data, through the inverse procedure;
ii. Aggregation of hourly flows to the daily scale;
iii. Extraction of error time series for different error types, by contrasting the aggregated daily flows to the actual ones;
iv. Statistical analysis of errors, and selection of suitable error type on the basis of error characteristics;
v. Determination of stochastic model (in our case, AR(1)) and of its parameters;
vi. Generation of synthetic error realizations through the stochastic model;

vii. Synthesis of 100 ensembles of stochastic daily flow data, by adding synthetic errors to simulated data;

viii. Empirical estimation of target flow values for three characteristic quantiles (5, 50 and 95%), representing the low and upper limits of confidence intervals and the median estimation of the retrieved flows;

Apparently, since we compare real flow and energy data, after employing the inverse procedure we expect to detect errors that reflect all uncertainties that are embedded in the data and the rest of computational assumptions. Actually, in this system we detected multiple issues of uncertainty, as discussed below.

The first origins from the different time scale of data (hourly for energy, daily for inflow). From a first point-of-view, this should only be a straightforward problem of data aggregation. In our study, as the beginning point to measure the flow is midnight but it's possible due to change of work shift this time not to be constant.

According to the general experience, we consider that the Pelton turbine is starting to operate at 10% of its nominal discharge. For a maximum power capacity 1.4 MW and a maximum efficiency 0.89, we get a maximum discharge at approximately 1.057 m³/s. As for the Francis, we assume that the turbine is starting to operate at 20% of its nominal discharge, which is approximately 1.995 m³/s (for power capacity 2.3 MW and maximum efficiency).

8.5   Results

Initially, we tested the three types of errors, as explained in **Chapter 5**, and estimated their statistical characteristics. As made for the hypothetical problem, we finally kept the type I error; its summary statistics for the two turbines are given in **Table 8.2**. We remark that in the case of Pelton, the skewness is negative, while it known that the Gamma distribution describes processes with positive skewness. So, the random variable is expressed as $Z = -X$ and thus the mean and the skewness become -0.001 and 1.782, respectively. Regarding Francis, we demonstrate two sub-cases, one with the empirical curve and one the analytical ones, which is derived via calibration. Details are provided in next section.

Table 8.2: Statistical characteristics of error type 1 for Francis and Pelton turbines.

|	Mean	Standard deviation	Skewness	Autocorrelation	Cross-correlation
Pelton	-0.001	0.041	-1.782	-0.184	0.165
Francis, empirical	-0.026	0.142	6.795	0.850	-0.015
Francis, analytical	-0.002	0.085	5.947	0.045	0.083
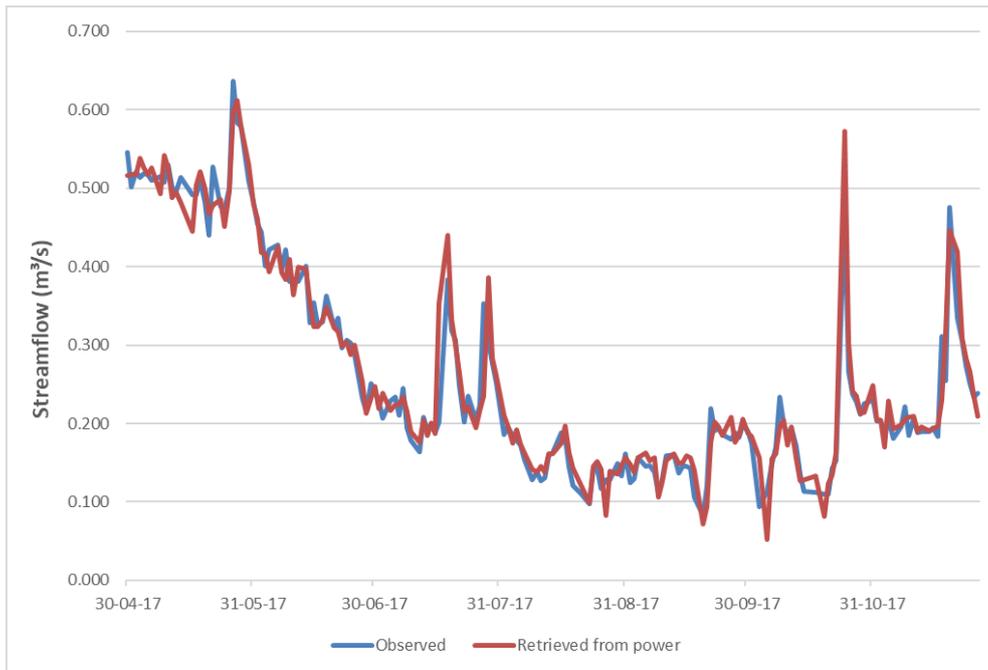
Figure 8.8: Simulated flow from May to November 2017, for the continuous operation of Pelton turbine (deterministic approach).
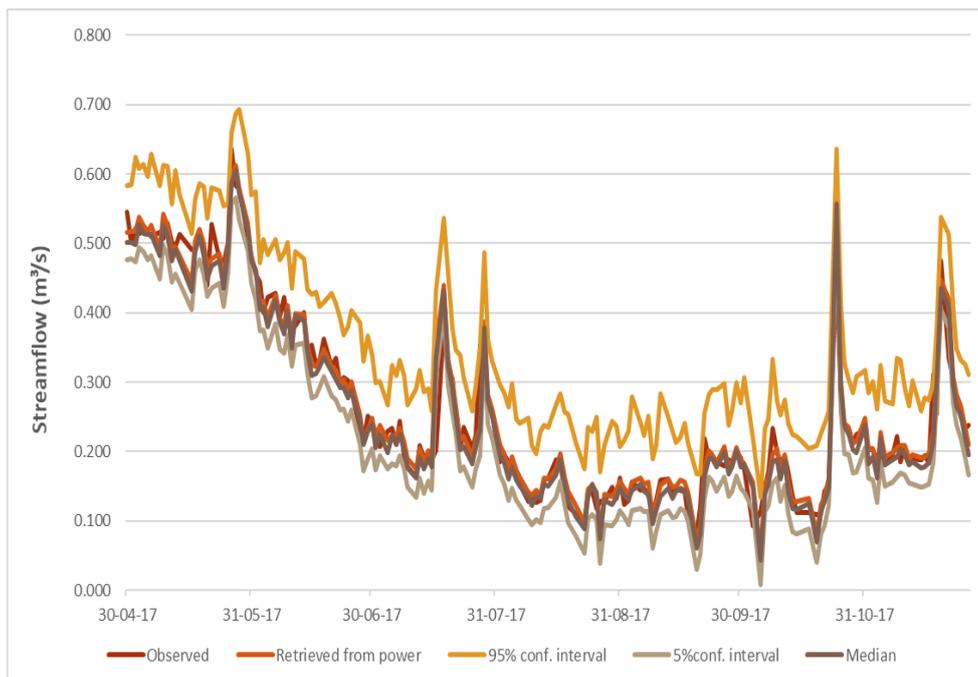

Figure 8.9: Simulated flows and its uncertainty from May to November 2017, for the continuous operation of Pelton turbine.

From **Table 8.2** we remark that the derived errors for both turbines are unbiased and exhibit limited auto- and cross-correlations, which is desirable. On the other hand, in both cases the skewness is very high, particularly for the Francis turbine. This may due to few yet important errors in flow and/or energy observations. In general, the inverse modelling for the case of Francis results to larger errors that the Pelton, as indicated by the more than double

value of the standard deviation. This systematically poorer performance is probably explained by the larger uncertainty of the efficiency curve of Francis over the Pelton.

In **Figures 8.8** and **8.9** we contrast the two approaches for extracting the turbine flows from observed energy, i.e. deterministic and stochastic, respectively, for the continuous operation of Pelton from May to November 2017. From the first approach, it seems that the flows extracted by the (deterministic) reverse engineering procedure fit very well to the observed ones, thus the model performance is excellent. However, by adding the stochastic error term, the actual model uncertainty, as quantified in terms of confidence limits, is much larger than expected. In particular, the upper limit of the confidence interval is much wider, resulted from the large positive skewness of the error. Nevertheless, the stochastic approach allows to quantify the uncertainty induced even from small errors of the observed data. Apparently, the same conclusion stands for the forward problem, i.e. if the streamflow has been measured with errors, the prediction of energy production will be uncertain as well.

Regarding the Francis case, its period of continuous operation is quite small, namely approximately one month. By repeating the same procedures with Pelton, i.e. deterministic and stochastic, we extract the reproduced, the median and the upper and lower confidence limits, which are shown in **Figure 8.10**. The contrasting of the aforementioned time series with the observed data indicates a remarkable uncertainty. Specifically, the median estimation is very close to the low (5%) confidence limit, while the actual data are very close and even exceed the upper (95%) limit.
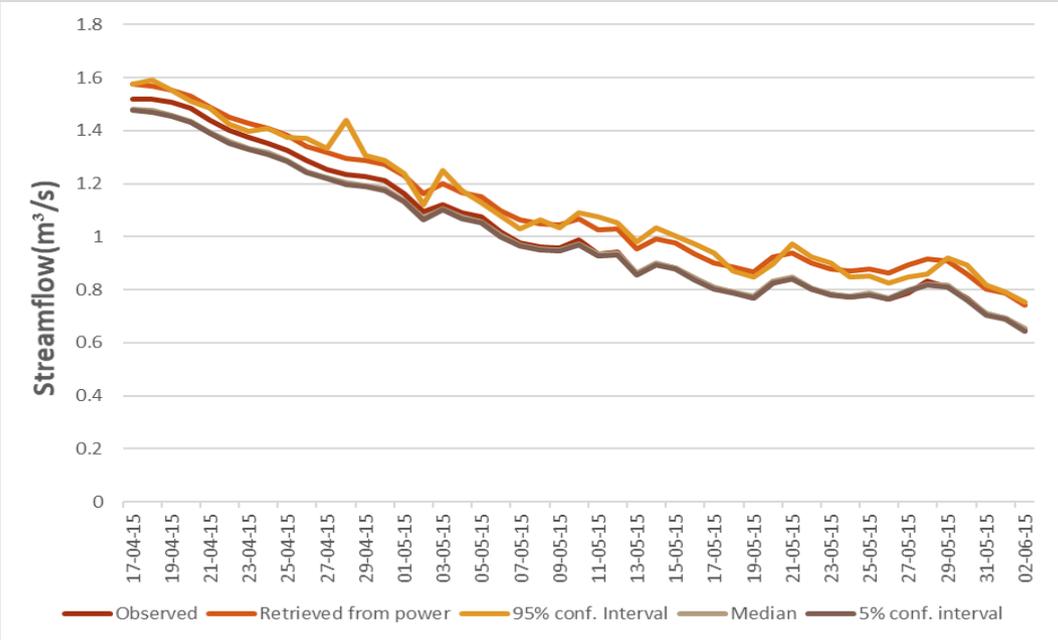
Figure 8.10: Simulated flows and its uncertainty by using the empirical efficiency curve for specific speed $n_s = 100$.
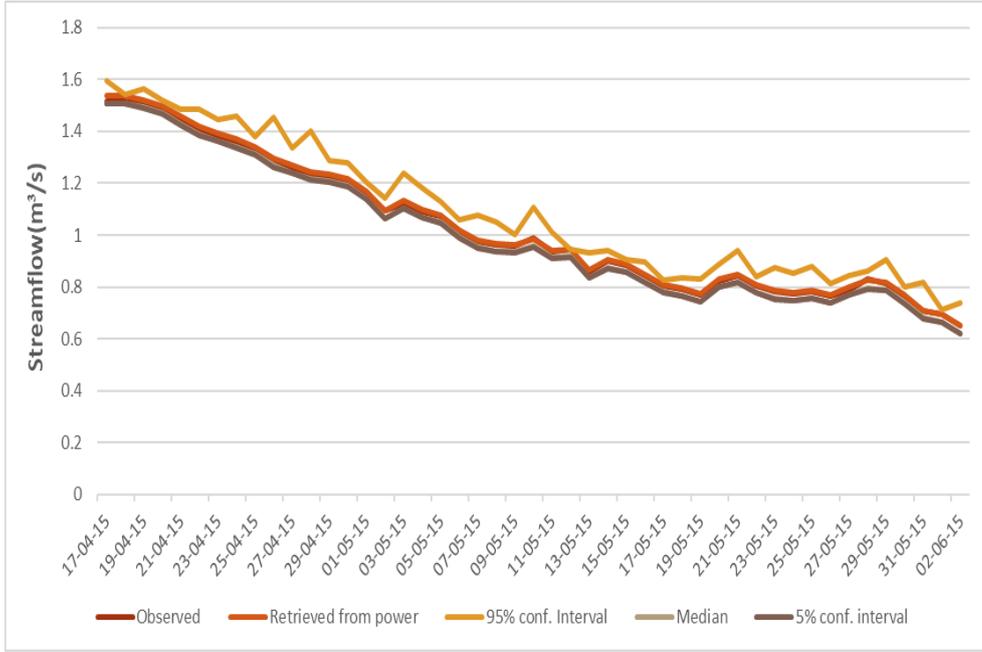
Figure 8.11: Simulated flows and its uncertainty by using the analytical efficiency formula.

This abnormal behaviour reveals that the most essential problem at the study of this turbine is the uncertainty of its efficiency curve. As mentioned in **section 4.4** the efficiency of this type of turbine varies significantly with discharge, thus the modelling procedure is expected to be sensitive against this input element. In order to better fit the simulated to the actual inflow data, and consequently reduce the uncertainty of the inverse modelling procedure, we first extracted an optimized efficiency curve, by applying the analytical formula (5.26) on the basis of simultaneous flow and energy data, and next run the inverse problem to extract the inflows, for the given efficiency. The calibration was carried out by employing the evolutionary algorithm which is embedded in MATLAB. The optimized parameters are n_{min} = 0.70, n_{max} = 0.95, a = 0.59 and b = 3.95. As expected, the new curve ensures better fitting, with the deterministic approach, and little more narrow confidence limits, with the stochastic one, as shown in **Figure 8.11**.

8.6   Combined operation of Pelton and Francis turbines

As discussed before, the period of mixed operation of the two turbines introduced further uncertainties and makes the modelling of this small hydropower plant even more challenging. In fact, the management policy for the combined operation of the two turbines was unknown. In addition, the common period of operation was very limited, namely only 20 days, thus making difficult to extract safe conclusions for the entire range of feasible flow values. In this respect, the beginning and end of mixing was beyond reach. However, the inverse problem was easy to set, since energy production data from each individual turbine were available. Under this premise, the deterministic inverse modelling procedure, described in section 5.3.1, fits also in the mixing of turbines, since the total inflow is just the addition of the two individual flow values that are extracted from the associated energy data, i.e.:

$$Q_{total} = Q_{francis} + Q_{pelton} \qquad (8.1)$$
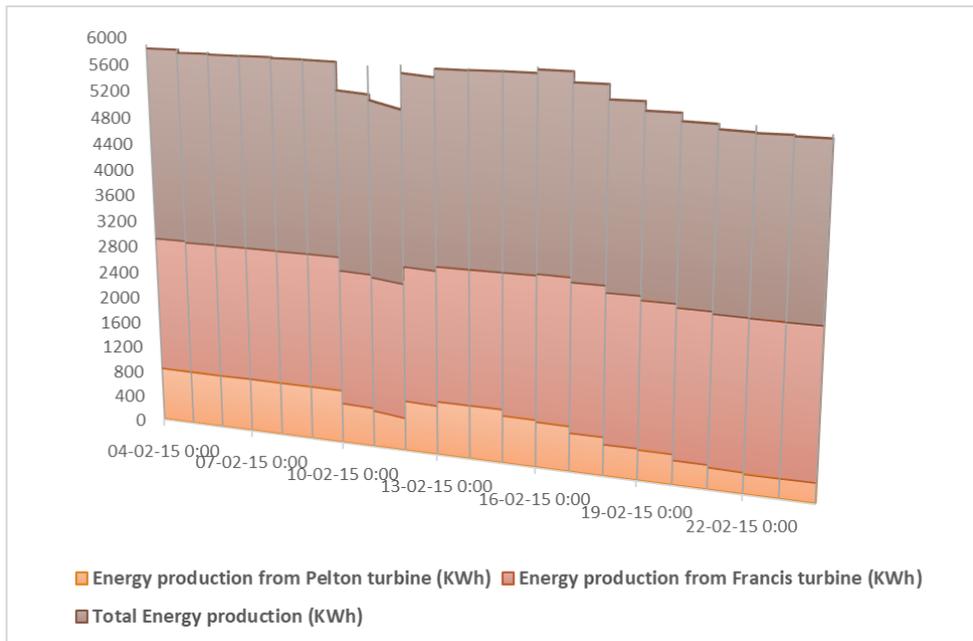
Figure 8.12: Hourly energy production for 20 days of continuous operation of both turbines.
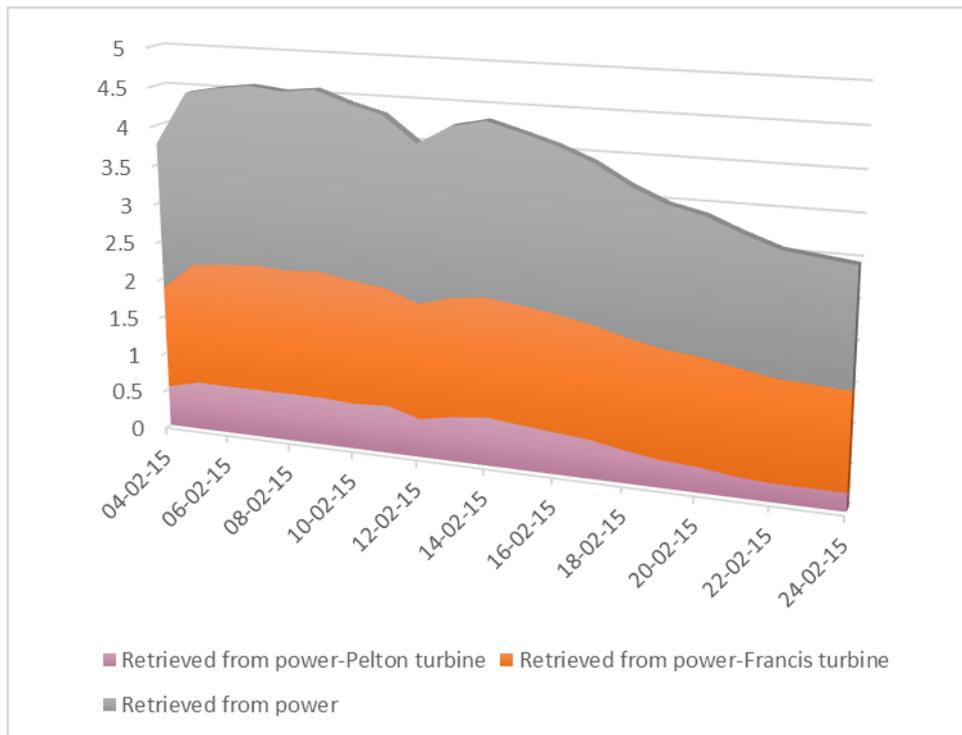

**Figure 8.13**: Simulated flows over 20 days of continuous operation for both turbines.
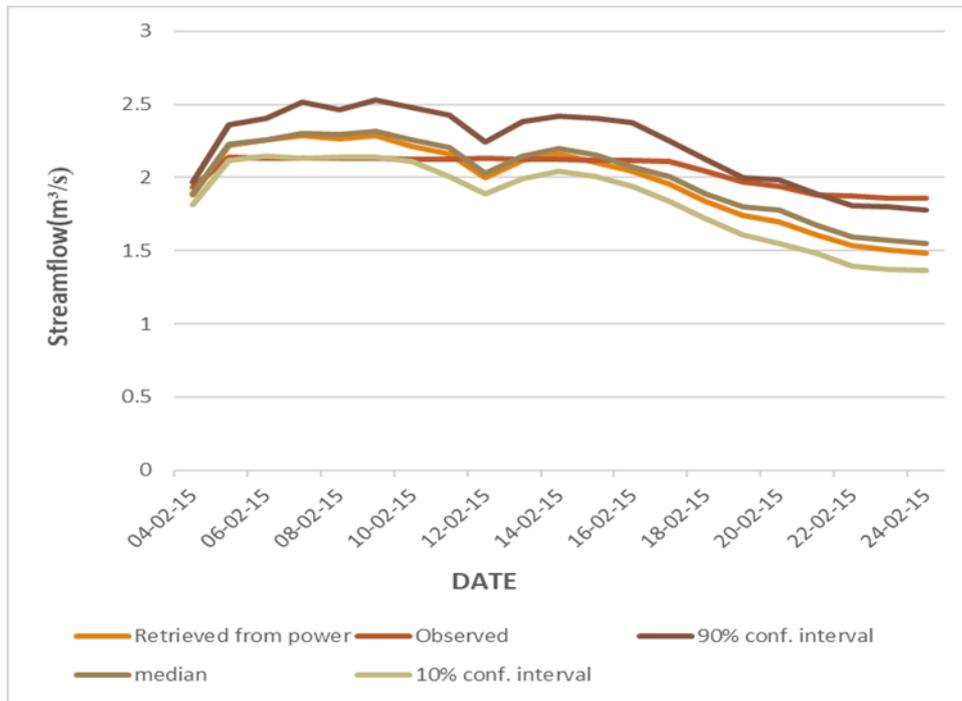
Figure 8.14: Simulated flows and its uncertainty for the mixture of turbines.

In **Table 3** we demonstrate the results of our analysis, which are yet not representative since the available sample is too small, i.e. only 20 days, thus the estimation of the statistical characteristics of error may not be reliable enough. Nevertheless, for the completeness of the study we provided a stochastic model for the errors and used it to estimate the confidence intervals of the retrieved streamflow. As shown in the table, both the auto- and the cross-correlations are too large, which is evidently due to sample uncertainty.

Table 8.3: Statistical characteristics of error type 1 for the mixing of turbines.

Mean	Standard deviation	Skewness	Autocorrelation	Cross-correlation
0.078	0.179	0.279	0.920	-0.852

9 Conclusions and perspectives

9.1 Synopsis and conclusions

The aim of this research was to investigate the non-linear flow-energy transformations across small hydropower plants as well as their complexities and uncertainties. This problem has three possible configurations, the forward (from flow to energy), the inverse (from energy to flow), and the calibration when both flow and energy data are available.

We mainly emphasised on the reverse engineering aspect, i.e. the retrieval of streamflow from energy production data, here called the inverse problem of hydroelectricity. Initially, we developed a deterministic model, which is based on an iterative numerical scheme, that was next formulated in stochastic terms. This approach allows to express the overall uncertainties that are embedded in the aforementioned reverse transformation in typical statistical terms (e.g. marginal statistics and confidence intervals). Here we focused on two key uncertain issues, i.e. the observed output (energy production) and the efficiency curve of turbines.

A well-known peculiarity of SHPPs is the fact that these systems only operate within a specific range of inflows. This challenging task was the opportunity to implement a semi-empirical methodology for extrapolating the part of hydrograph, which is above the nominal flow of turbines or below the minimum flow to produce energy. Our key principle is that the rising limb follows a linear increasing law while the falling one is described as a linear reservoir recession, thus following an exponentially decreasing formula.

Moreover, we discussed another interesting configuration, the extraction of unknown or uncertain technical characteristics of the system, through calibration. In particular, we analysed the efficiency curves, for which we provided a generic parametric expression that can fit to any empirical curve, to facilitate calibration. Our literature research, as well as, our tests on both hypothetical and real-world cases indicated that the efficiency is the most uncertain component of flow-energy transformations for the small hydropower plants.

We first studied an hypothetical small hydroelectric plant for two types of turbines, i.e. Pelton and Francis. In order to investigate the effects of observational errors we added synthetic errors in energy production data. Furthermore, the uncertainty on efficiency curves of turbines was described through multiple curves around the "true" one. The confidence intervals of the extracted flows, considering the artificial errors and the alternative efficiency curves, point the importance of this research.

The spearhead of this research was the study of the real-world small hydroelectric station at Glafkos. This SHPP includes two turbines, i.e. Pelton and Francis. The mixing of turbines, the unknown efficiency curves, the different temporal resolution of flow and energy data, and the possible observational errors in both types of data render this case more challenging. Our analyses indicated that efficiency is the major source of uncertainty, particularly for the case of Francis machines, in which efficiency drops rapidly as discharge decreases. This observation

was the motivation to calibrate the efficiency curve and to further investigate the impact of efficiency on flow-energy transformations.

9.2   Future research perspectives

From the experience gained so far, we have detected several issues for future research, regarding the modelling of small hydropower plants. Specifically:

- Application of the proposed framework to a large number of small hydropower plants (particularly real-world ones), to test the methodology under different system configurations, flow regimes and error sources;
- Modelling of additional uncertain factors, which affect the relationship between inflows-energy production, namely the parameters used in the estimation of hydraulic losses such as pipe roughness;
- Investigation of alternative error expressions and statistical/stochastic approaches for the generation of synthetic error data;
- Adjusting of the new analytical expression of efficiency curves to a wide range of commercial turbines of all types;
- Generalisation of the calibration approach to include several unknown characteristics of the flow-energy transformation, such as the parameters of the analytical efficiency curves and other technical quantities.

The proposed framework may be used in a multidimensional context that span over the three configurations of the flow-energy transformation problem. In particular:
- The design of small hydropower plants under uncertainty, by expressing the forward problem in stochastic terms;
- The management policy of turbines, by using the inverse engineering approach as a driver for optimizing their operation, specifically in the more complex case of turbine mixing;
- The scheduling of energy production, where the prediction of energy can be better formalised as a flow prediction problem. In this formulation we can first implement the inverse approach in order to extract the recent flow sequence, next employ a short-term forecasting scheme to obtain future flow ensembles and finally run the forward model to transform them in energy terms.

This last point triggers a wider perspective of the reverse engineering problem in hydroelectricity, which is the extrapolation of the current status of hydrometric information across Greece by obtaining past flow data in the existing SHPP sites (about 130). This may solve the major shortcomings caused by the lack or low quality of flow data, mainly in small and medium-scale catchments that generally lack of hydrometric infrastructure.

References

Abbas, A., and A. Kumar, Evaluation of uncertainty in flow and performance parameters in Francis turbine test rig, *Flow Measurement and Instrumentation*, 65, 297-308, doi:10.1016/j.flowmeasinst.2019.01.009, 2019.

Anagnostopoulos, J. S., and D. E. Papantonis, Optimal sizing of a run-of-river small hydropower plant, *Energy Conversion and Management*, 48(10), 2663-2670, doi:10.1016/j.enconman.2007.04.016, 2007.

Cobb, B. R., and K. V. Sharp, Impulse (Turgo and Pelton) turbine performance characteristics and their impact on pico-hydro installations, *Renewable Energy*, 50, 959-964, doi:10.1016/j.renene.2012.08.010, 2013.

Efstratiadis, A., I. Nalbantis, and D. Koutsoyiannis, Hydrological modelling of temporally-varying catchments: Facets of change and the value of information, *Hydrological Sciences Journal*, 60(7-8), 1438–1461, doi:10.1080/02626667.2014.982123, 2015.

Efstratiadis, A., N. Mamassis, and D. Koutsoyiannis, *Lecture Notes on Renewable Energy and Hydroelectric Works*, Department of Water Resources and Environmental Engineering, National Technical University of Athens, 2020.

Efstratiadis, A., Y. Dialynas, S. Kozanis, and D. Koutsoyiannis, A multivariate stochastic model for the generation of synthetic time series at multiple time scales reproducing long-term persistence, *Environmental Modelling and Software*, 62, 139–152, doi:10.1016/j.envsoft.2014.08.017, 2014.

Elbatran, A. H., O. B. Yaakob, Y. M.Ahmed, and H. M. Shabara, Operation, performance and economic analysis of low head micro-hydropower turbines for rural and remote areas: A review, *Renewable and Sustainable Energy Reviews*, 43, 40-50, doi:10.1016/j.rser.2014.11.045, 2015.

Evangellatos, A., *Installation study for power production from the small hydropower plant of Glafkos*, Undergraduate thesis, Department of Mechanical Engineering, Technological Educational Institute of Western Greece, Patras, 2016 (in Greek).

Hidalgo, I. G., D. G. Fontane, J. E. G. Lopes; J. G. P. Andrade, and A. F. de Angelis, Efficiency curves for hydroelectric generating units, *Journal of Water Resources Planning & Management*, 140(1), 86-91, doi:10.1061/(ASCE)WR.1943-5452.0000258, 2014.

Koutsoyiannis, D., A generalized mathematical framework for stochastic simulation and forecast of hydrologic time series, *Water Resources Research*, 36(6), 1519–1533, doi:10.1029/2000WR900044, 2000.

Koutsoyiannis, D., A power-law approximation of the turbulent flow friction factor useful for the design and simulation of urban water networks, *Urban Water Journal*, 5(2), 117-115, doi:10.1080/15730620701712325, 2008.

Koutsoyiannis, D., C. Makropoulos, A. Langousis, S. Baki, A. Efstratiadis, A. Christofides, G. Karavokiros, and N. Mamassis, Climate, hydrology, energy, water: recognizing uncertainty and seeking sustainability, *Hydrology and Earth System Sciences*, 13, 247–257, doi:10.5194/hess-13-247-2009, 2009.

Kumaraswamy, P. A generalized probability density function for double-bounded random processes, *Journal of Hydrology*, 46(1-2), 79-88, doi:10.1016/0022-1694(80)90036-0, 1980.

Kumar, R., and S. K. Singal, Operation and maintenance problems in hydro turbine material in small hydro power plant, *Materials Today: Proceedings*, 2(4-5), 2323-2331, doi:10.1016/j.matpr.2015.07.284, 2015.

Langousis, A., and V. Kaleris, Theoretical framework to estimate spatial rainfall averages conditional on river discharges and point rainfall measurements from a single location: an application to western Greece, *Hydrology and Earth System Sciences*, 17, 1241-1263, doi:10.5194/hess-17-1241-2013, 2013.

Mamassis, N., A. Efstratiadis, P. Dimitriadis, T. Iliopoulou, R. Ioannidis, and D. Koutsoyiannis, Water and Energy, *Handbook of Water Resources Management: Discourses, Concepts and Examples*, edited by J. Bogardi, K. D. Wasantha, R. R. P. Nandalal, R. van Nooyen, and A. Bhaduri, Chapter 20, Springer Nature, Switzerland, 2020, (in press).

Michailidi, E., *Flood risk assessment in gauged and ungauged basins in a multidimensional context*, PhD thesis, Universita Degli Studi di Brescia, March 2018.

Mishra, S., S. K. Singal, and D. K. Khatod, Optimal installation of small hydropower plant – A review, *Renewable and Sustainable Energy Reviews*, 15(8), 3862-3869, doi:10.1016/j.rser.2011.07.008, 2011.

Montanari, R., Criteria for the economic planning of a low power hydroelectric plant, *Renewable Energy*, 28(13), 2129-2145, doi:10.1016/S0960-1481(03)00063-6, 2003.

Paish, O., Small hydro power: technology and current status, *Renewable and Sustainable Energy Reviews*, 6(6), 537–556, doi:10.1016/S1364-0321(02)00006-0, 2002.

Papantonis, D. E., *Small Hydroelectric Works*, 2nd edition, Symeon Editions, Athens, 2008 (in Greek).

Risva, K., D. Nikolopoulos, A. Efstratiadis, and I. Nalbantis, A framework for dry period low flow forecasting in Mediterranean streams, *Water Resources Management*, 32(15), 4911–1432, doi:10.1007/s11269-018-2060-z, 2018.

Roberson, J.A., J. J. Cassidy, and M. H. Chaudhry, *Hydraulic Engineering*, Wiley, New York, 1998.

Sadegh, M., J. A. Vrugt, H. V. Gupta, and C. Xu, The soil water characteristic as new class of closed-form parametric expressions for the flow duration curve, *Journal of Hydrology*, 535, 438-456, doi:10.1016/j.jhydrol.2016.01.027, 2015.

Sakki, G.-K., V. Papalamprou, I. Tsoukalas, N. Mamassis, and A. Efstratiadis, Stochastic modelling of hydropower generation from small hydropower plants under limited data availability: from post-assessment to forecasting, *European Geosciences Union General Assembly 2020, Geophysical Research Abstracts, Vol. 22*, Vienna, EGU2020-8129, doi:10.5194/egusphere-egu2020-812, 2020.

Santolin, A., G. Cavazzini, G. Pavesi, G. Ardizzon, and A. Rossetti, Techno-economical method for the capacity sizing of a small hydropower plant, *Energy Conversion and Management*, 52(7), 2533-2541, doi:10.1016/j.enconman.2011.01.001, 2011.

Skjelbred, H. I., and J. Kong, A comparison of linear interpolation and spline interpolation for turbine efficiency curves in short-term hydropower scheduling problems, *IOP Conference Series Earth and Environmental Science*, 240(4), 042011, doi:10.1088/1755-1315/240/4/042011, 2011.

Tsoukalas, I., A. Efstratiadis, and C. Makropoulos, Building a puzzle to solve a riddle: A multi-scale disaggregation approach for multivariate stochastic processes with any marginal distribution and correlation structure, *Journal of Hydrology*, 575, 354–380, doi:10.1016/j.jhydrol.2019.05.017, 2019.

Tsoukalas, I., P. Kossieris, and C. Makropoulos, Simulation of non-Gaussian correlated random variables, stochastic processes and random fields: Introducing the anySim R-Package for environmental applications and beyond, *Water*, 12(6), 1645, doi:10.3390/w12061645, 2020.

Vrugt, J. A., C. J. F. ter Braak, H. V. Gupta, and B. A. Robinson, Equifinality of formal (DREAM) and informal (GLUE) Bayesian approaches in hydrologic modeling, *Stochastic Environmental Research and Risk Assessment*, 23(7) 1011-1026, 10.1007/s00477-008-0274-y, 2009.

Yildiz, V., and J. A. Vrugt, A toolbox for the optimal design of run-of-river hydropower plants, *Environmental Modelling and Software*, 111, 134-152, doi:10.1016/j.envsoft.2018.08.018, 2019.

Appendix: Extrapolated inflow hydrographs for the hypothetical SHPP
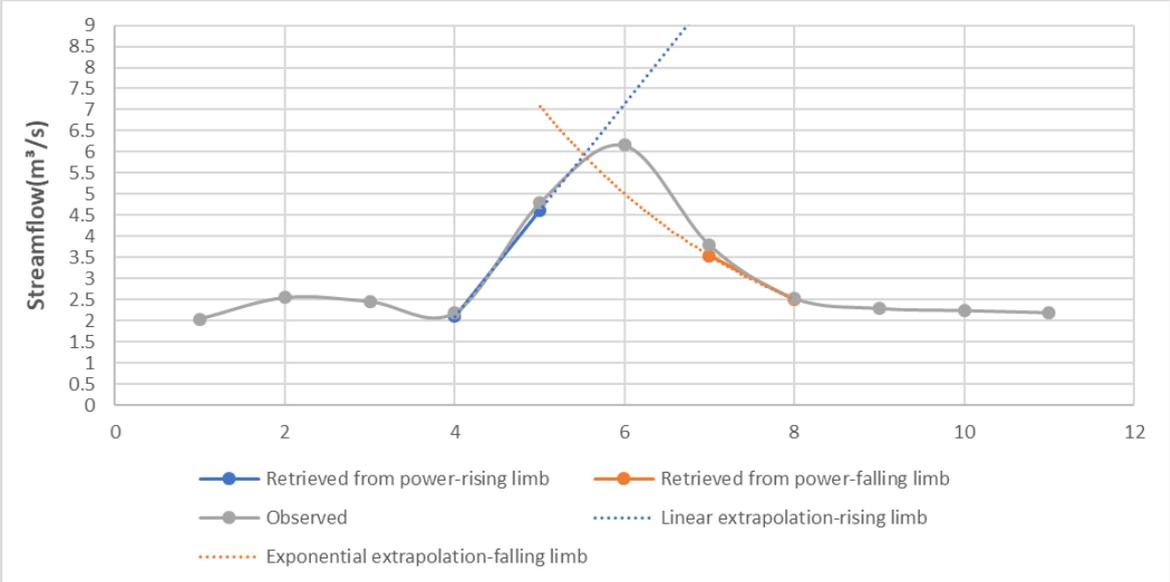

Figure A.1: Example of extrapolating high flow values, when the streamflow exceeds the upper discharge limit (turbine capacity) of 5.0 m³/s.
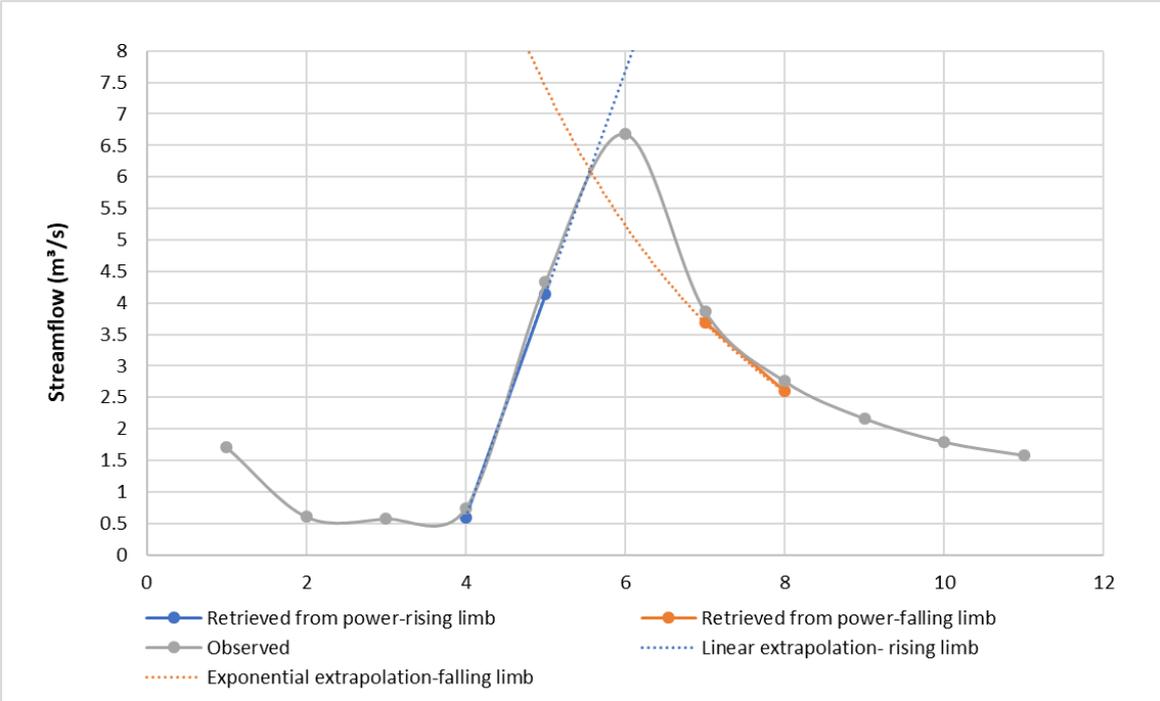

Figure A.2: Example of extrapolating high flow values, when the streamflow exceeds the upper discharge limit (turbine capacity) of 5.0 m³/s.
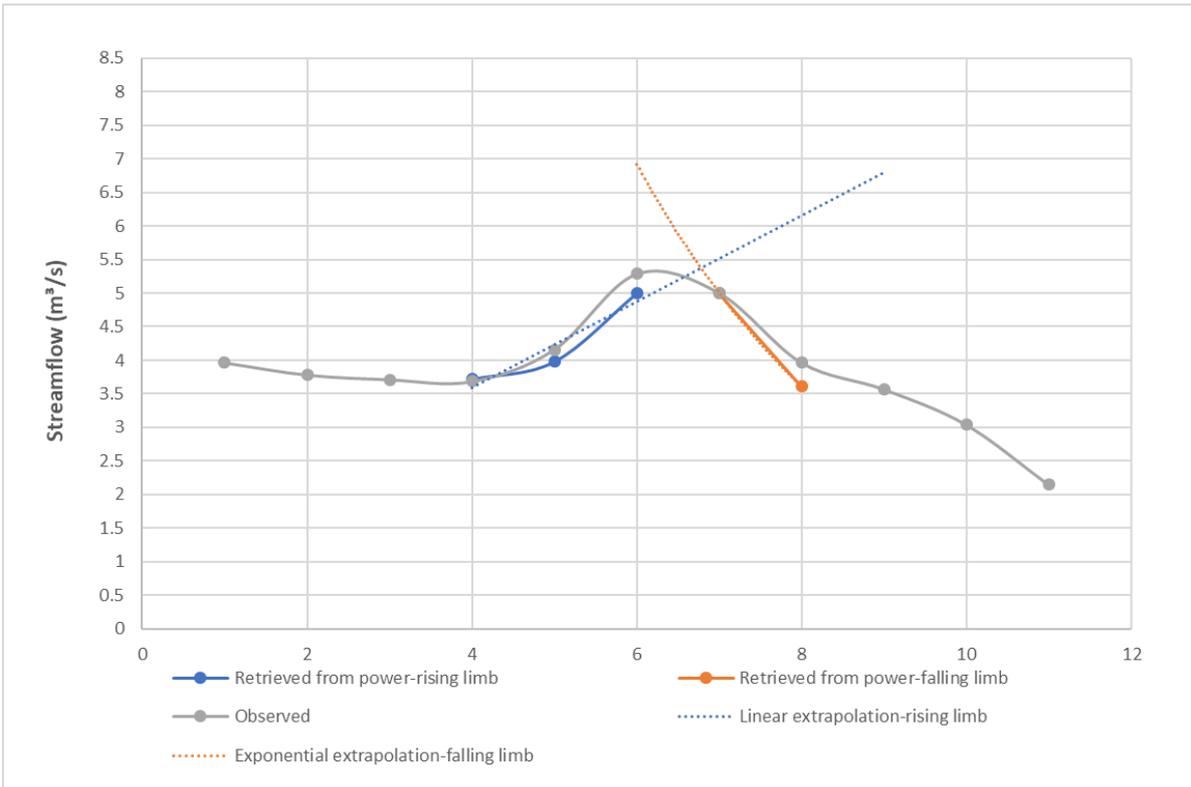
Figure A.3: Example of extrapolating high flow values, when the streamflow exceeds the upper discharge limit (turbine capacity) of 5.0 m^3/s.
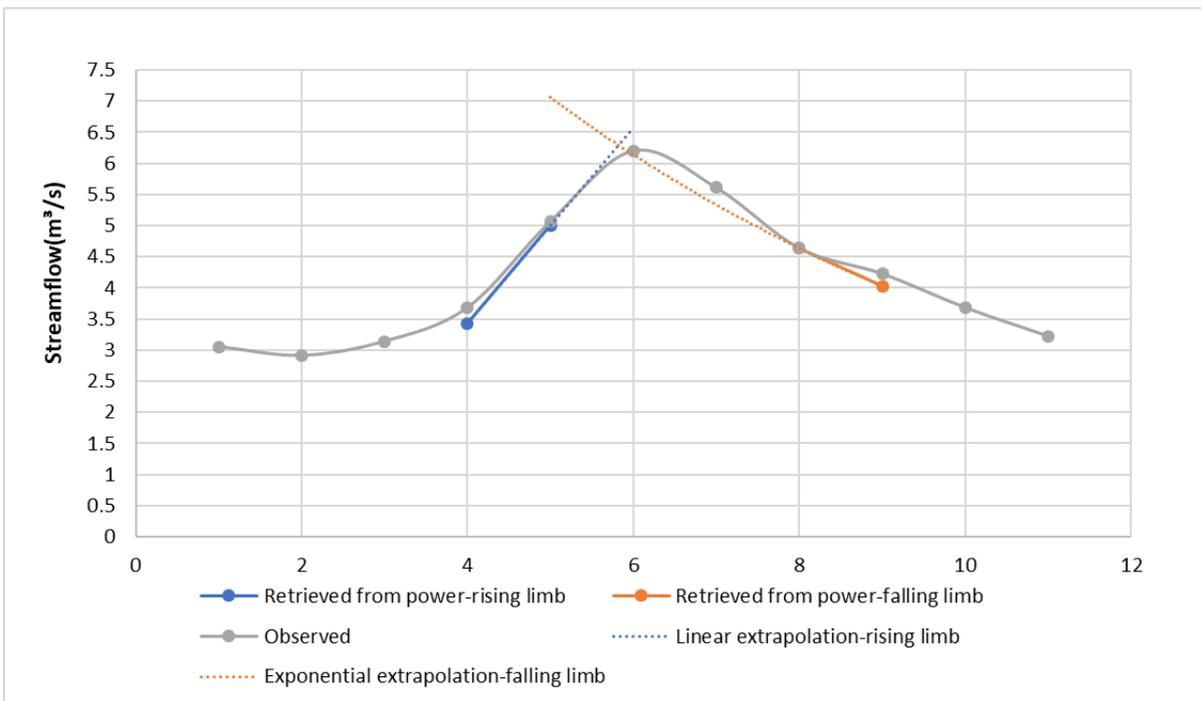
Figure A.4: Example of extrapolating high flow values, when the streamflow exceeds the upper discharge limit (turbine capacity) of 5.0 m^3/s.
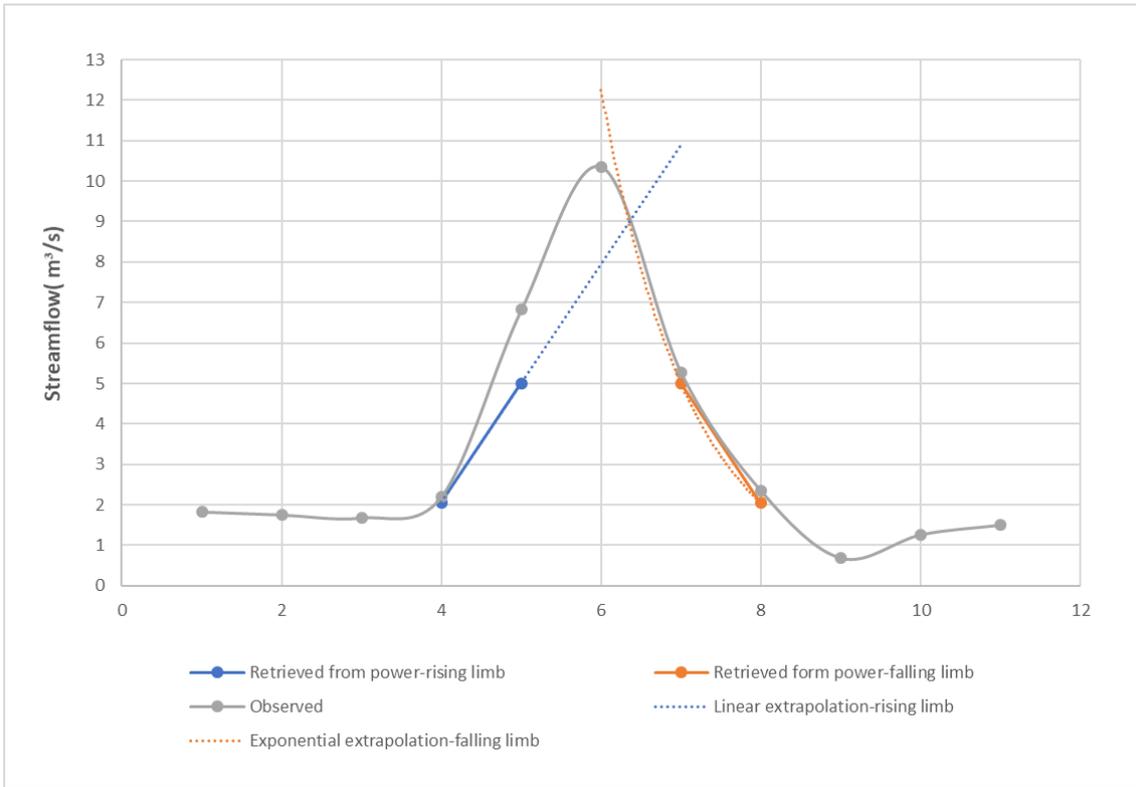
Figure A.5: Example of extrapolating high flow values, when the streamflow exceeds the upper discharge limit (turbine capacity) of 5.0 m³/s.
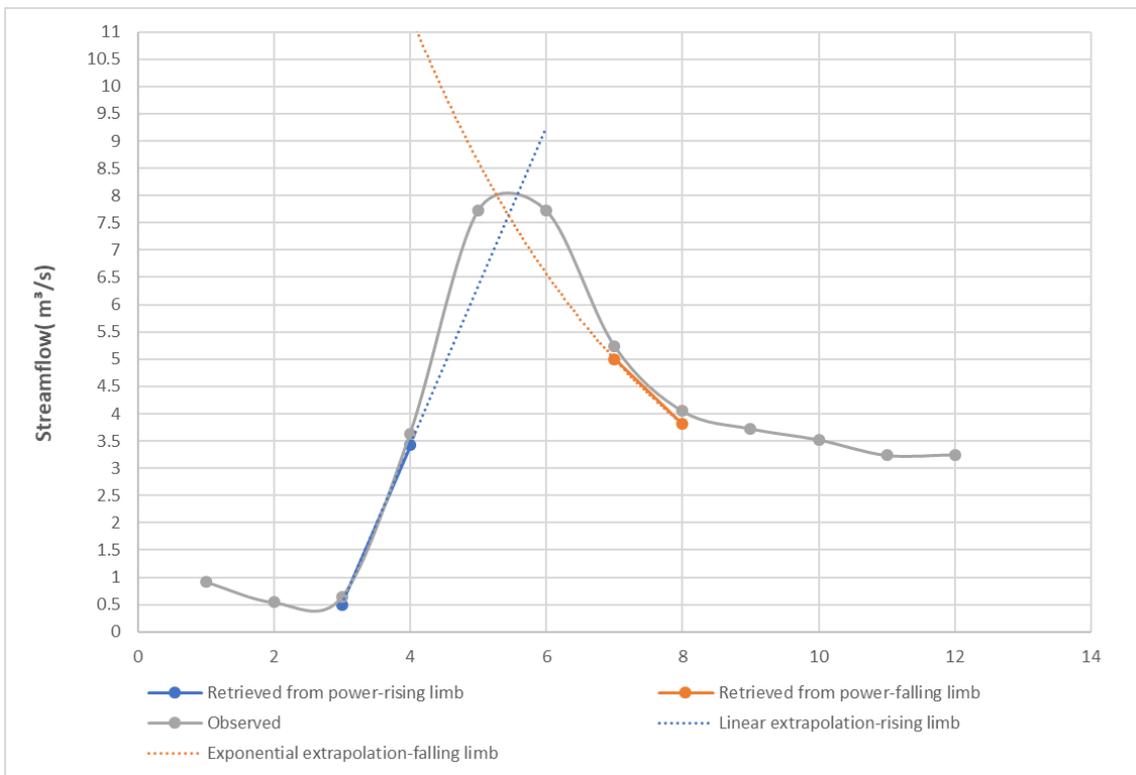
Figure A.6: Example of extrapolating high flow values, when the streamflow exceeds the upper discharge limit (turbine capacity) of 5.0 m³/s.
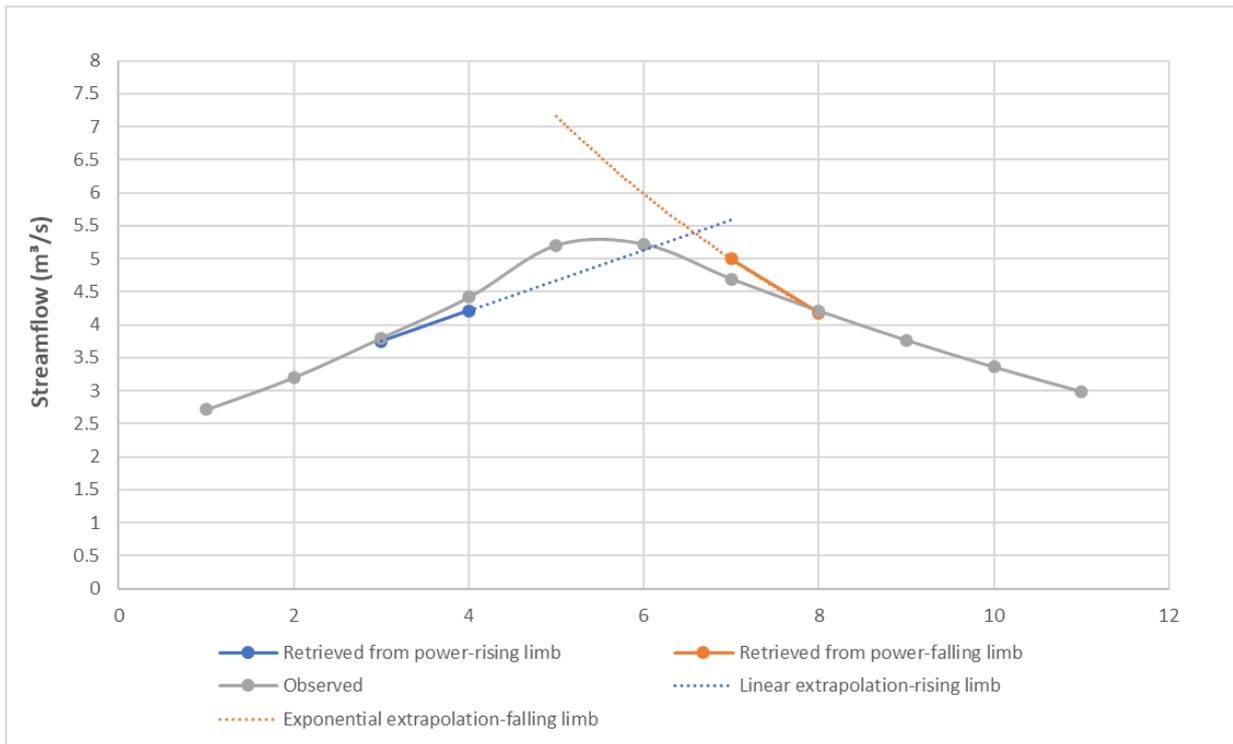
Figure A.7: Example of extrapolating high flow values, when the streamflow exceeds the upper discharge limit (turbine capacity) of 5.0 m^3/s.
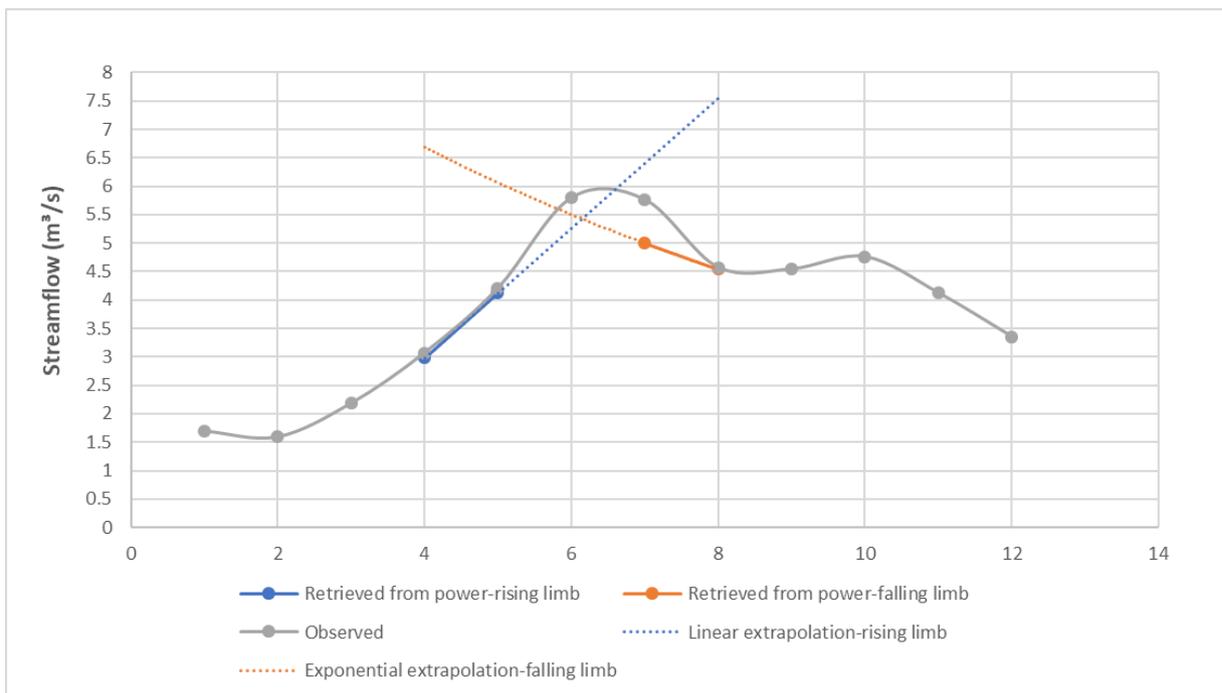
Figure A.8: Example of extrapolating high flow values, when the streamflow exceeds the upper discharge limit (turbine capacity) of 5.0 m^3/s.
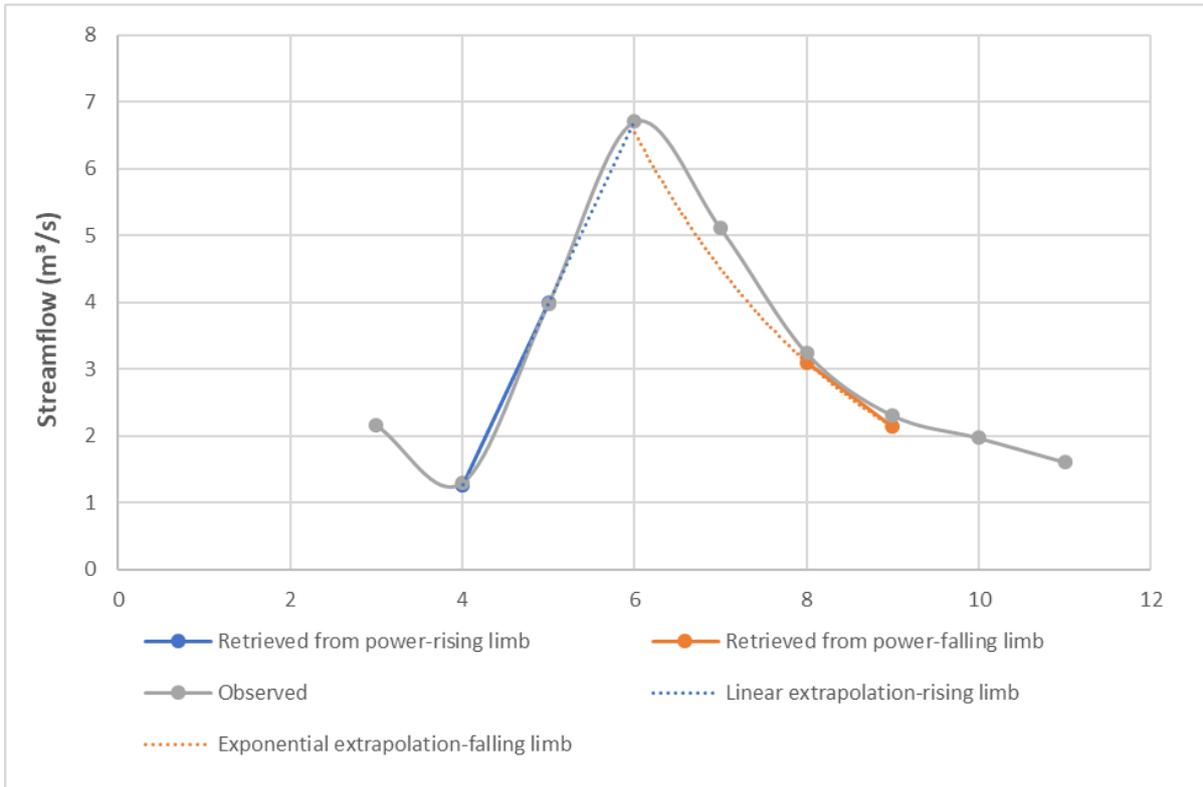
Figure A.9: Example of extrapolating high flow values, when the streamflow exceeds the upper discharge limit (turbine capacity) of 5.0 m³/s.
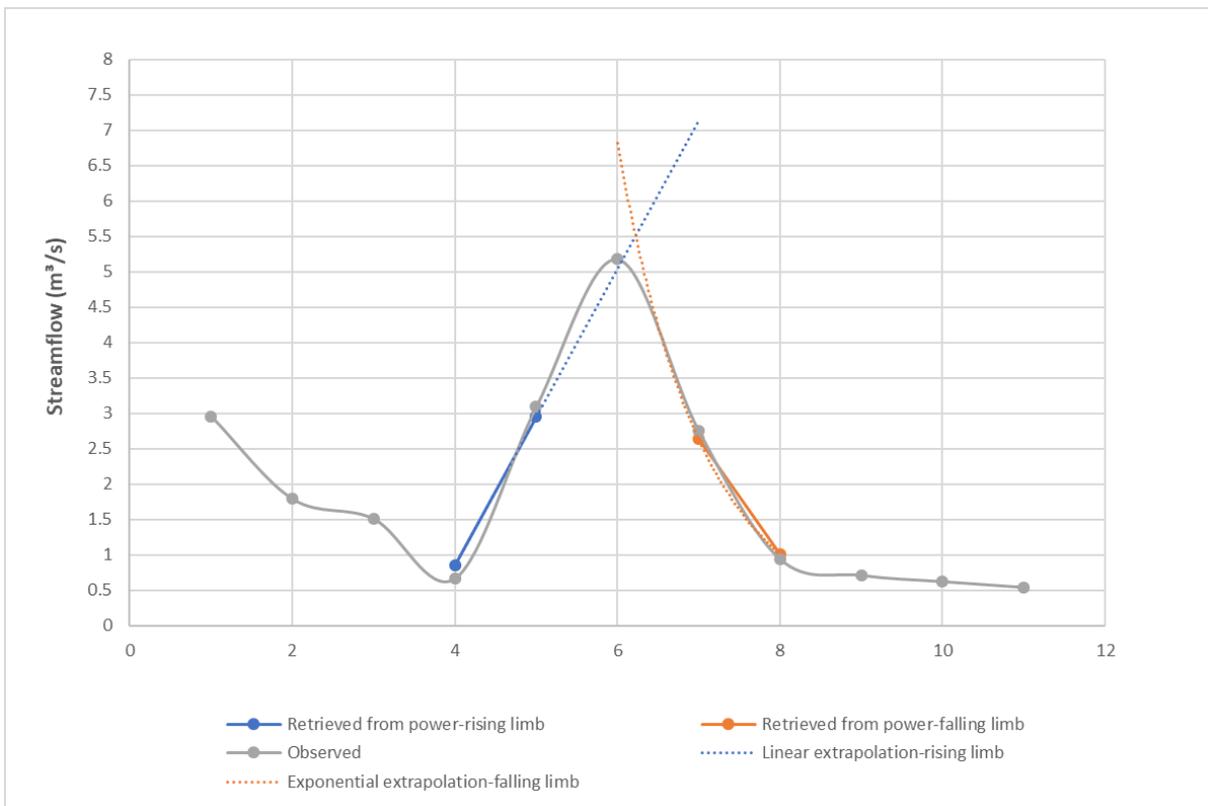
Figure A.10: Example of extrapolating high flow values, when the streamflow exceeds the upper discharge limit (turbine capacity) of 5.0 m³/s.
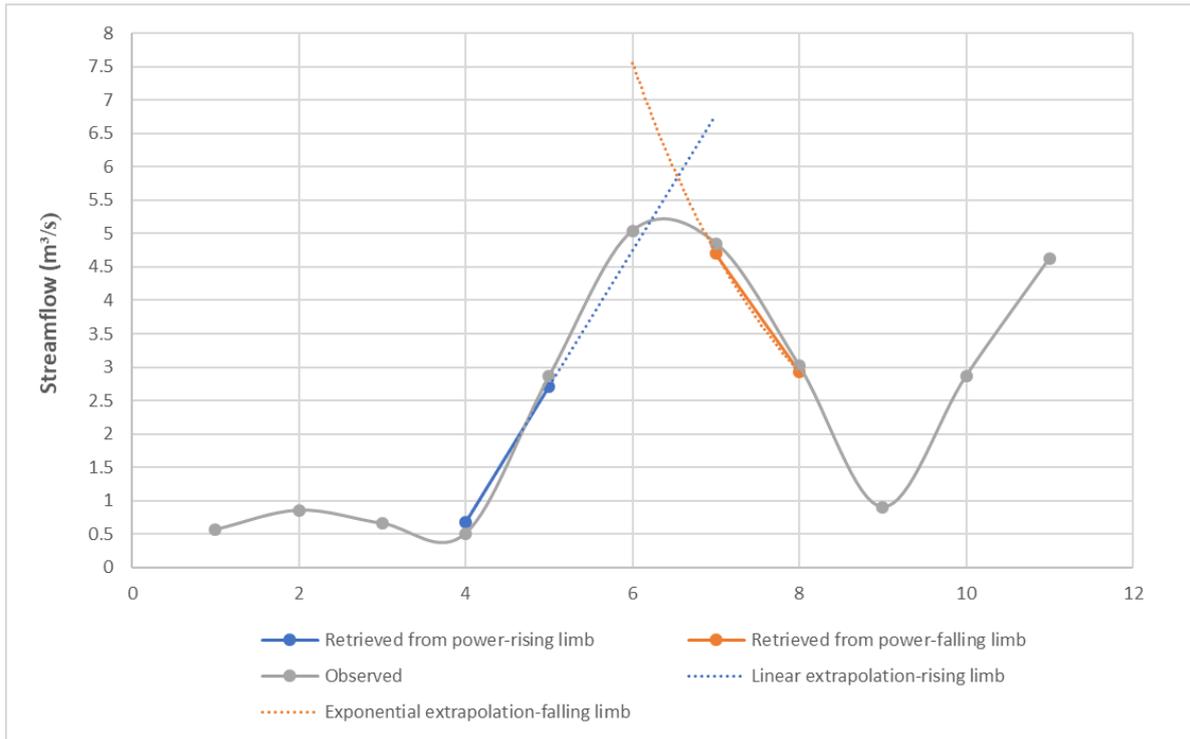
Figure A.11: Example of extrapolating high flow values, when the streamflow exceeds the upper discharge limit (turbine capacity) of 5.0 m³/s.
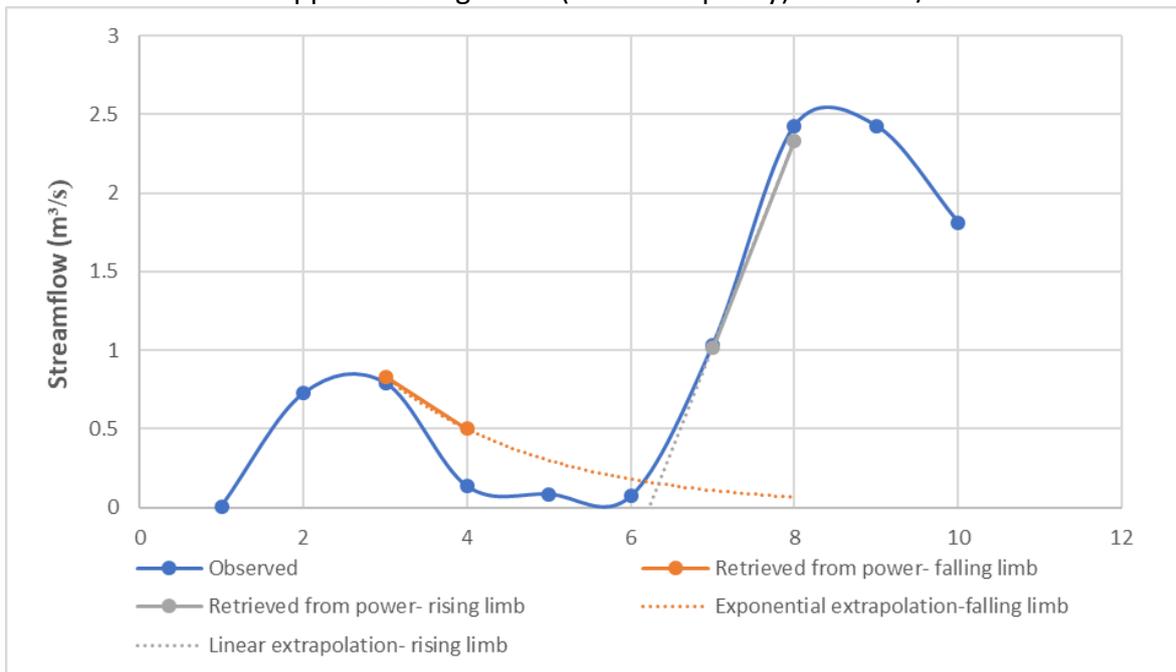
Figure A.12: Example of extrapolating low flow values for missing days 5, 6 and 7, when the streamflow is below the lower operational discharge limit of 0.5 m³/s.
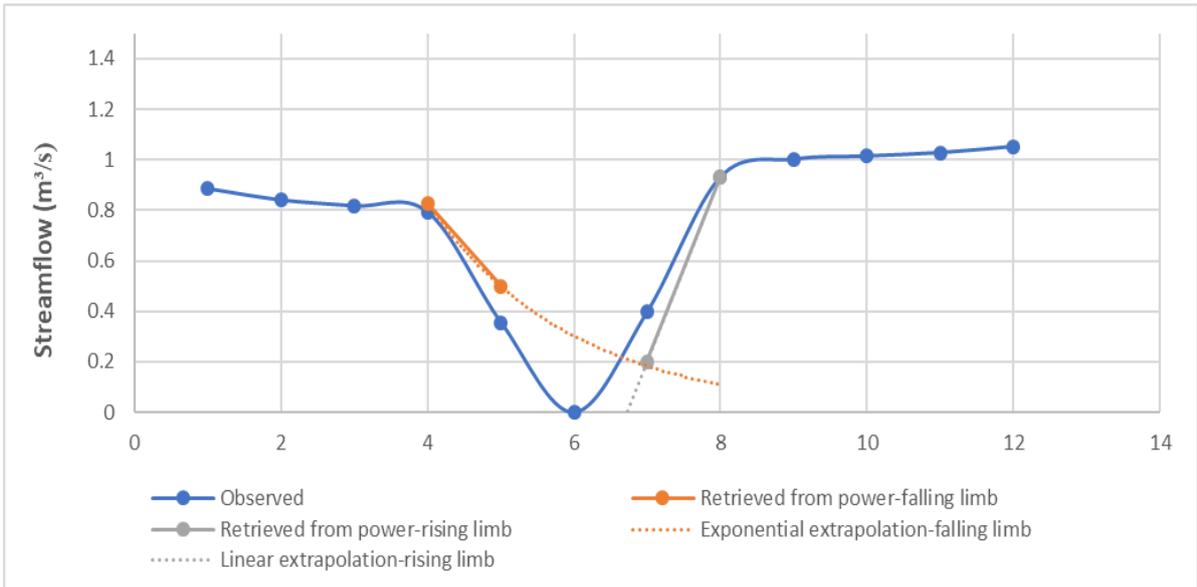
Figure A.13: Example of extrapolating low flow values for missing days 5, 6 and 7, when the streamflow is below the lower operational discharge limit of 0.5 m^3/s.
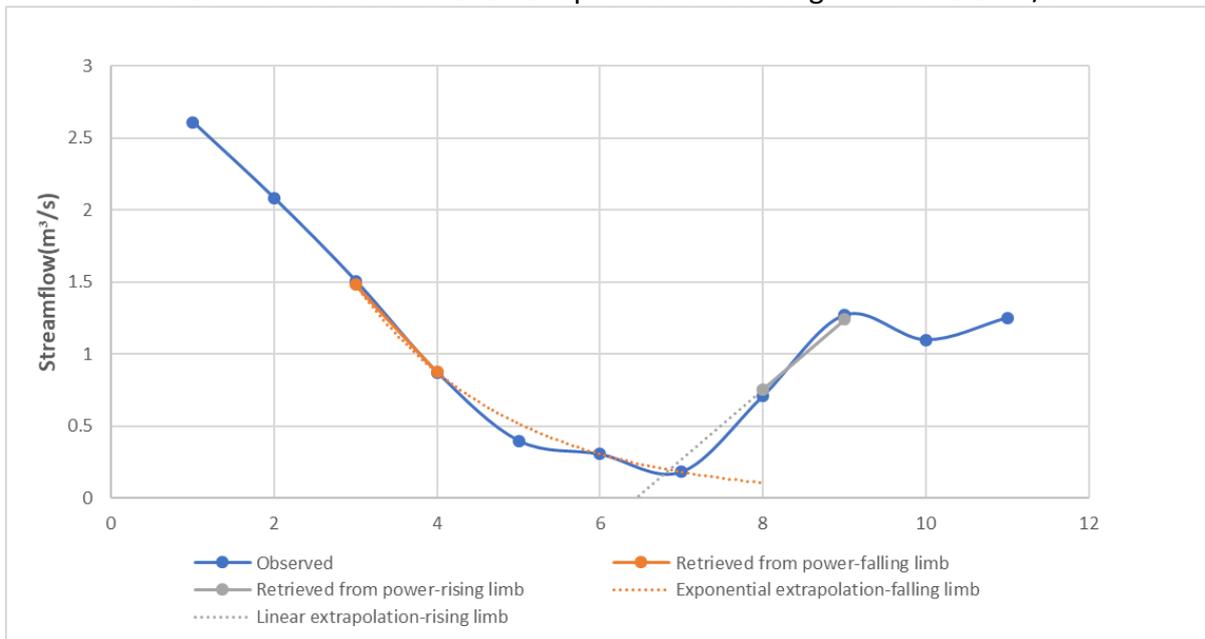
Figure A.14: Example of extrapolating low flow values for missing days 5, 6 and 7, when the streamflow is below the lower operational discharge limit of 0.5 m^3/s.
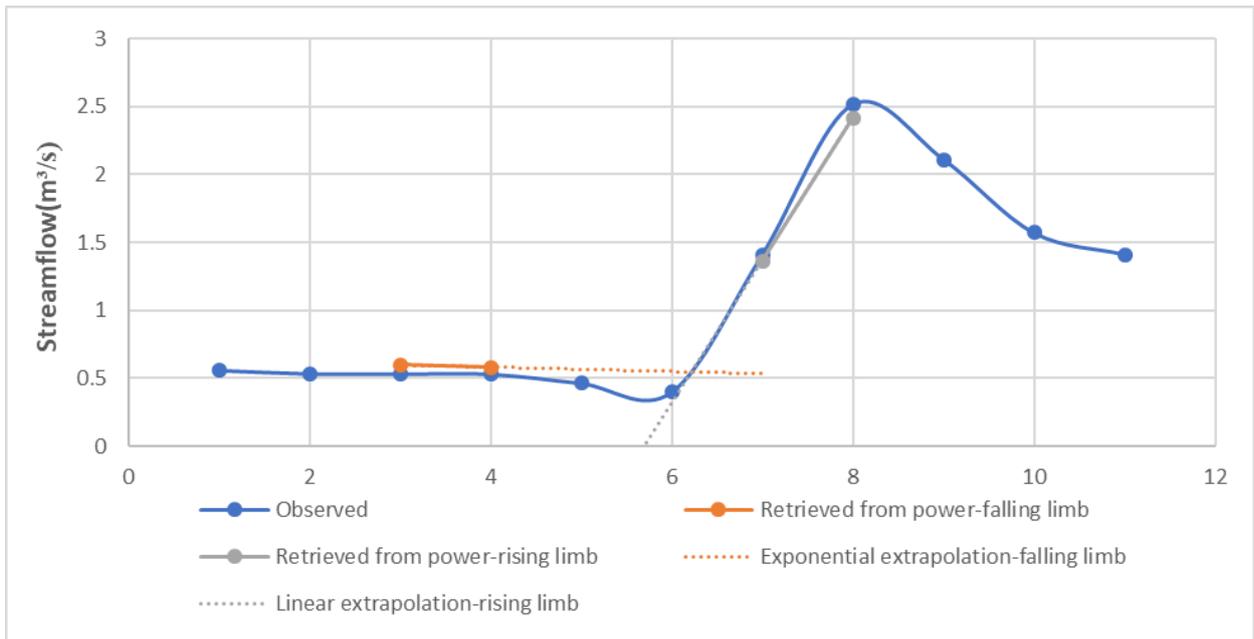
Figure A.15: Example of extrapolating low flow values for missing days 5, 6 and 7, when the streamflow is below the lower operational discharge limit of 0.5 m³/s.
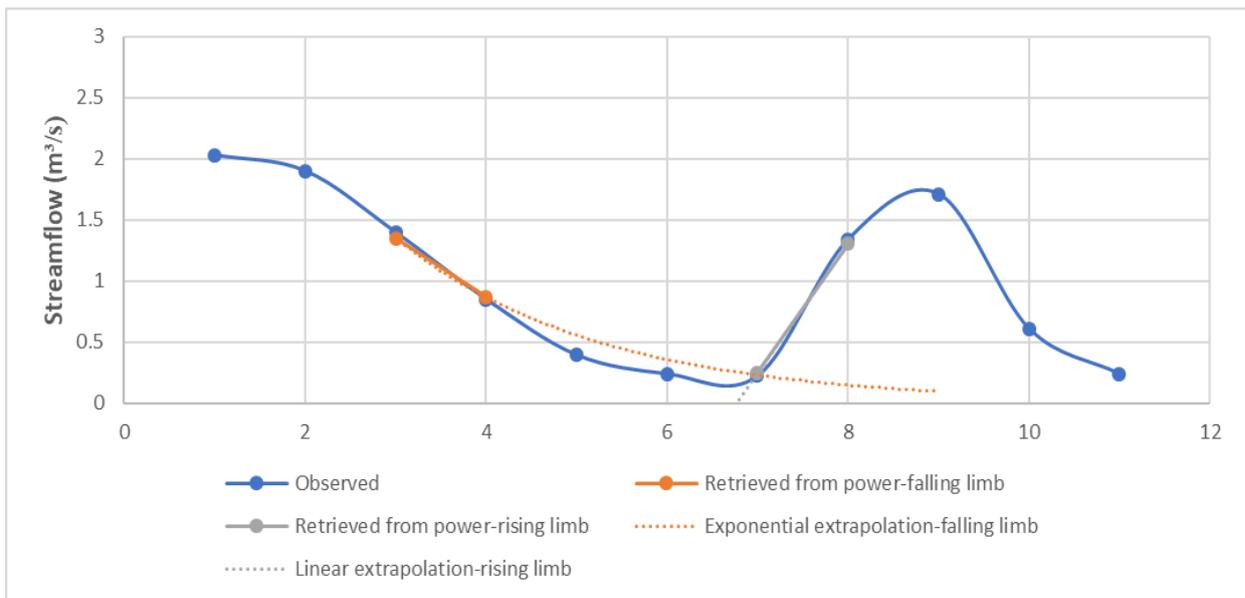

Figure A.16: Example of extrapolating low flow values for missing days 5, 6 and 7, when the streamflow is below the lower operational discharge limit of 0.5 m³/s.
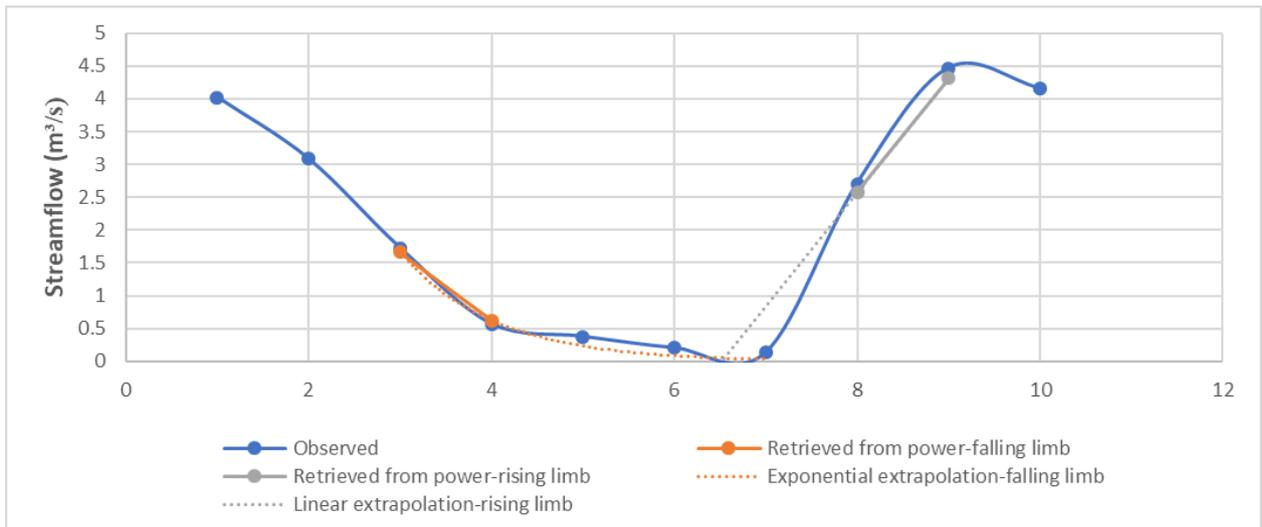
Figure A.17: Example of extrapolating low flow values for missing days 5, 6 and 7, when the streamflow is below the lower operational discharge limit of 0.5 m³/s.
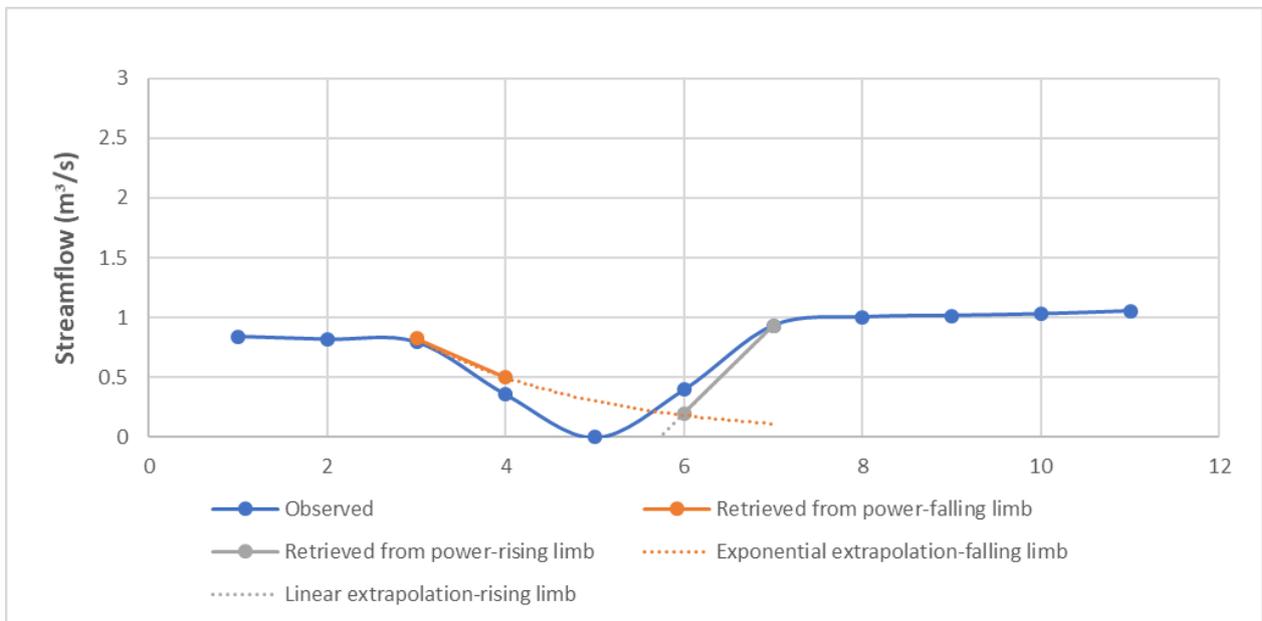
Figure A.18: Example of extrapolating low flow values for missing days 5, 6 and 7, when the streamflow is below the lower operational discharge limit of 0.5 m³/s.

95
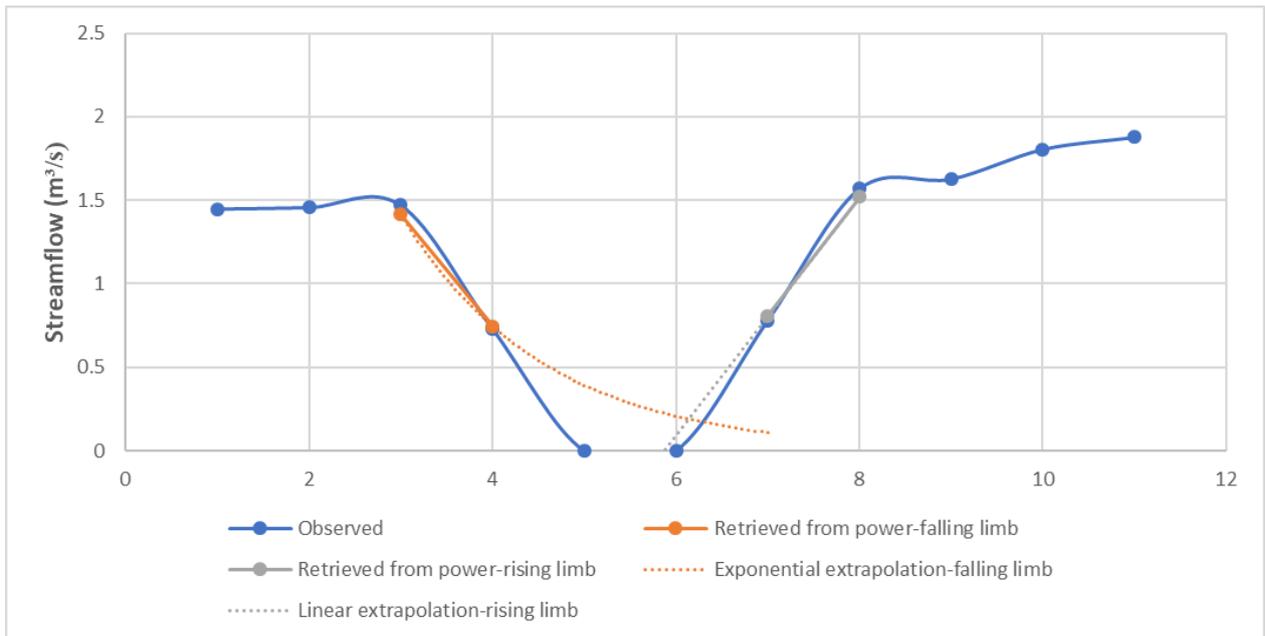
Figure A.19: Example of extrapolating low flow values for missing days 5, 6 and 7, when the streamflow is below the lower operational discharge limit of 0.5 m³/s.